NAVAL POSTGRADUATE SCHOOL

MONTEREY, CALIFORNIA

THESIS

PARAMETER ESTIMATION AND MODELING OF INTERFERENCE CANCELLATION TECHNIQUE FOR MULTIPLE SIGNAL RECOVERY

by

Alexander Rios

June 2013

Thesis Advisors: Ric A. Romero
Tri T. Ha

Approved for public release; distribution is unlimited

THIS PAGE INTENTIONALLY LEFT BLANK

REPORT DOCUMENTATION PAGE			*Form Approved OMB No. 0704–0188*
Public reporting burden for this collection of information is estimated to average 1 hour per response, including the time for reviewing instruction, searching existing data sources, gathering and maintaining the data needed, and completing and reviewing the collection of information. Send comments regarding this burden estimate or any other aspect of this collection of information, including suggestions for reducing this burden, to Washington headquarters Services, Directorate for Information Operations and Reports, 1215 Jefferson Davis Highway, Suite 1204, Arlington, VA 22202–4302, and to the Office of Management and Budget, Paperwork Reduction Project (0704–0188) Washington DC 20503.			
1. AGENCY USE ONLY ***(Leave blank)***	**2. REPORT DATE** June 2013	**3. REPORT TYPE AND DATES COVERED** Master's Thesis	
4. TITLE AND SUBTITLE PARAMETER ESTIMATION AND MODELING OF INTERFERENCE CANCELLATION TECHNIQUE FOR MULTIPLE SIGNAL RECOVERY		**5. FUNDING NUMBERS**	
6. AUTHOR(S) Alexander Rios			
7. PERFORMING ORGANIZATION NAME(S) AND ADDRESS(ES) Naval Postgraduate School Monterey, CA 93943–5000		**8. PERFORMING ORGANIZATION REPORT NUMBER**	
9. SPONSORING /MONITORING AGENCY NAME(S) AND ADDRESS(ES) N/A		**10. SPONSORING/MONITORING AGENCY REPORT NUMBER**	
11. SUPPLEMENTARY NOTES The views expressed in this thesis are those of the author and do not reflect the official policy or position of the Department of Defense or the U.S. government. IRB Protocol number ____N/A____.			
12a. DISTRIBUTION / AVAILABILITY STATEMENT Approved for public release; distribution is unlimited		**12b. DISTRIBUTION CODE** A	

13. ABSTRACT (maximum 200 words)

In this thesis, the amplitude gain of received quadrature phase shift keying (QPSK) signals and interferences are estimated via the least squares error method in order to facilitate the implementation of reference-based successive interference cancellation (RSIC). In the scenario considered for this thesis, a system of multi-platform receivers is assumed to be positioned within the overlapping coverage areas of transmitting base stations. The first receiver initiates the RSIC technique by obtaining a demodulated reference signal and forwarding that reference to the second receiver that separately collects a second signal corrupted by interference, which is actually a scaled version of the first signal with an unknown amplitude gain. This amplitude gain is estimated and applied to the known reference signal so that it is subtracted from the collected signal at the second receiver. The process continues with a third and fourth receiver (or potentially more receivers) until the final desired signal is separated from all the interferences. Finally, the accuracy of the estimations is evaluated and the symbol error rate performances via Monte Carlo simulations for QPSK modulation in a multi-platform system are presented.

14. SUBJECT TERMS Parameter Estimation, Amplitude Gain Estimation, Successive Interference Cancellation, Least Squares Error			**15. NUMBER OF PAGES** 105
			16. PRICE CODE
17. SECURITY CLASSIFICATION OF REPORT Unclassified	**18. SECURITY CLASSIFICATION OF THIS PAGE** Unclassified	**19. SECURITY CLASSIFICATION OF ABSTRACT** Unclassified	**20. LIMITATION OF ABSTRACT** UU

NSN 7540–01–280–5500 Standard Form 298 (Rev. 2–89)
Prescribed by ANSI Std. 239–18

THIS PAGE INTENTIONALLY LEFT BLANK

Approved for public release; distribution is unlimited

PARAMETER ESTIMATION AND MODELING OF INTERFERENCE CANCELLATION TECHNIQUE FOR MULTIPLE SIGNAL RECOVERY

Alexander Rios
Lieutenant, United States Navy
B.S., United States Naval Academy, 2007

Submitted in partial fulfillment of the
requirements for the degree of

MASTER OF SCIENCE IN ELECTRICAL ENGINEERING

from the

NAVAL POSTGRADUATE SCHOOL
June 2013

Author: Alexander Rios

Approved by: Ric A. Romero
Thesis Co-Advisor

Tri T. Ha
Thesis Co-Advisor

Clark R. Robertson
Chair, Department of Electrical and Computer Engineering

THIS PAGE INTENTIONALLY LEFT BLANK

ABSTRACT

In this thesis, the amplitude gain of received quadrature phase shift keying (QPSK) signals and interferences are estimated via the least squares error method in order to facilitate the implementation of reference-based successive interference cancellation (RSIC). In the scenario considered for this thesis, a system of multi-platform receivers is assumed to be positioned within the overlapping coverage areas of transmitting base stations. The first receiver initiates the RSIC technique by obtaining a demodulated reference signal and forwarding that reference to the second receiver that separately collects a second signal corrupted by interference, which is actually a scaled version of the first signal with an unknown amplitude gain. This amplitude gain is estimated and applied to the known reference signal so that it is subtracted from the collected signal at the second receiver. The process continues with a third and fourth receiver (or potentially more receivers) until the final desired signal is separated from all the interferences. Finally, the accuracy of the estimations is evaluated and the symbol error rate performances via Monte Carlo simulations for QPSK modulation in a multi-platform system are presented.

THIS PAGE INTENTIONALLY LEFT BLANK

TABLE OF CONTENTS

THIS PAGE INTENTIONALLY LEFT BLANK

LIST OF FIGURES

THIS PAGE INTENTIONALLY LEFT BLANK

LIST OF ACRONYMS AND ABBREVIATIONS

AWGN	Additive White Gaussian Noise
BS	Base Station
CRLB	Cramer-Rao Lower Bound
IC	Interference Cancellation
LSE	Least Squares Error
MLD	Maximum Likelihood Detector
PDF	Probability Density Function
QPSK	Quadrature Phase Shift Keying
Rd	Round
RSIC	Reference-Based Successive Interference Cancellation
Rx	Receiver
SER	Symbol Error Rate
SIC	Successive Interference Cancellation
SIR	Signal-to-Interference Ratio
SNR	Signal-to-Noise Ratio
SOI	Signal of Interest
vs.	versus

THIS PAGE INTENTIONALLY LEFT BLANK

EXECUTIVE SUMMARY

Wireless communication has made huge advances in the ability to transmit and receive at high data rates in almost every populated region in the world. The amount of interference experienced by these systems may seem overwhelming at times, but innovations in technology and modulation continue to provide the world with reliable exchange of information. Another technique exists that is utilized by a multi-platform system to remove extraneous interference from a received signal so that only the desired signal of interest (SOI) remains.

Successive interference cancellation (SIC) is considered a member of the family of post-interference cancellation techniques which are focused on the cancellation or suppression of interference on an a-posteriori basis [1]. This means that a system using the low complexity SIC method must first collect a signal in order to then "demodulate and/or decode desired information, and use this information along with channel estimates to cancel received interference from the received signal" [2]. A related SIC scheme known as reference-based successive interference cancellation (RSIC) makes use of a multi-platform system with what is called a reference signal to eliminate interference in received signals.

RSIC makes use of multiple receivers placed in favorable locations so that each can collect a specific combination of signals. An iterative process ensues in which a receiver in one area successfully collects a signal (called the reference), demodulates and then transmits it to the successive receiver in the next area. Reference signals are assumed to be mostly interference-free. The second receiver separately collects a different signal in addition to interference, which is a scaled version of the first signal (scaled due to amplitude gain or loss). By calculating an estimate of the amplitude gain and applying it to the reference signal that is obtained from the first receiver, the second receiver can subtract this interference from the overall signal it has received. This effectively provides the second receiver with its own reference signal to pass on (in addition to the first reference signal) to the next receiver in the system and thus continuing the RSIC process.

Previous work related to RSIC uses this described technique to model systems with different amplitude gain configurations with the intention of observing the performance provided by the interference cancellation [3]. For that study, the amplitude gain parameter values are chosen arbitrarily simply to examine how the cancellation technique functions in different interference environments. The purpose of this thesis is therefore to provide a method to estimate the values of the gain parameters experienced by a multi-platform system, in order to allow the RSIC technique to successfully remove extraneous unwanted interference from SOIs. The performance and accuracy of these estimates will also be analyzed.

As seen in Figure 1, the overlapping base station (BS) coverage areas contain sectors where different sets of signals coincide.

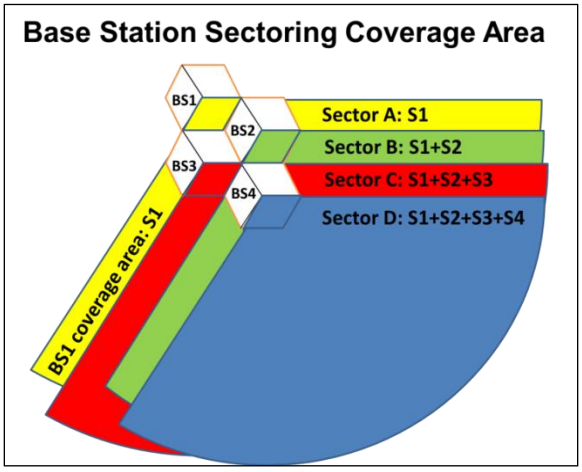

Figure 1. Configuration of multiple BSs with overlapping antenna coverage which has different signal combinations received in each sector. From [3].

The received signals from each sector are given by

$$y_1 = s_1 + w_1, \tag{1.1}$$

$$y_2 = s_2 + \alpha_{1,2} s_1 + w_2, \tag{1.2}$$

$$y_3 = s_3 + \alpha_{2,3} s_2 + \alpha_{1,3} s_1 + w_3, \tag{1.3}$$

$$y_4 = s_4 + \alpha_{3,4} s_3 + \alpha_{2,4} s_2 + \alpha_{1,4} s_1 + w_4, \tag{1.4}$$

where $\alpha_{m,n}$ is the amplitude gain (or loss) of the signal from BS *m* received by receiver *n*, and *w* is the additive white Gaussian noise in the receiver. The transmitted signals *s* are assumed to have perfect synchronization and the same energy while the amplitude gain is assumed to be real and positive. Receivers in each sector are assumed to only have the knowledge of the signal *y* they collect, and the reference signals that are sent to them by the other receivers (i.e., receiver two (Rx2) only knows y_2 and s_1; Rx3 only knows y_3, s_2 and s_1; Rx4 only knows y_4, s_3, s_2 and s_1). If for example s_2 is considered the SOI, then in order to conduct RSIC, the receiver placed in Sector A would collect (1.1), demodulate the information, then transmit this reference signal to receiver two. At Rx2, the received signal y_2 and the obtained reference signal would be used to calculate an estimate for the amplitude gain $\alpha_{1,2}$ so that the estimate could be multiplied to the reference and then subtracted from the received signal y_2. The SOIs from each sector are therefore

$$\hat{s}_1 = y_1 - w_1, \tag{1.5}$$

$$\hat{s}_2 = y_2 - \beta_{1,2}s_1 - w_2, \tag{1.6}$$

$$\hat{s}_3 = y_3 - \beta_{2,3}s_2 - \beta_{1,3}s_1 - w_3, \tag{1.7}$$

$$\hat{s}_4 = y_4 - \beta_{3,4}s_3 - \beta_{2,4}s_2 - \beta_{1,4}s_1 - w_4, \tag{1.8}$$

where β is the amplitude gain estimate for the respective α parameter and the noise *w* may be considered negligible for high signal-to-noise ratios (SNR).

In order to obtain these β parameters, the least squares error (LSE) method from [4] is used to calculate estimations for each sector. In the example where $\mathbf{s}_2$ is the SOI, Rx1 collects $\mathbf{y}_1$ which it passes through a maximum likelihood detector (MLD) [5] to decide on what information is received, or

$$\hat{\mathbf{s}}_1 = dec(\mathbf{y}_1) = dec(s_1 + w_1), \tag{1.9}$$

where *dec*( ) is the MLD, $\mathbf{y}_1 = [y_1[0] y_1[1] ... y_1[N-1]]^T$ and $\mathbf{s}_i = [s_i[0] s_i[1] ... s_i[N-1]]^T$ for *i* = 1, 2. Next, the decision as to what symbols are received by Rx2 is made based on $\mathbf{y}_2$ alone, such that we have an initial (*pre*) calculation for $\mathbf{s}_2$, or simply $\tilde{\mathbf{s}}_2$ where

$$\tilde{\mathbf{s}}_2 = dec(\mathbf{y}_2). \tag{1.10}$$

This *pre* calculation is used to determine an estimate for $\alpha_{1,2}$, which is defined as $\beta_{1,2}$. The value for $\beta_{1,2}$ is now used to determine a final (*post*) calculation for the information of $\mathbf{s}_2$ in (1.6), or

$$\hat{\mathbf{s}}_2 = dec(\mathbf{y}_2 - \beta_{1,2}\hat{\mathbf{s}}_1). \tag{1.11}$$

If the concept of making decisions to obtain reference signals is executed on a three-receiver system, by utilizing $\tilde{\mathbf{s}}_3 = dec(\mathbf{y}_3)$ we calculate the estimates for the gain parameters, $\beta_{2,3}$ and $\beta_{1,3}$. Utilizing these estimations, we make a new *post* calculation based on (1.7), yielding

$$\hat{\mathbf{s}}_3 = dec(\mathbf{y}_3 - \beta_{2,3}\hat{\mathbf{s}}_2 - \beta_{1,3}\hat{\mathbf{s}}_1). \tag{1.12}$$

For the four-receiver system where we define $\tilde{\mathbf{s}}_4 = dec(\mathbf{y}_4)$, the gain estimates are $\beta_{3,4}$, $\beta_{2,4}$ and $\beta_{1,4}$. These estimations are now used in the *post* calculation, or

$$\hat{\mathbf{s}}_4 = dec(\mathbf{y}_4 - \beta_{3,4}\hat{\mathbf{s}}_3 - \beta_{2,4}\hat{\mathbf{s}}_2 - \beta_{1,4}\hat{\mathbf{s}}_1). \tag{1.13}$$

With the formulas ready for use, the Monte Carlo simulations involve first iterating through different gain parameter values with fixed SNR levels. The estimates are compared to the actual values of α. These simulations are also conducted at various SNRs to observe the effects of noise on the estimators. From the simulation results, we observe that as any of the α gain parameters approach 1.0, the performance of the estimators begins to degrade. The performance is degraded as additional receiver noise is added to the system. In our simulations, we also investigate fixing the α parameters while the SNR is varied to different levels. Improving accuracies of the estimates are

observed when the SNR is increased. With the generation of the post calculation signals, the performance of the RSIC technique is illustrated by comparing the SER between the $\hat{\mathbf{s}}$ signals and theoretical values for QPSK modulation.

It is made clear that in the four-receiver system the compounding effect of additional interferences has a negative effect on estimator performance. Estimate accuracy is seen to decrease with the slightest addition of interference amplitude gain. A method to mitigate this is to use the post calculation obtained from (1.13) and substitute those values into a new calculation of the gain estimate. New β parameters are obtained and can again be used to calculate a new $\hat{\mathbf{s}}_4$. These additional rounds of estimate re-calculation are seen to greatly improve the accuracy of the β parameters as well as SER performance of the new $\hat{\mathbf{s}}_4$ signal.

A useful metric in each of these systems is the signal-to-interference ratio (SIR) that is present due to the extraneous transmissions from the other BSs. It is useful to compare the accuracy of the estimates as a function of SIR to see how overall interference in the system affects the performance of the estimators. Specifically, in the four-receiver system, it is clear that SIR plays a large role since there are three signals interfering with the SOI. Even small values of amplitude gain from one of these signals make a considerable effect on performance when compounded with the gains from the others. It is shown in the simulation results that as the SIR for a specific system increased, the estimator performance improves and in turn, the SER of the *post* calculations is diminished.

RSIC is an effective method for extracting a desired signal(s) from a receiver(s) in an interference-filled environment, provided of course that the estimates calculated for the amplitude gain of interference signals are accurate. Favorable placement of each receiver is essential to minimize the effect of interference gain and maximize the received strength of the SOI, so that the estimators in the system perform effectively. This thesis successfully provides a method of providing accurate estimates in multiple systems located in interference-filled environments.

THIS PAGE INTENTIONALLY LEFT BLANK

LIST OF REFERENCES

[1] N. I. Miridakis and D. D. Vergados, "A survey on the successive interference cancellation performance for single-antenna and multiple-antenna OFDM systems," *IEEE Comms. Surveys & Tutorials*, vol.15, no. 1, pp. 312–335, 2013.

[2] J. G. Andrews, "Interference cancellation for cellular systems: A contemporary overview," *IEEE Wireless Comms.*, pp. 19–29, 2005.

[3] C. Ni, "Signal Reception Via Multi-Platform Receivers," M.S. thesis, Naval Postgraduate School, Monterey, CA, 2012.

[4] S. M. Kay, *Fundamentals of Statistical Signal Processing, Volume I: Estimation Theory*, Upper Saddle River, NJ: Prentice Hall PTR, 1993.

[5] S. M. Kay, *Fundamentals of Statistical Signal Processing, Volume II: Detection Theory*, Upper Saddle River, NJ: Prentice Hall PTR, 1998.

THIS PAGE INTENTIONALLY LEFT BLANK

ACKNOWLEDGMENTS

I would like to thank my advisors Ric Romero and Tri Ha for the guidance and direction they have provided over the last several quarters. Your knowledge and mentorship taught me about the proper way to think and learn.

To my wife Julie, your unwavering love and support helped me get this thesis finished. Thank you for always being there to provide me with the motivation I needed when I didn't think I could get it completed.

And to my son, Nathan, thanks for giving me a reason to get this thesis done—so I could get back home for Tummy Time!!

THIS PAGE INTENTIONALLY LEFT BLANK

I. INTRODUCTION

A. OVERVIEW

The increased use of cellular technology has provided an unparalleled advancement of communication in today's world. Cell phone towers and base stations (BS) number in the hundreds in just a small geographic area making signal interference an unavoidable consequence. While several methods are currently used to mitigate the amount of attenuation and multipath interference to provide clearer links, another method exists that allows the removal of interferences from a received signal so that only the desired information remains. This method is accomplished with the use of multiple receivers positioned so that an initial reference signal is collected that is passed on to the next receiver to effectively conduct interference cancellation (IC). Consequently, this method does not allow an immediate demodulation of the clean signal. In a multi-platform scenario, with more receivers involved in the cancellation procedure, more latency and error is expected in the final signal demodulation. Even so, the additional time and processing power necessary to execute this procedure will still benefit those conducting long-term surveillance and collection, where some latency is acceptable or real-time signal processing may not be required.

Successive interference cancellation (SIC) is considered a member of the family of post-IC techniques which are focused on the cancellation or suppression of interference on an *a-posteriori* basis [1]. This means that the low complexity SIC method must first collect a signal in order to then "demodulate and/or decode desired information, and use this information along with channel estimates to cancel received interference from the received signal" [2]. A related SIC scheme known as reference-based successive interference cancellation (RSIC) makes use of a multi-platform system and what is called a reference signal to eliminate interference in received signals.

Previous work concerning RSIC [3] explains how by placing a receiver in a favorable location, a signal is collected and demodulated so that it is mostly interference-free (now known as a reference signal) and then transmitted to the following receiver in

this multi-platform system. This next receiver, which is positioned so that it collects a second signal interfered with a scaled version of the first signal (scaled due to amplitude gain or loss), can now use that clean reference signal and a calculated estimate of the gain to subtract the interference from its overall received signal. Now a cleaned up version of the second signal is available and is also called a reference, but for the second signal. This reference signal, in addition to the one from the first receiver is passed on to a third receiver. The cancellation procedure is repeated and a cleaned up reference for signal three is available to a fourth receiver.

Thus, the procedure applies to multiple receivers. In practice, the subsequent receivers are the ones to calculate the amplitude gain estimates for any interfering signal and to conduct the cancellation to allow the signal of interest (SOI) demodulation. To note, the study in [3] simply utilizes various arbitrary values for the amplitude gains and estimates solely to simulate and observe the performance of the cancellation technique. The purpose of this thesis is therefore to model several communication systems with multiple interference configurations and estimate the gains of the received interfering signals and evaluate the performance of the RSIC technique in terms of symbol error rate (SER) of the SOI using quadrature phase shift keying (QPSK) modulation. In addition, we evaluate the accuracy of the estimates.

B. SCOPE AND ORGANIZATION

In order to successfully estimate these gains, a mathematical signal model is needed to describe the received signals and interferences in the multiple systems. Next, the least squares error (LSE) method of estimation is performed to calculate the amplitude gain parameters of the unwanted signals. These calculations are compared to the actual gain values from the interference and then the reference signals are computed with the help of these estimates and passed on to the next receiver in order to continue the RSIC technique. Utilizing Monte Carlo simulations, we calculate SER against various signal-to-noise ratios (SNR).

In Chapter II, the concept of how the multi-platform system uses the RSIC technique is discussed in detail. The necessary gain parameter estimators are calculated

and the accuracy of the estimates is investigated for a two-receiver system using QPSK modulation. The results of Monte Carlo simulation for a two-receiver system are examined by observing how the estimates change while first holding different SNRs constant followed by next holding the gain parameters constant.

In Chapter III, a third receiver is added to the system and the mathematical formulas needed for the parameter estimation are discussed. The performances of the estimators for a three-receiver QPSK system are reviewed.

In Chapter IV, a fourth receiver is added and the calculations for the four-receiver system are discussed and the system is simulated. The performances of the estimators for a four-receiver QPSK system are then discussed.

In Chapter V, we present our conclusions and provide recommendations for follow on work.

THIS PAGE INTENTIONALLY LEFT BLANK

II. INTERFERENCE CANCELLATION AND PARAMETER ESTIMATION FOR A TWO-RECEIVER SYSTEM

A. REFERENCE-BASED SUCCESSIVE INTERFERENCE CANCELLATION

RSIC, or SIC for short, is a technique that removes unwanted signal interferences from a set of receivers in order to obtain one or multiple SOIs from a set of transmitters. These transmitters can exist in one of several configurations. A good example of a configuration is shown in Figure 1, where the coverage areas of multiple cellular BSs overlap with those from subsequent BSs, resulting in a layout where different regions contain multiple signals. Certain sectors of the coverage areas exist that contain only a specific number of these signals.

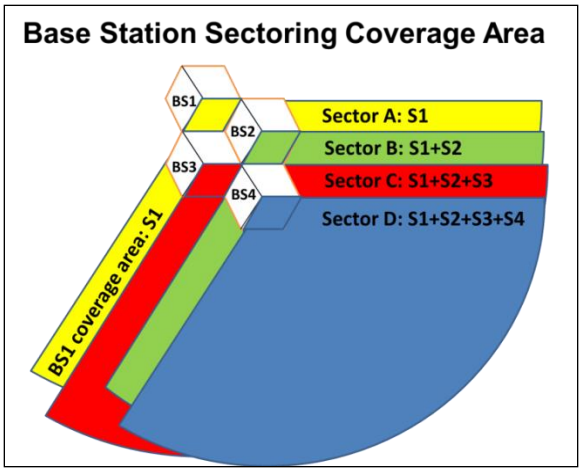

Figure 1. Configuration of multiple BSs with overlapping antenna coverage which has different signal combinations received in each sector. From [3].

Each sector is modeled so that it contains a received signal y_i that is described by:

$$y_1 = s_1 + w_1, \tag{2.1}$$

$$y_2 = s_2 + \alpha_{1,2} s_1 + w_2, \tag{2.2}$$

$$y_3 = s_3 + \alpha_{2,3} s_2 + \alpha_{1,3} s_1 + w_3, \tag{2.3}$$

$$y_4 = s_4 + \alpha_{3,4} s_3 + \alpha_{2,4} s_2 + \alpha_{1,4} s_1 + w_4, \tag{2.4}$$

where $\alpha_{m,n}$ is the amplitude gain (or loss) of the signal from BS *m* received by receiver *n* and is assumed real and positive, and where *w* is the additive white Gaussian noise (AWGN) in the receiver. For purposes of this thesis, the energies of each QPSK signal s_i for $i = 1,2,3,4$ are made identical, the signals are assumed to have perfect phase synchronization with one another and the α values define their amplitude ratio. Receivers in each sector are assumed to only have the knowledge of the signal *y* they collect and the reference signals sent by the other receivers (i.e., receiver two (Rx2) only knows y_2 and s_1; Rx3 only knows y_3, s_2 and s_1; Rx4 only knows y_4, s_3, s_2 and s_1). If for example s_4 is the SOI transmitted by base station four (BS4), then Rx4 placed in Sector D picks up the SOI as well as interference from the three other BSs (i.e., y_4 is the received signal in Sector D). Analytically, each one of these received signals has a signal-to-interference ratio (SIR) that affects the performance of the cancellation technique. (This concept is discussed in detail in Section C of this chapter.) SIC is implemented with Rx1 located in Sector A collecting an interference-free or clean version of s_1 and transmitting it to Rx2 located in Sector B. Next, Rx2 conducts the calculations needed for gain parameter estimation and subtracts or cancels the scaled version of s_1 from the received signal y_2, resulting in an estimate for s_2 (a new reference signal). Rx2 now transmits this new reference signal in addition to the first reference signal over to Rx3. This iteration of cancellation continues until only the clean estimate of s_4 is left.

Clearly for this method to effectively work, the receivers need to have a good estimate of the values of $\alpha_{i,j}$ to properly conduct the IC. This gain parameter estimate is called β, which is eventually used for the estimated signals given by

$$\hat{s}_1 = y_1 - w_1, \tag{2.5}$$

$$\hat{s}_2 = y_2 - \beta_{1,2} s_1 - w_2, \tag{2.6}$$

$$\hat{s}_3 = y_3 - \beta_{2,3} s_2 - \beta_{1,3} s_1 - w_3, \tag{2.7}$$

$$\hat{s}_4 = y_4 - \beta_{3,4} s_3 - \beta_{2,4} s_2 - \beta_{1,4} s_1 - w_4, \tag{2.8}$$

where *w* is the noise in the receiver. For high SNR, the noise is considered negligible and thus the receiver becomes interference-limited. For low SNR, the receiver becomes noise-limited and therefore the noise may even have a greater effect on receiver performance than the interferences themselves. In our simulation results (presented in each chapter), varying cases of noise and interference powers are considered. The previous work on this topic [3] explored the performance of various types of IC, the best of which is demodulated RSIC where the receiver first demodulates, or makes the decision, as to what information is collected. This clean signal is then passed on to the next receiver to continue the SIC process. The decision-making process is discussed in the next section.

B. PARAMETER ESTIMATION FOR A TWO-RECEIVER SYSTEM

1. Least Squares Error (LSE) Method

Starting with the notion of a simple two-receiver system using Equations (2.1) and (2.2), we utilize the LSE approach from [4] to determine an estimate for the α values. In this thesis we assume discrete-time signal models. This is appropriate as receiver signals are almost always sampled prior to signal processing. The equation to determine the estimation of the amplitude gain first seeks to minimize the magnitude of squared difference between the received signal y_2 and the combined data of $s_2 + \alpha_{1,2} s_1$. It is given by

$$J(\alpha_{1,2}) = \sum_{n=0}^{N-1} \left| y_2[n] - (s_2[n] + \alpha_{1,2} s_1[n]) \right|^2 \tag{2.9}$$

where $J(\alpha)$ is clearly the square-error magnitude, $y_2[n]$, $s_1[n]$ and $s_2[n]$ are the discrete-time complex signals collected by Rx2 which is located in Sector B. If we let $\mathbf{y}_2 = [y_2[0] y_2[1] ... y_2[N-1]]^T$ and $\mathbf{s}_i = [s_i[0] s_i[1] ... s_i[N-1]]^T$ for *i* = 1, 2 we get

$$J(\alpha_{1,2}) = \left\| \mathbf{y}_2 - (\mathbf{s}_2 + \alpha_{1,2}\mathbf{s}_1) \right\|^2 = (\mathbf{y}_2 - \mathbf{s}_2 - \alpha_{1,2}\mathbf{s}_1)^H (\mathbf{y}_2 - \mathbf{s}_2 - \alpha_{1,2}\mathbf{s}_1), \tag{2.10}$$

where $(\cdot)^H$ is the Hermitian, or complex conjugate transpose operation. Expanding Equation (2.10) yields

$$J(\alpha_{1,2}) = \mathbf{y}_2{}^H\mathbf{y}_2 - \mathbf{y}_2{}^H\mathbf{s}_2 - \alpha_{1,2}\mathbf{y}_2{}^H\mathbf{s}_1 - \mathbf{s}_2{}^H\mathbf{y}_2 + \mathbf{s}_2{}^H\mathbf{s}_2 + \alpha_{1,2}\mathbf{s}_2{}^H\mathbf{s}_1 - \alpha_{1,2}\mathbf{s}_1{}^H\mathbf{y}_2 + \alpha_{1,2}\mathbf{s}_1{}^H\mathbf{s}_2 + \alpha_{1,2}^2\mathbf{s}_1{}^H\mathbf{s}_1 \tag{2.11}$$

and taking the partial derivative of (2.11) with respect to $a_{1,2}$ yields

$$\frac{\partial J}{\partial \alpha_{1,2}} = -\mathbf{y}_2{}^H\mathbf{s}_1 + \mathbf{s}_2{}^H\mathbf{s}_1 - \mathbf{s}_1{}^H\mathbf{y}_2 + \mathbf{s}_1{}^H\mathbf{s}_2 + 2\alpha_{1,2}\mathbf{s}_1{}^H\mathbf{s}_1. \tag{2.12}$$

Setting the derivative to zero and then solving for the estimate, we get

$$2\alpha_{1,2}\mathbf{s}_1{}^H\mathbf{s}_1 = \mathbf{y}_2{}^H\mathbf{s}_1 + \mathbf{s}_1{}^H\mathbf{y}_2 - \mathbf{s}_1{}^H\mathbf{s}_2 - \mathbf{s}_2{}^H\mathbf{s}_1 \tag{2.13}$$

and thus

$$\alpha_{1,2} = \frac{\mathbf{y}_2{}^H\mathbf{s}_1 + \mathbf{s}_1{}^H\mathbf{y}_2 - \mathbf{s}_1{}^H\mathbf{s}_2 - \mathbf{s}_2{}^H\mathbf{s}_1}{2\mathbf{s}_1{}^H\mathbf{s}_1}. \tag{2.14}$$

Using the definition of a real number, we can reduce Equation (2.14) to

$$\alpha_{1,2} = \frac{2\,\mathrm{Re}\{\mathbf{y}_2{}^H\mathbf{s}_1\} - 2\,\mathrm{Re}\{\mathbf{s}_1{}^H\mathbf{s}_2\}}{2\mathbf{s}_1{}^H\mathbf{s}_1}, \tag{2.15}$$

or simply

$$\alpha_{1,2} = \frac{\mathrm{Re}\{\mathbf{y}_2{}^H\mathbf{s}_1\} - \mathrm{Re}\{\rho_{1,2}\}}{E_{\mathbf{s}_1}}, \tag{2.16}$$

where $\rho_{1,2} = \mathbf{s}_1{}^H\mathbf{s}_2$ and $E_{\mathbf{s}_1} = \mathbf{s}_1{}^H\mathbf{s}_1$.

The first hurdle in this estimation problem is apparent in (2.16). In order to solve for $\alpha_{1,2}$, we need $\mathbf{s}_1$ and $\mathbf{s}_2$ which are currently unknown. The best chance of obtaining the first clean reference signal is with the receiver placed in Sector A. Here, Rx1 only has its own internal noise and chances of a successful demodulation are reasonable given a high SNR. Once received, the signal $\mathbf{y}_1$ is sent through a maximum likelihood detector (MLD) [5] in Rx1, which estimates, or *decides*, which symbols are obtained. This estimate made from (2.5) is designated as $\hat{\mathbf{s}}_1$, that is

$$\hat{\mathbf{s}}_1 = dec(\mathbf{y}_1) = dec(s_1 + w_1), \tag{2.17}$$

where *dec*( ) signifies MLD operation. Next, the decision as to what symbols are received by Rx2 is made based on $\mathbf{y}_2$ alone, such that we have an initial (*pre*) calculation for $\mathbf{s}_2$, or simply $\tilde{\mathbf{s}}_2$ where

$$\tilde{\mathbf{s}}_2 = dec(\mathbf{y}_2). \tag{2.18}$$

This estimate is then used in (2.16) to determine an estimate for $\alpha_{1,2}$, which is given as

$$\beta_{1,2} = \frac{\mathrm{Re}\{\mathbf{y}_2{}^H \hat{\mathbf{s}}_1\} - \mathrm{Re}\{\hat{\mathbf{s}}_1{}^H \tilde{\mathbf{s}}_2\}}{\hat{\mathbf{s}}_1{}^H \hat{\mathbf{s}}_1} \tag{2.19}$$

The value for $\beta_{1,2}$ is now used to compute a final (*post*) calculation for the QPSK symbols of $\mathbf{s}_2$ in (2.6), or

$$\hat{\mathbf{s}}_2 = dec(\mathbf{y}_2 - \beta_{1,2}\hat{\mathbf{s}}_1). \tag{2.20}$$

2. Cramer-Rao Lower Bound (CRLB)

The CRLB is calculated in order obtain a lower bound on the variance of our estimator in (2.19). This is to determine whether or not the estimator is the mean value unbiased estimator, which would indicate that (2.19) has the lowest variance of any other unbiased estimator for all possible values of $\alpha_{1,2}$. Starting with a general approach from [4] of a real signal in white Gaussian noise, we assume that a deterministic signal with its dependence on an unknown parameter θ is observed in AWGN as

$$y[n] = s[n;\theta] + w[n] \qquad n = 0,1,...,N-1. \tag{2.21}$$

The probability density function (PDF) is

$$p(\mathbf{y};\theta) = \frac{1}{(2\pi\sigma^2)^{N/2}} \exp\left\{-\frac{1}{2\sigma^2}\sum_{n=0}^{N-1}(y[n] - s[n;\theta])^2\right\}. \tag{2.22}$$

Taking the expected value of the second derivative of the log-likelihood function, we get

$$E\left(\frac{\partial^2 \ln p(\mathbf{y};\theta)}{\partial\theta^2}\right) = -\frac{1}{\sigma^2}\sum_{n=0}^{N-1}\left(\frac{\partial s[n;\theta]}{\partial\theta}\right)^2 \tag{2.23}$$

so that the CRLB on the variance of the estimator $\hat{\theta}$ of θ is expressed as

$$\text{var}(\hat{\theta}) \geq \frac{1}{-E\left(\frac{\partial^2 \ln p(\mathbf{y};\theta)}{\partial\theta^2}\right)} = \frac{\sigma^2}{\sum_{n=0}^{N-1}\left(\frac{\partial s[n;\theta]}{\partial\theta}\right)^2}. \tag{2.24}$$

For use in this thesis, if the complex terms from (2.2) are used and we allow $s[n;\theta] \triangleq \alpha_{1,2}s_1[n]$, then the PDF for complex valued signals is

$$p(\mathbf{y}_2;\alpha_{1,2}) = \frac{1}{\pi^N \left|C_{\mathbf{y}_2}\right|}\exp\left\{-(\mathbf{y}_2 - \mathbf{s}_2 - \alpha_{1,2}\mathbf{s}_1)^H C_{\mathbf{y}_2}^{-1}(\mathbf{y}_2 - \mathbf{s}_2 - \alpha_{1,2}\mathbf{s}_1)\right\}. \tag{2.25}$$

If we assume that $C_{\mathbf{y}_2} = \sigma^2 I$ and $C_{\mathbf{y}_2}^{-1} = \frac{1}{\sigma^2} I$, the log-likelihood yields

$$\begin{aligned}\ln p(\mathbf{y}_2;\alpha_{1,2}) &= \ln\left(\frac{1}{\pi^N\sigma^{2N}}\right) + \ln\cdot\exp\left\{-\frac{1}{\sigma^2}(\mathbf{y}_2 - \mathbf{s}_2 - \alpha_{1,2}\mathbf{s}_1)^H(\mathbf{y}_2 - \mathbf{s}_2 - \alpha_{1,2}\mathbf{s}_1)\right\} \\ &= \ln\left(\frac{1}{\pi^N\sigma^{2N}}\right) - \frac{1}{\sigma^2}(\mathbf{y}_2{}^H\mathbf{y}_2 - \mathbf{y}_2{}^H\mathbf{s}_2 - \alpha_{1,2}\mathbf{y}_2{}^H\mathbf{s}_1 - \mathbf{s}_2{}^H\mathbf{y}_2 + \mathbf{s}_2{}^H\mathbf{s}_2 \\ &\quad + \alpha_{1,2}\mathbf{s}_2{}^H\mathbf{s}_1 - \alpha_{1,2}\mathbf{s}_1{}^H\mathbf{y}_2 + \alpha_{1,2}\mathbf{s}_1{}^H\mathbf{s}_2 + \alpha_{1,2}^2\mathbf{s}_1{}^H\mathbf{s}_1).\end{aligned} \tag{2.26}$$

We assume that $\mathbf{s}_1$ and $\mathbf{s}_2$ are known at this point. In practice, these are merely estimates themselves and contribute to the overall variance of the estimate. Taking the first derivative with respect to $\alpha_{1,2}$ gives

$$\frac{\partial \ln p(\mathbf{y}_2;\alpha_{1,2})}{\partial\alpha_{1,2}} = -\frac{1}{\sigma^2}\left(-\mathbf{y}_2{}^H\mathbf{s}_1 + \mathbf{s}_2{}^H\mathbf{s}_1 - \mathbf{s}_1{}^H\mathbf{y}_2 + \mathbf{s}_1{}^H\mathbf{s}_2 + 2\alpha_{1,2}\mathbf{s}_1{}^H\mathbf{s}_1\right), \tag{2.27}$$

and a second differentiation results in

$$\frac{\partial^2 \ln p(\mathbf{y}_2;\alpha_{1,2})}{\partial\alpha_{1,2}^2} = -\frac{2}{\sigma^2}\left(\mathbf{s}_1{}^H\mathbf{s}_1\right). \tag{2.28}$$

The expected value of this provides

$$E\left(\frac{\partial^2 \ln p(\mathbf{y}_2;\alpha_{1,2})}{\partial \alpha_{1,2}^2}\right) = -\frac{2\cdot\|\mathbf{s}_1\|^2}{\sigma^2}, \tag{2.29}$$

which yields a CRLB of

$$\text{var}(\hat{\alpha}_{1,2}) \geq \frac{1}{-E\left(\frac{\partial^2 \ln p(\mathbf{y}_2;\alpha_{1,2})}{\partial \alpha_{1,2}^2}\right)} = \frac{\sigma^2}{2\cdot\|\mathbf{s}_1\|^2}, \tag{2.30}$$

where σ^2 is the variance caused by the random AWGN and $\hat{\alpha}_{1,2} = \beta_{1,2}$. Therefore, Equation (2.30) shows the variance of $\beta_{1,2}$ is in terms of the energy of the first signal and is effectively the theoretical value as if there is no $\mathbf{s}_2$ present.

C. RESULTS FOR A TWO RECEIVER SYSTEM

1. Fix S_2NR, Vary $\alpha_{1,2}$

As $\mathbf{y}_2$ is made up of signal $\mathbf{s}_2$ and the interference of the scaled form of $\mathbf{s}_1$, the SIR is therefore defined as

$$SIR \triangleq \frac{E_{\mathbf{s}_2}}{E_{\mathbf{s}_1}} = \frac{\|\mathbf{s}_2\|^2}{\|\alpha_{1,2}\mathbf{s}_1\|^2}. \tag{2.31}$$

With the energy of each signal normalized to have the same value, the equation that defines the relationship between $\mathbf{s}_2$ and the interference from $\mathbf{s}_1$ simplifies to

$$S_2IR = \frac{1}{\alpha_{1,2}^2}. \tag{2.32}$$

Furthermore, the SNR of each signal is varied by simply changing the energy of the noise power P_n in the received signals. In our Monte Carlo simulation, we generate two random QPSK symbol streams combined with accompanying noise and interference to create (2.1) and (2.2). The values of $\alpha_{1,2}$ that are examined range from 0.01 to 1.0 at

steps of 0.01 while setting the SNR for $\mathbf{s}_2$, or S_2NR, at multiple levels to observe the effect on the accuracy of the gain estimate $\beta_{1,2}$. With their inverse relationship, as $\alpha_{1,2}$ is increased, the value of S_2IR decreases. Initially, P_n is set very low in order to first model a system where there is a very high S_2NR, which is then followed by modifying P_n to have values closer to unity (i.e., equal to normalized signal energy) to model low S_2NR. From Figure 2, we see that the dashed blue line represents the actual $\alpha_{1,2}$ amplitude gain parameter used in the simulation. At high S_2NR levels, the calculated estimate values lie closely along the theoretical line until $\alpha_{1,2}$ approaches 1.0. If the noise is increased and the S_2NRs are changed to low levels, the performance of the estimator begins to decline. Even at minimal values of $\alpha_{1,2}$, the estimates deviate from the line representing no interference and the deviation becomes significant when P_n = 0.8. Interestingly, as these estimates get worse, they begin to converge towards the value of 0.5. This is most likely due to the fact that the estimator from (2.19) is more accurate for systems where $E_{\mathbf{s}_2}$ is much greater than $E_{\mathbf{s}_1}$, and therefore does not yield good estimates for high $\alpha_{1,2}$ levels.

Another way to see how effective the estimates are for $\beta_{1,2}$ is to plot them against the actual $\alpha_{1,2}$ parameter values as displayed in Figure 3. Again, the dashed blue line represents actual amplitude gain parameter values and the subsequent curves show the estimates at various S_2NRs. At low P_n levels, the estimates are fairly accurate until $\alpha_{1,2}$ reaches a value of about 0.7. At higher $\alpha_{1,2}$ values, the simulation results show estimates that again diverge from the theoretical line and approach a value of 0.5. Thus, we can appreciate the effect of increasing noise and interference on the accuracy of the amplitude gain estimations.

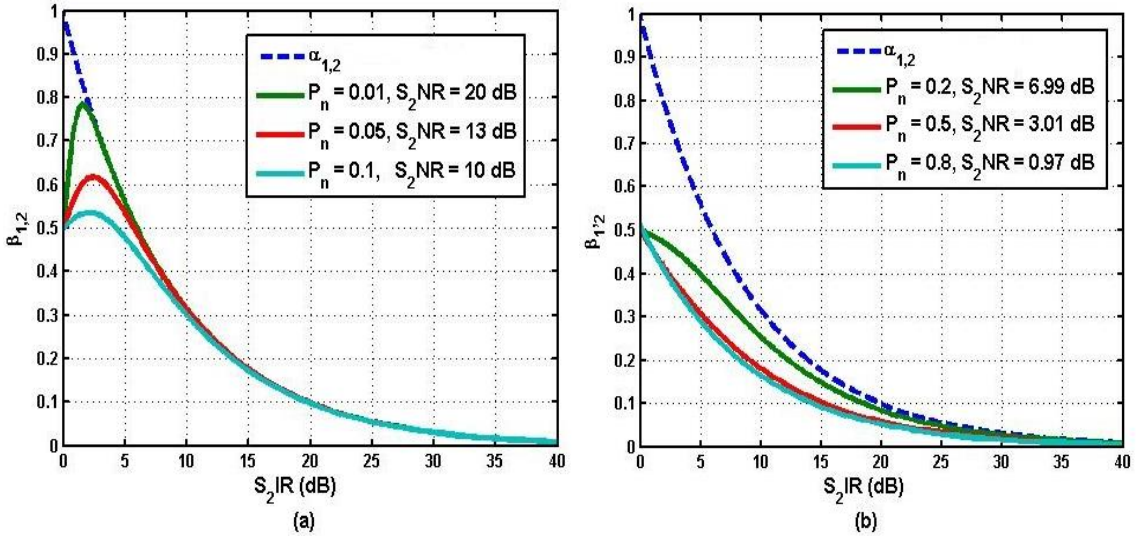

Figure 2. Curves of $\beta_{1,2}$ versus (vs.) S_2IR at various noise levels: (a) Performance curves with high S_2NR; (b) Performance curves with low S_2NR.

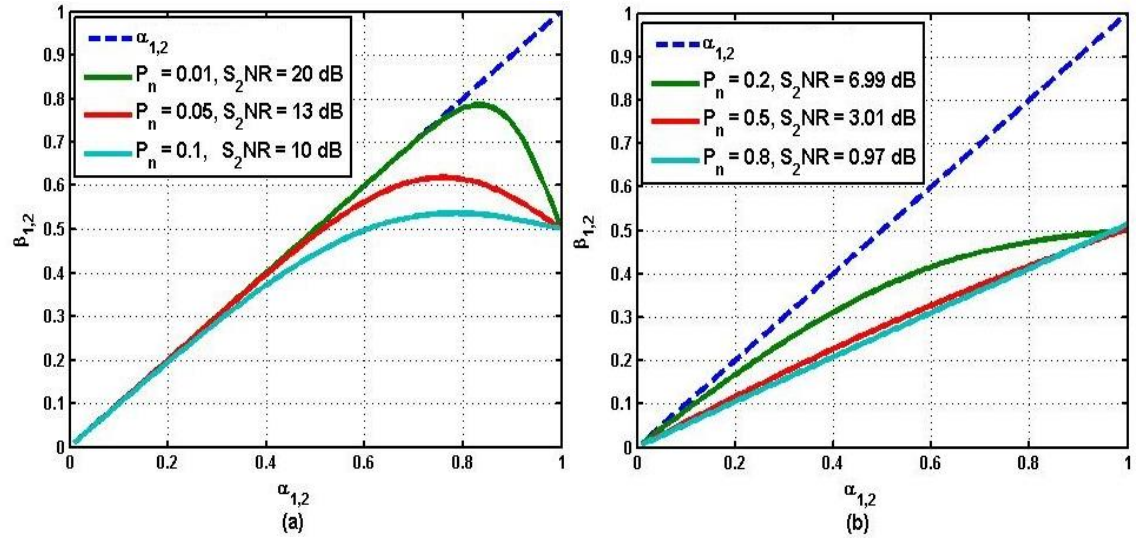

Figure 3. Curves of $\beta_{1,2}$ vs. $\alpha_{1,2}$ at various noise levels: (a) Performance curves with high S_2NR; (b) Performance curves with low S_2NR.

2. Fix $\boldsymbol{\alpha}_{1,2}$, Vary S_2NR

A second approach to observing the performance of the estimators is to hold the interference gain values constant, and while the SNR of $\mathbf{s}_2$ is increased, examine the performance of the SIC technique. The simulation is conducted at different $\alpha_{1,2}$ values while decreasing the amount of noise in the receivers and thus we are able to calculate the SER for the increasing S_2NR. It is important to remember that on the figures, the *pre* calculations are the estimates made from making a decision based solely on $\mathbf{y}_2$, or (2.18), whereas the *post* calculations from (2.20) provide better signal estimates. From Figure 4, it is seen that at low $\alpha_{1,2}$, both the SER for the *pre* and *post* calculations of the $\mathbf{s}_2$ symbols closely follow the theoretical values obtained for QPSK. Also, due to the relationship from (2.32), a better performance is therefore expected for higher S_2IR levels. When the amount of interference is increased (i.e., increased amplitude gain on the energy of $\mathbf{s}_1$), the performance decreases (i.e., SER starts to suffer). Clearly the incorporation of $\beta_{1,2}$ in the IC makes an impact to the quality of the cleaned up signal, as *pre* calculations are severely affected by increased interference while *post* calculations show only a slight to moderate deviation from the theoretical line.

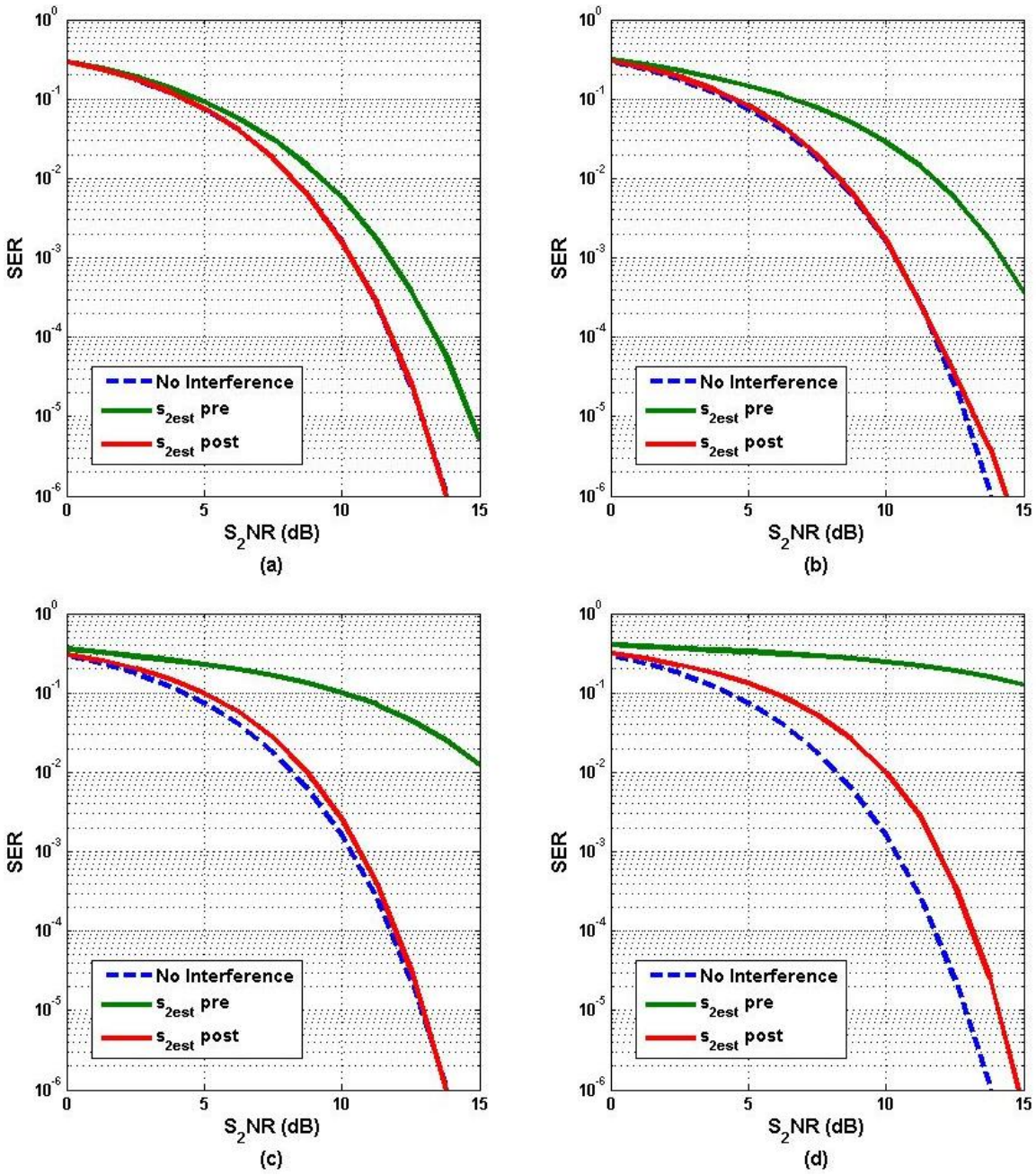

Figure 4. Performance curves of SER vs. S_2NR for *pre*/*post* decisions of $\mathbf{s}_2$ at different interference combinations: (a) $\alpha_{1,2}$ = 0.2, S_2IR = 14 dB; (b) $\alpha_{1,2}$ = 0.4, S_2IR = 7.96 dB; (c) $\alpha_{1,2}$ = 0.6, S_2IR = 4.4 dB; (d) $\alpha_{1,2}$ = 0.8, S_2IR = 1.94 dB.

Using the same approach of setting different $\alpha_{1,2}$ values and varying SNR, we see the accuracy of the $\beta_{1,2}$ estimates shown in Figure 5. By plotting a line of the actual gain

value $\alpha_{1,2}$ and then showing how the estimates approach that line, a clear understanding is made of how greater S_2NR plays a role in parameter estimation. Estimates obviously improve with reduction of noise in the system. However, with higher interference levels such as when $\alpha_{1,2}$ = 0.8, increased S_2NR does not provide the same level of accuracy previously seen for the gain estimate at lower $\alpha_{1,2}$ values.

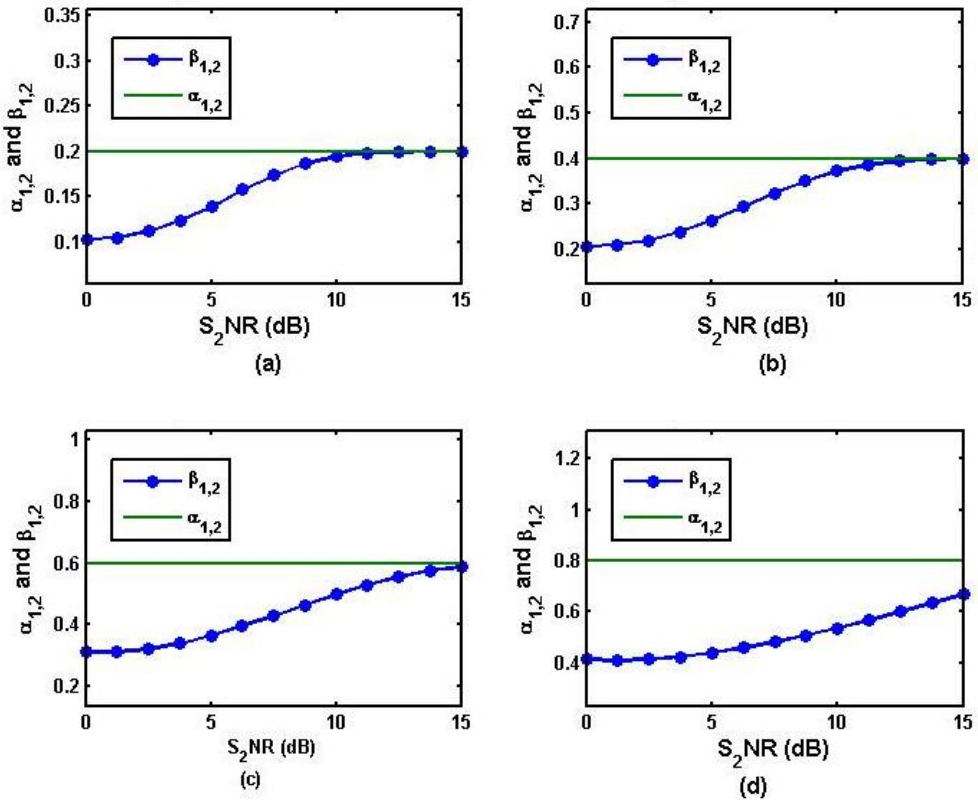

Figure 5. Plots of the actual gain parameter $\alpha_{1,2}$ and the estimator $\beta_{1,2}$ vs. S_2NR values for multiple simulations of $\mathbf{y}_2$: (a) $a_{1,2}$ = 0.2, S_2IR = 14 dB; (b) $a_{1,2}$ = 0.4, S_2IR = 7.9 dB; (c) $a_{1,2}$ = 0.6, S_2IR = 4.4 dB; (d) $a_{1,2}$ = 0.8, S_2IR = 1.9 dB.

If we refer back to the CRLB, it is possible to plot the variance of the $\beta_{1,2}$ estimates calculated from (2.30) against the theoretical variance as if the system is without interference. From Figure 6, it is seen that while $\alpha_{1,2}$ remains low, it is possible to

attain a very low variance, which corresponds to a more accurate estimate $\beta_{1,2}$. However, once $\alpha_{1,2}$ starts to approach 1.0, even very high levels of S_1NR result in poor variance of the estimate.

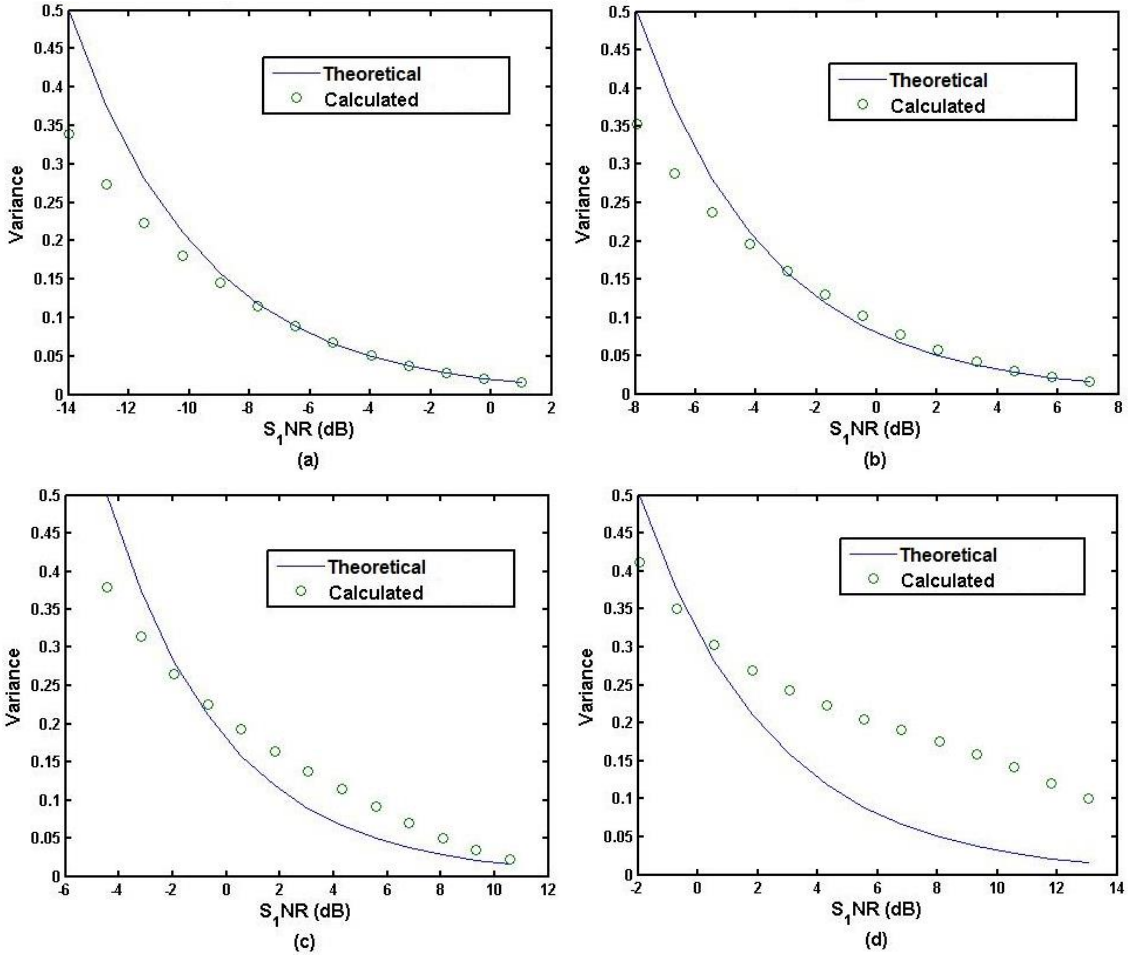

Figure 6. Plots of the variance of the estimator $\beta_{1,2}$ vs. S_1NR values: (a) $a_{1,2}$ = 0.2, S_2IR = 14 dB; (b) $a_{1,2}$ = 0.4, S_2IR = 7.9 dB; (c) $a_{1,2}$ = 0.6, S_2IR = 4.4 dB; (d) $a_{1,2}$ = 0.8, S_2IR = 1.9 dB.

With the basic understanding of how RSIC is applied and performs for two receivers, we next observe the IC technique for the simulation of a three-receiver system.

THIS PAGE INTENTIONALLY LEFT BLANK

III. ADDITION OF A THIRD RECEIVER

Continuing with the idea of successive receivers within a multi-platform system, we assume that a third signal is obtained by Rx3 located in Sector C and contains information from BS1, BS2 and BS3, as seen in Figure 1. Clearly the procedure involved for this estimation is more involved as the received signal $\mathbf{y}_3$ contains two interfering signals.

A. PARAMETER ESTIMATION FOR A THREE-RECEIVER SYSTEM

Following the same method from Chapter II, we see that a third receiver would make use of (2.3) and the LSE approach gives

$$J(\alpha)=\sum_{n=0}^{N-1}\left|y_3[n]-(s_3[n]+\alpha_{2,3}s_2[n]+\alpha_{1,3}s_1[n])\right|^2. \tag{3.1}$$

Taking the vector form of (3.1) and expanding, we get

$$\begin{aligned} J(\alpha)&=\left\|\mathbf{y}_3-(\mathbf{s}_3+\alpha_{2,3}\mathbf{s}_2+\alpha_{1,3}\mathbf{s}_1)\right\|^2 \\ &=(\mathbf{y}_3-\mathbf{s}_3-\alpha_{2,3}\mathbf{s}_2-\alpha_{1,3}\mathbf{s}_1)^H(\mathbf{y}_3-\mathbf{s}_3-\alpha_{2,3}\mathbf{s}_2-\alpha_{1,3}\mathbf{s}_1) \end{aligned} \tag{3.2}$$

and

$$\begin{aligned} J(\alpha)=&\mathbf{y}_3{}^H\mathbf{y}_3-\mathbf{y}_3{}^H\mathbf{s}_3-\alpha_{2,3}\mathbf{y}_3{}^H\mathbf{s}_2-\alpha_{1,3}\mathbf{y}_3{}^H\mathbf{s}_1-\mathbf{s}_3{}^H\mathbf{y}_3+\mathbf{s}_3{}^H\mathbf{s}_3+\alpha_{2,3}\mathbf{s}_3{}^H\mathbf{s}_2 \\ &+\alpha_{1,3}\mathbf{s}_3{}^H\mathbf{s}_1-\alpha_{2,3}\mathbf{s}_2{}^H\mathbf{y}_3+\alpha_{2,3}\mathbf{s}_2{}^H\mathbf{s}_3+\alpha_{2,3}^2\mathbf{s}_2{}^H\mathbf{s}_2+\alpha_{1,3}\alpha_{2,3}\mathbf{s}_2{}^H\mathbf{s}_1 \\ &-\alpha_{1,3}\mathbf{s}_1{}^H\mathbf{y}_3+\alpha_{1,3}\mathbf{s}_1{}^H\mathbf{s}_3+\alpha_{1,3}\alpha_{2,3}\mathbf{s}_1{}^H\mathbf{s}_2+\alpha_{1,3}^2\mathbf{s}_1{}^H\mathbf{s}_1. \end{aligned} \tag{3.3}$$

The important difference from the two-receiver system is the need to now estimate for two gain parameters. Taking the partial derivatives with respect to the individual gains, we get

$$\begin{aligned} \frac{\partial J}{\partial\alpha_{2,3}}&=-\mathbf{y}_3{}^H\mathbf{s}_2+\mathbf{s}_3{}^H\mathbf{s}_2-\mathbf{s}_2{}^H\mathbf{y}_3+\mathbf{s}_2{}^H\mathbf{s}_3+2\alpha_{2,3}\mathbf{s}_2{}^H\mathbf{s}_2+\alpha_{1,3}\mathbf{s}_2{}^H\mathbf{s}_1+\alpha_{1,3}\mathbf{s}_1{}^H\mathbf{s}_2, \\ \frac{\partial J}{\partial\alpha_{1,3}}&=-\mathbf{y}_3{}^H\mathbf{s}_1+\mathbf{s}_3{}^H\mathbf{s}_1+\alpha_{2,3}\mathbf{s}_2{}^H\mathbf{s}_1-\mathbf{s}_1{}^H\mathbf{y}_3+\mathbf{s}_1{}^H\mathbf{s}_3+\alpha_{2,3}\mathbf{s}_1{}^H\mathbf{s}_2+2\alpha_{1,3}\mathbf{s}_1{}^H\mathbf{s}_1. \end{aligned} \tag{3.4}$$

Setting to zero and solving for each one of the estimates we get

$$\alpha_{2,3} = \frac{\mathbf{y}_3{}^H\mathbf{s}_2 + \mathbf{s}_2{}^H\mathbf{y}_3 - \mathbf{s}_3{}^H\mathbf{s}_2 - \mathbf{s}_2{}^H\mathbf{s}_3 - \alpha_{1,3}(\mathbf{s}_2{}^H\mathbf{s}_1 + \mathbf{s}_1{}^H\mathbf{s}_2)}{2\mathbf{s}_2{}^H\mathbf{s}_2},$$

$$\alpha_{1,3} = \frac{\mathbf{y}_3{}^H\mathbf{s}_1 + \mathbf{s}_1{}^H\mathbf{y}_3 - \mathbf{s}_3{}^H\mathbf{s}_1 - \mathbf{s}_1{}^H\mathbf{s}_3 - \alpha_{2,3}(\mathbf{s}_2{}^H\mathbf{s}_1 + \mathbf{s}_1{}^H\mathbf{s}_2)}{2\mathbf{s}_1{}^H\mathbf{s}_1}. \quad (3.5)$$

We can utilize the definition of a real number to simplify the equations and get

$$\alpha_{2,3} = \frac{2\,\mathrm{Re}\{\mathbf{y}_3{}^H\mathbf{s}_2\} - 2\,\mathrm{Re}\{\mathbf{s}_3{}^H\mathbf{s}_2\} - \left[\frac{2\,\mathrm{Re}\{\mathbf{y}_3{}^H\mathbf{s}_1\} - 2\,\mathrm{Re}\{\mathbf{s}_3{}^H\mathbf{s}_1\} - \alpha_{2,3}(2\,\mathrm{Re}\{\mathbf{s}_2{}^H\mathbf{s}_1\})}{2\mathbf{s}_1{}^H\mathbf{s}_1}\right](2\,\mathrm{Re}\{\mathbf{s}_2{}^H\mathbf{s}_1\})}{2\mathbf{s}_2{}^H\mathbf{s}_2},$$

$$= \frac{2\,\mathrm{Re}\{\mathbf{y}_3{}^H\mathbf{s}_2\} - 2\,\mathrm{Re}\{\rho_{3,2}\} - \left[\frac{2\,\mathrm{Re}\{\rho_{2,1}\}\,\mathrm{Re}\{\mathbf{y}_3{}^H\mathbf{s}_1\} - 2\,\mathrm{Re}\{\rho_{2,1}\}\,\mathrm{Re}\{\rho_{3,1}\} - \alpha_{2,3}(2\,\mathrm{Re}\{\rho_{2,1}\}^2)}{E_{\mathbf{s}_1}}\right]}{2E_{\mathbf{s}_2}}, \quad (3.6)$$

$$= \frac{E_{\mathbf{s}_1}\,\mathrm{Re}\{\mathbf{y}_3{}^H\mathbf{s}_2\} - E_{\mathbf{s}_1}\,\mathrm{Re}\{\rho_{3,2}\} - \mathrm{Re}\{\rho_{2,1}\}\,\mathrm{Re}\{\mathbf{y}_3{}^H\mathbf{s}_1\} + \mathrm{Re}\{\rho_{2,1}\}\,\mathrm{Re}\{\rho_{3,1}\} + \alpha_{2,3}\,\mathrm{Re}\{\rho_{2,1}\}^2}{E_{\mathbf{s}_1}E_{\mathbf{s}_2}},$$

$$\alpha_{2,3}(E_{\mathbf{s}_1}E_{\mathbf{s}_2}) - \alpha_{2,3}\,\mathrm{Re}\{\rho_{2,1}\}^2 = \left(E_{\mathbf{s}_1}\right)\left(\mathrm{Re}\{\mathbf{y}_3{}^H\mathbf{s}_2\} - \mathrm{Re}\{\rho_{3,2}\}\right) - \left(\mathrm{Re}\{\rho_{2,1}\}\right)\left(\mathrm{Re}\{\mathbf{y}_3{}^H\mathbf{s}_1\} - \mathrm{Re}\{\rho_{3,1}\}\right).$$

The same approach is taken for the estimator of $\alpha_{1,3}$ and the following sequence of equations is obtained:

$$\alpha_{1,3} = \frac{2\,\mathrm{Re}\{\mathbf{y}_3{}^H\mathbf{s}_1\} - 2\,\mathrm{Re}\{\mathbf{s}_3{}^H\mathbf{s}_1\} - \left[\dfrac{2\,\mathrm{Re}\{\mathbf{y}_3{}^H\mathbf{s}_2\} - 2\,\mathrm{Re}\{\mathbf{s}_3{}^H\mathbf{s}_2\} - \alpha_{1,3}(2\,\mathrm{Re}\{\mathbf{s}_2{}^H\mathbf{s}_1\})}{2\mathbf{s}_2{}^H\mathbf{s}_2}\right](2\,\mathrm{Re}\{\mathbf{s}_2{}^H\mathbf{s}_1\})}{2\mathbf{s}_1{}^H\mathbf{s}_1},$$

$$= \frac{2\,\mathrm{Re}\{\mathbf{y}_3{}^H\mathbf{s}_1\} - 2\,\mathrm{Re}\{\rho_{3,1}\} - \left[\dfrac{2\,\mathrm{Re}\{\rho_{2,1}\}\,\mathrm{Re}\{\mathbf{y}_3{}^H\mathbf{s}_2\} - 2\,\mathrm{Re}\{\rho_{2,1}\}\,\mathrm{Re}\{\rho_{3,2}\} - \alpha_{1,3}(2\,\mathrm{Re}\{\rho_{2,1}\}^2)}{E_{\mathbf{s}_2}}\right]}{2E_{\mathbf{s}_1}}, \tag{3.7}$$

$$= \frac{E_{\mathbf{s}_2}\,\mathrm{Re}\{\mathbf{y}_3{}^H\mathbf{s}_1\} - E_{\mathbf{s}_2}\,\mathrm{Re}\{\rho_{3,1}\} - \mathrm{Re}\{\rho_{2,1}\}\,\mathrm{Re}\{\mathbf{y}_3{}^H\mathbf{s}_2\} + \mathrm{Re}\{\rho_{2,1}\}\,\mathrm{Re}\{\rho_{3,2}\} + \alpha_{1,3}\,\mathrm{Re}\{\rho_{2,1}\}^2}{E_{\mathbf{s}_1}E_{\mathbf{s}_2}},$$

$$\alpha_{1,3}(E_{\mathbf{s}_1}E_{\mathbf{s}_2}) - \alpha_{1,3}\,\mathrm{Re}\{\rho_{2,1}\}^2 = \left(E_{\mathbf{s}_2}\right)\left(\mathrm{Re}\{\mathbf{y}_3{}^H\mathbf{s}_1\} - \mathrm{Re}\{\rho_{3,1}\}\right) - \left(\mathrm{Re}\{\rho_{2,1}\}\right)\left(\mathrm{Re}\{\mathbf{y}_3{}^H\mathbf{s}_2\} - \mathrm{Re}\{\rho_{3,2}\}\right).$$

Now solving for the α values in (3.6) and (3.7), we arrive at the final estimators for the amplitude gains of a three-receiver system which are given by

$$\alpha_{2,3} = \frac{E_{\mathbf{s}_1}\left(\mathrm{Re}\{\mathbf{y}_3{}^H\mathbf{s}_2\} - \mathrm{Re}\{\rho_{3,2}\}\right) - \left(\mathrm{Re}\{\rho_{2,1}\}\right)\left(\mathrm{Re}\{\mathbf{y}_3{}^H\mathbf{s}_1\} - \mathrm{Re}\{\rho_{3,1}\}\right)}{E_{\mathbf{s}_1}E_{\mathbf{s}_2} - \mathrm{Re}\{\rho_{2,1}\}^2},$$

$$\alpha_{1,3} = \frac{E_{\mathbf{s}_2}\left(\mathrm{Re}\{\mathbf{y}_3{}^H\mathbf{s}_1\} - \mathrm{Re}\{\rho_{3,1}\}\right) - \left(\mathrm{Re}\{\rho_{2,1}\}\right)\left(\mathrm{Re}\{\mathbf{y}_3{}^H\mathbf{s}_2\} - \mathrm{Re}\{\rho_{3,2}\}\right)}{(E_{\mathbf{s}_1}E_{\mathbf{s}_2} - \mathrm{Re}\{\rho_{2,1}\}^2)}. \tag{3.8}$$

There is however the same problem that is experienced in Equation (2.16) where the calculations in (3.8) require the signal $\mathbf{s}_3$. Therefore the system must first make a decision as to what symbols are transmitted based only on the received signal. In this scenario, Rx3 makes the *pre* decision on the received signal, which is given by

$$\tilde{\mathbf{s}}_3 = dec(\mathbf{y}_3). \tag{3.9}$$

Substituting (3.9) into (3.8) yields

$$\beta_{2,3} = \frac{E_{\mathbf{s}_1}\left(\mathrm{Re}\{\mathbf{y}_3{}^H\hat{\mathbf{s}}_2\} - \mathrm{Re}\{\tilde{\rho}_{3,2}\}\right) - \left(\mathrm{Re}\{\hat{\rho}_{2,1}\}\right)\left(\mathrm{Re}\{\mathbf{y}_3{}^H\hat{\mathbf{s}}_1\} - \mathrm{Re}\{\tilde{\rho}_{3,1}\}\right)}{(E_{\mathbf{s}_1}E_{\mathbf{s}_2} - \mathrm{Re}\{\hat{\rho}_{2,1}\}^2)}$$

$$\beta_{1,3} = \frac{E_{\mathbf{s}_2}\left(\mathrm{Re}\{\mathbf{y}_3{}^H\hat{\mathbf{s}}_1\} - \mathrm{Re}\{\tilde{\rho}_{3,1}\}\right) - \left(\mathrm{Re}\{\hat{\rho}_{2,1}\}\right)\left(\mathrm{Re}\{\mathbf{y}_3{}^H\hat{\mathbf{s}}_2\} - \mathrm{Re}\{\tilde{\rho}_{3,2}\}\right)}{(E_{\mathbf{s}_1}E_{\mathbf{s}_2} - \mathrm{Re}\{\hat{\rho}_{2,1}\}^2)}, \tag{3.10}$$

where $\tilde{\rho}_{3,2} = \tilde{\mathbf{s}}_3{}^H \hat{\mathbf{s}}_2$, $\tilde{\rho}_{3,1} = \tilde{\mathbf{s}}_3{}^H \hat{\mathbf{s}}_1$ and $\hat{\rho}_{2,1} = \hat{\mathbf{s}}_2{}^H \hat{\mathbf{s}}_1$. Utilizing the calculated gain estimates, we make a new *post* calculation based on (2.7) yielding

$$\hat{\mathbf{s}}_3 = dec(\mathbf{y}_3 - \beta_{2,3}\hat{\mathbf{s}}_2 - \beta_{1,3}\hat{\mathbf{s}}_1). \tag{3.11}$$

1. CRLB Calculation

If we tailor the complex PDF from (2.25) for a three-receiver system, we get

$$p(\mathbf{y}_3;\alpha) = \frac{1}{\pi^N \left|C_{\mathbf{y}_2}\right|} \exp\left\{-(\mathbf{y}_3 - \mathbf{s}_3 - \alpha_{2,3}\mathbf{s}_2 - \alpha_{1,3}\mathbf{s}_1)^H C_{\mathbf{y}_2}^{-1}(\mathbf{y}_3 - \mathbf{s}_3 - \alpha_{2,3}\mathbf{s}_2 - \alpha_{1,3}\mathbf{s}_1)\right\}. \tag{3.12}$$

The second derivative of the log-likelihood for each gain parameter yields

$$\begin{aligned} \frac{\partial^2 \ln p(\mathbf{y}_3;\alpha_{2,3})}{\partial \alpha_{2,3}^2} &= -\frac{2}{\sigma^2}\left(\mathbf{s}_2{}^H \mathbf{s}_2\right), \\ \frac{\partial^2 \ln p(\mathbf{y}_3;\alpha_{1,3})}{\partial \alpha_{1,3}^2} &= -\frac{2}{\sigma^2}\left(\mathbf{s}_1{}^H \mathbf{s}_1\right), \end{aligned} \tag{3.13}$$

from which the CRLB for each parameter is

$$\begin{aligned} \mathrm{var}(\hat{\alpha}_{2,3}) &\geq \frac{1}{-E\left(\dfrac{\partial^2 \ln p(\mathbf{y}_2;\alpha_{2,3})}{\partial \alpha_{2,3}^2}\right)} = \frac{\sigma^2}{2\cdot\left\|\mathbf{s}_2\right\|^2}, \\ \mathrm{var}(\hat{\alpha}_{1,3}) &\geq \frac{1}{-E\left(\dfrac{\partial^2 \ln p(\mathbf{y}_2;\alpha_{1,3})}{\partial \alpha_{1,3}^2}\right)} = \frac{\sigma^2}{2\cdot\left\|\mathbf{s}_1\right\|^2}, \end{aligned} \tag{3.14}$$

where $\hat{\alpha}_{2,3} = \beta_{2,3}$ and $\hat{\alpha}_{1,3} = \beta_{1,3}$.

As can be seen from (3.14), the theoretical variance of an estimate solely depends on the noise of the system and energy of the signal corresponding to the amplitude gain. The actual variance calculated in the simulation will depend on the overall interference experienced at the receiver.

B. RESULTS FOR A THREE-RECEIVER SYSTEM

In order to best illustrate the effect of different amplitude gains of the interfering signals, the simulations are performed with the assumption that Rx3 has access to the good, clean reference signals $\hat{\mathbf{s}}_1$ and $\hat{\mathbf{s}}_2$. Therefore, in the simulations y_1 and y_2 from Equations (2.1) and (2.2) are assumed to have high SNRs and SIRs for their respective signals. For Equation (2.2), this means assuming that $\mathbf{s}_1$ includes only a small interference gain so that when a *decision* is made on $\mathbf{y}_2$, the reference signal passed to Rx3 is mostly error-free. To illustrate the result of the SIC technique on a three-receiver system, first the SNR levels are fixed and the α values are varied. This is followed by the reverse, through fixing the α values and varying the SNR of the signals and observing the performance of the estimators. With estimation needed for two gain parameters, the simulation is set up so that while the SNR of the system is fixed, we iterate through several different interference combinations by holding one gain at a certain level and running calculations through a range of the other gain values.

1. Fix S_3NR, Vary $\alpha_{2,3}$ and $\alpha_{1,3}$

With two signals now interfering with $\mathbf{s}_3$, the performance of the estimators depends on the signal-to-total-interference ratio of the system. As is seen with (2.31), this new relation is defined as

$$S_3IR \triangleq \frac{E_{\mathbf{s}_3}}{E_{\mathbf{s}_2} + E_{\mathbf{s}_1}} = \frac{\|\mathbf{s}_3\|^2}{\|\alpha_{2,3}\mathbf{s}_2\|^2 + \|\alpha_{1,3}\mathbf{s}_1\|^2}, \tag{3.15}$$

where $\mathbf{s}_2$ and $\mathbf{s}_1$ are considered uncorrelated based on being random QPSK signals generated by two different transmitters.

Since the energies of $\mathbf{s}_1$, $\mathbf{s}_2$ and $\mathbf{s}_3$ are the same, the resulting equation yields

$$S_3IR = \frac{1}{\alpha_{2,3}^2 + \alpha_{1,3}^2}. \tag{3.16}$$

Unless otherwise denoted as an individual signal interference (i.e., S_3I_2R and S_3I_1R), Equation (3.16) is used to describe the total signal-to-interference ratio. Consequently, as S_3IR describes the overall interference in the system, in many cases there is no need to hold $\alpha_{1,3}$ constant and then vary $\alpha_{2,3}$ since the resulting S_3IR is the same and would generate similar performance with regard to SER and estimation. For example, if $\alpha_{2,3}$ = 0.5 and $\alpha_{1,3}$ = 0.2, the overall S_3IR is $1/(0.5^2+0.2^2) = 5.4\ dB$. The performances of the estimators in the system are the same if $\alpha_{2,3}$ = 0.2 and $\alpha_{1,3}$ = 0.5. Further examination of this relationship is seen in the Appendix.

The first way to gauge the effect of the estimation accuracy is with various noise levels in the simulations held constant and having the gain parameters (and therefore S_3IR) change values. Viewing the results in this fashion, we observe how close the calculations of (3.10) are compared to the theoretical values. From Figure 7, it is seen that as $\alpha_{2,3}$ is varied at high S_2NR levels, the estimates remain accurate with low $\alpha_{1,2}$ values such as 0.01 and 0.2, but heavily degrade at 0.5 and 0.8. From Figure 8, we see that a three-receiver system suffers greatly in environments with low S_2NR, as the estimates barely approach the theoretical line. If the estimates are plotted against the actual interference values, a similar trend is observed in which the estimates fall back to the value of 0.5 under high amounts of interference as seen in Figures 9 and 10. From these results, we see that both noise and interference maintain a profound effect on the outcome on the estimators from Equation (3.10).

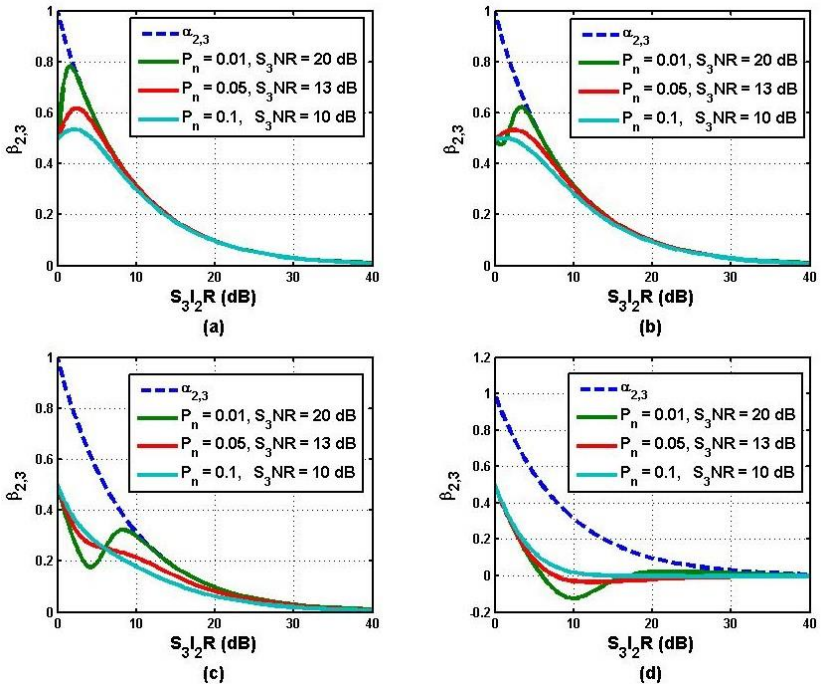

Figure 7. Plots of gain estimates $\beta_{2,3}$ vs. S_3I_2R values with fixed high S_3NR levels: (a) $\alpha_{1,3}$ = 0.01; (b) $\alpha_{1,3}$ = 0.2; (c) $\alpha_{1,3}$ = 0.5; (d) $\alpha_{1,3}$ = 0.8.

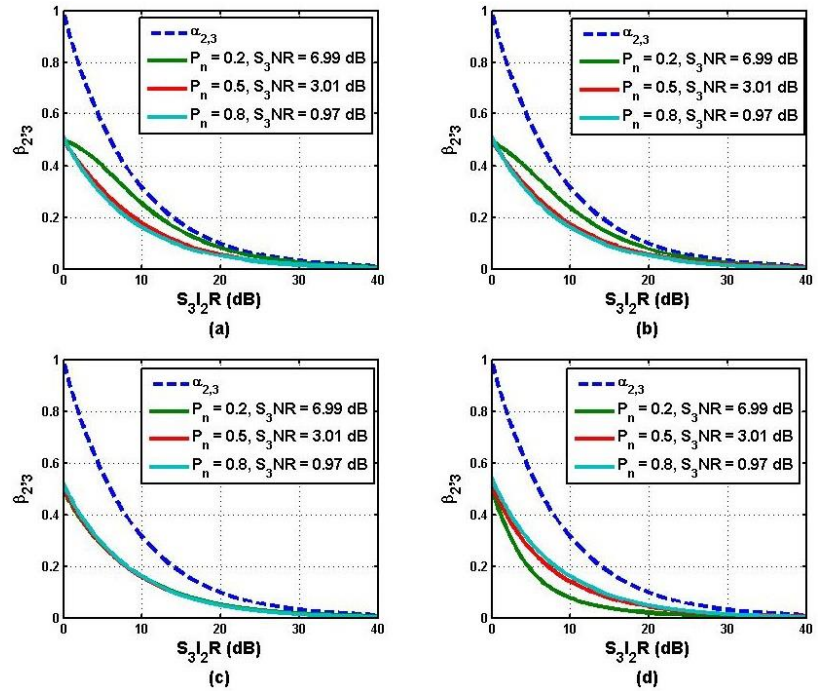

Figure 8. Plots of gain estimates $\beta_{2,3}$ vs. S_3I_2R values with fixed low S_3NR levels: (a) $\alpha_{1,3}$ = 0.01; (b) $\alpha_{1,3}$ = 0.2; (c) $\alpha_{1,3}$ = 0.5; (d) $\alpha_{1,3}$ = 0.8.

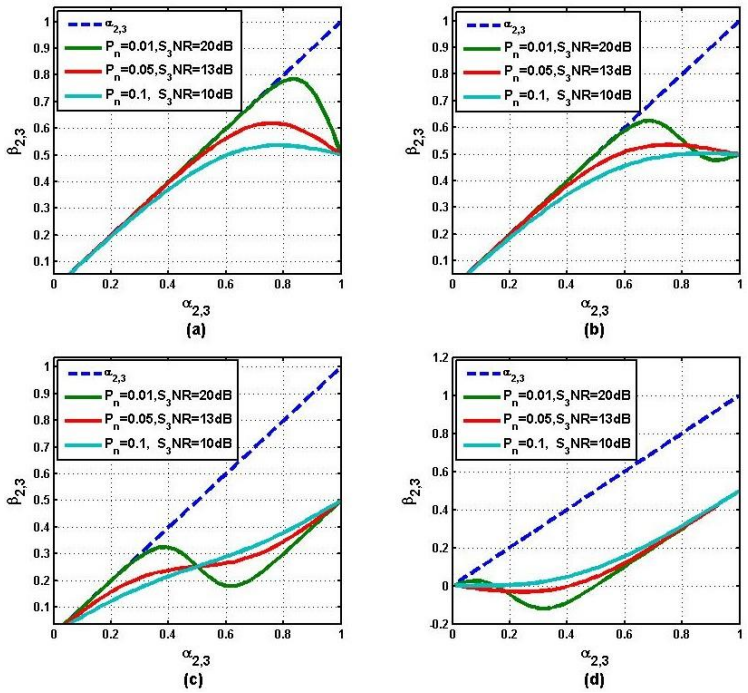

Figure 9. Plots of gain estimates $\beta_{2,3}$ vs. actual $\alpha_{2,3}$ parameter values with fixed high S_3NR levels: (a) $\alpha_{1,3}$ = 0.01; (b) $\alpha_{1,3}$ = 0.2; (c) $\alpha_{1,3}$ = 0.5; (d) $\alpha_{1,3}$ = 0.8.

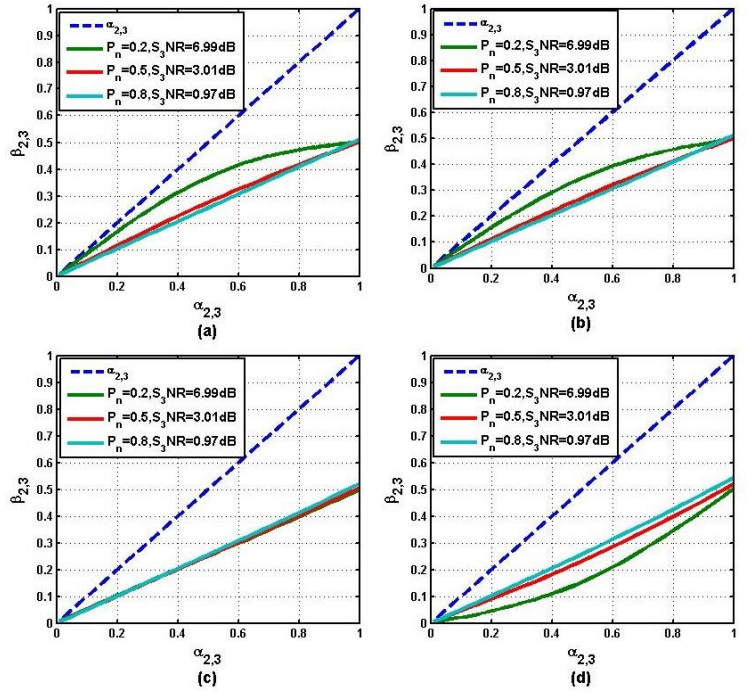

Figure 10. Plots of gain estimates $\beta_{2,3}$ vs. actual $\alpha_{2,3}$ parameter values with fixed low S_3NR levels: (a) $\alpha_{1,3}$ = 0.01; (b) $\alpha_{1,3}$ = 0.2; (c) $\alpha_{1,3}$ = 0.5; (d) $\alpha_{1,3}$ = 0.8.

2. Fix $\alpha_{2,3}$ and $\alpha_{1,3}$, Vary S_3NR

To observe the performance differences of the various scenarios in a different manner, we set one of the amplitude gains constant and the second is varied from almost zero to moderate/heavy interference. The simulation is performed with parameter $\alpha_{2,3}$ taking the values 0.01, 0.2, 0.5 and 0.8 while the parameter $\alpha_{1,3}$ changes to 0.01, 0.1, 0.2, 0.4, 0.6 and 0.8 to illustrate their respective SERs as shown in Figures 11–14.

Utilizing the same *pre* and *post* decision concepts from Chapter II, we see the differing performances resulting from the multiple combinations of interference gain values. For brevity, only the *post* SER curves are discussed since these are the results expected after the full application of the SIC technique. Starting at a low $\alpha_{2,3}$, we see that the *post* SERs realized with high S_3NR at each of the $\alpha_{1,3}$ values are quite small, around 10^{-5}–10^{-6}, which means that the SIC technique works well and provides a clean $\hat{\mathbf{s}}_3$ that is close to the original signal. This occurs until the interference amplitude from the first signal is set to 0.8. At this point, the SER begins to degrade as seen in Figure 11. If the $\alpha_{2,3}$ is increased to 0.2, then the performance starts to deteriorate earlier at $\alpha_{1,3}$ = 0.6 as shown in Figure 12. From Figure 13, it is seen that SER now has a noticeable decline at $\alpha_{1,3}$ = 0.4, and from Figure 14, we see there is an immediate decrease in SER performance at every S_3NR and $\alpha_{1,3}$ level due to the high value of $\alpha_{2,3}$ = 0.8. At interference levels this high, it is very difficult to successfully retrieve the SOI.

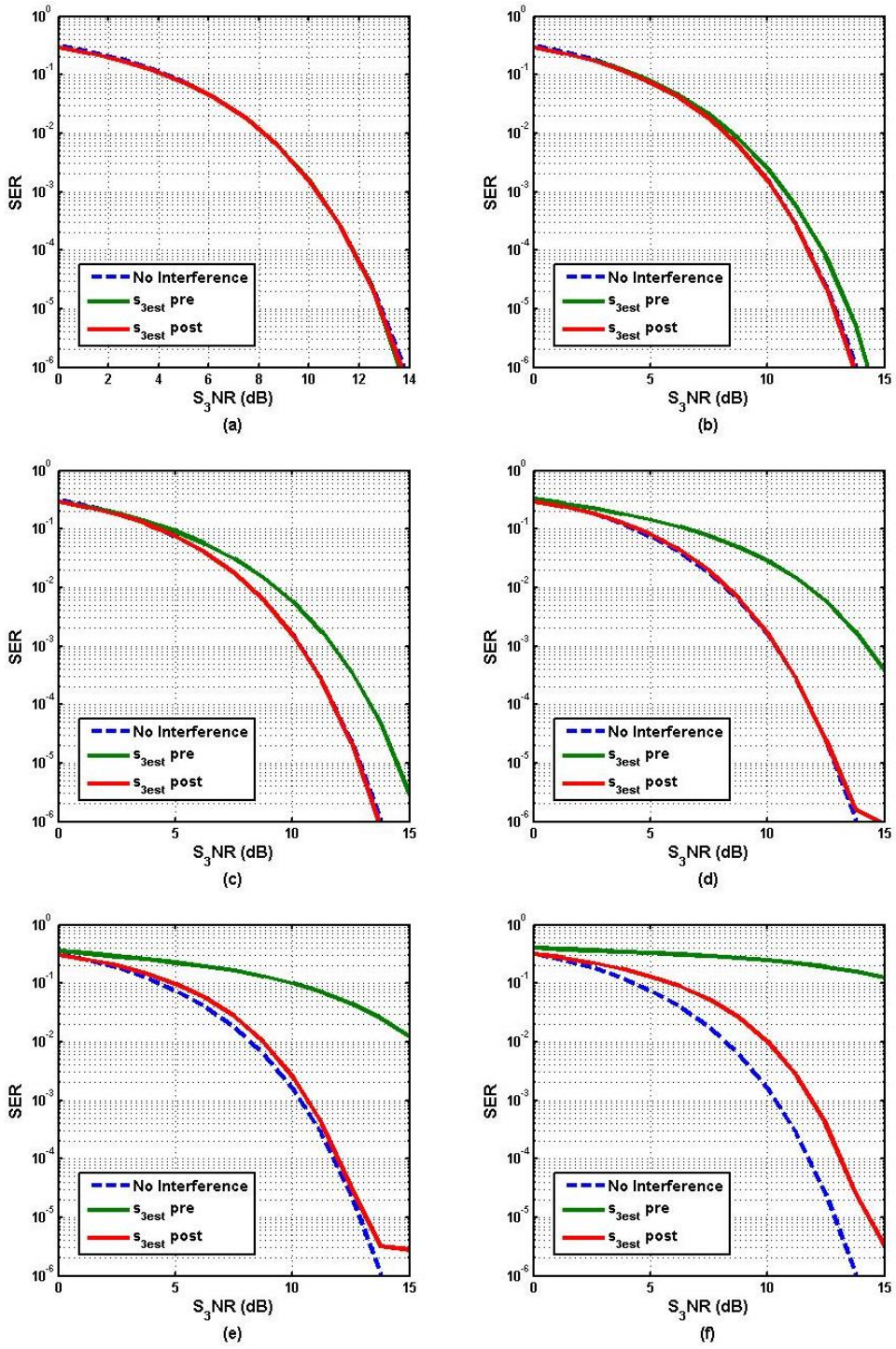

Figure 11. Performance curves of SER vs. S_3NR for *pre*/*post* decisions of $\mathbf{s}_3$ at different interference combinations when $\alpha_{2,3}$ = 0.01: (a) $\alpha_{1,3}$ = 0.01, S_3IR = 37 dB; (b) $\alpha_{1,3}$ = 0.1, S_3IR = 20 dB; (c) $\alpha_{1,3}$ = 0.2, S_3IR = 14 dB; (d) $\alpha_{1,3}$ = 0.4, S_3IR = 7.96 dB; (e) $\alpha_{1,3}$ = 0.6, S_3IR = 4.4 dB; (f) $\alpha_{1,3}$ = 0.8, S_3IR = 1.94 dB.

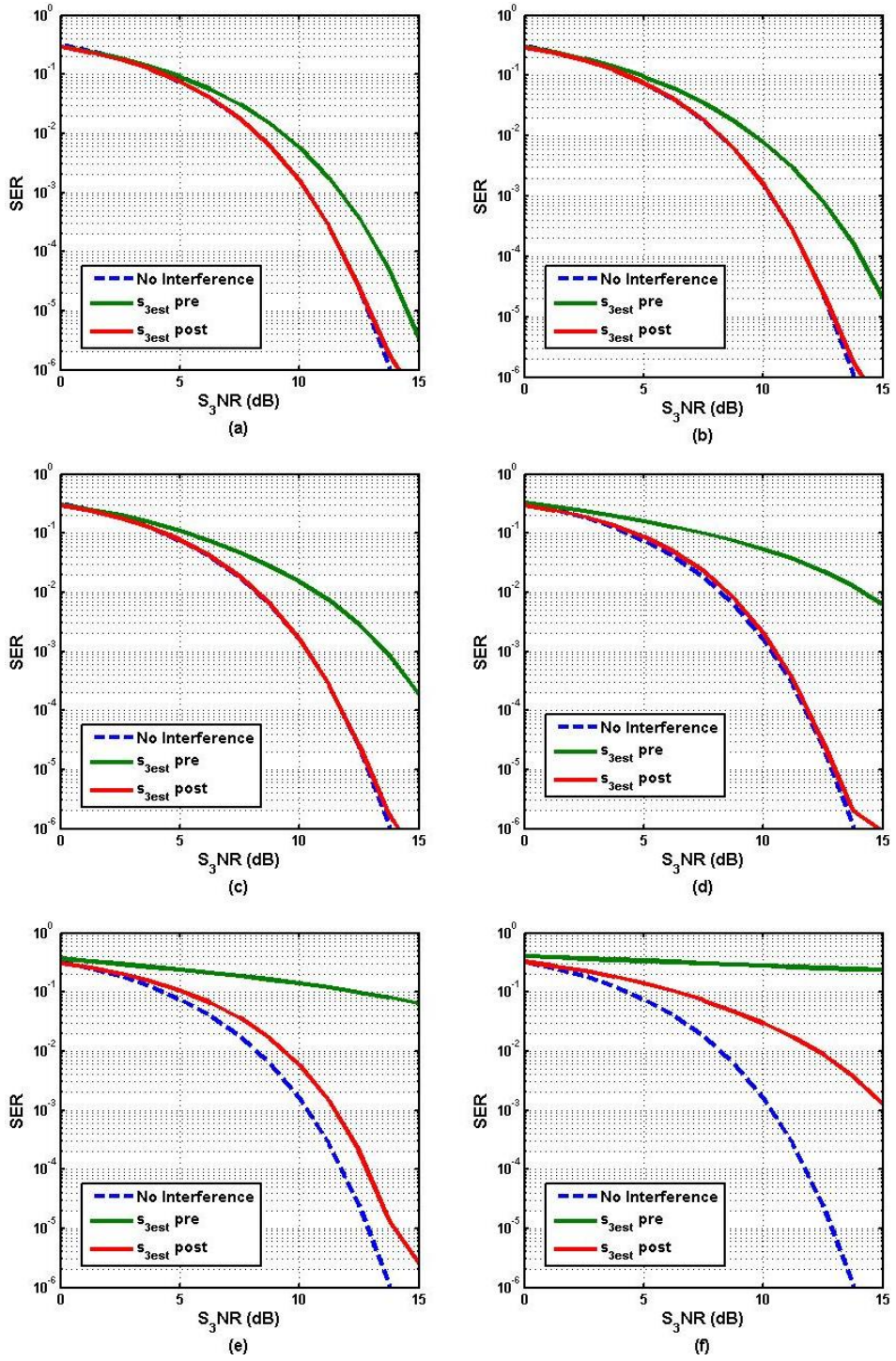

Figure 12. Performance curves of SER vs. S_3NR for *pre*/*post* decisions of $\mathbf{s}_3$ at different interference combinations when $\alpha_{2,3}$ = 0.2: (a) $\alpha_{1,3}$ = 0.01, S_3IR = 14 dB; (b) $\alpha_{1,3}$ = 0.1, S_3IR = 13 dB; (c) $\alpha_{1,3}$ = 0.2, S_3IR = 11 dB; (d) $\alpha_{1,3}$ = 0.4, S_3IR = 6.99 dB; (e) $\alpha_{1,3}$ = 0.6, S_3IR = 3.98 dB; (f) $\alpha_{1,3}$ = 0.8, S_3IR = 1.67 dB.

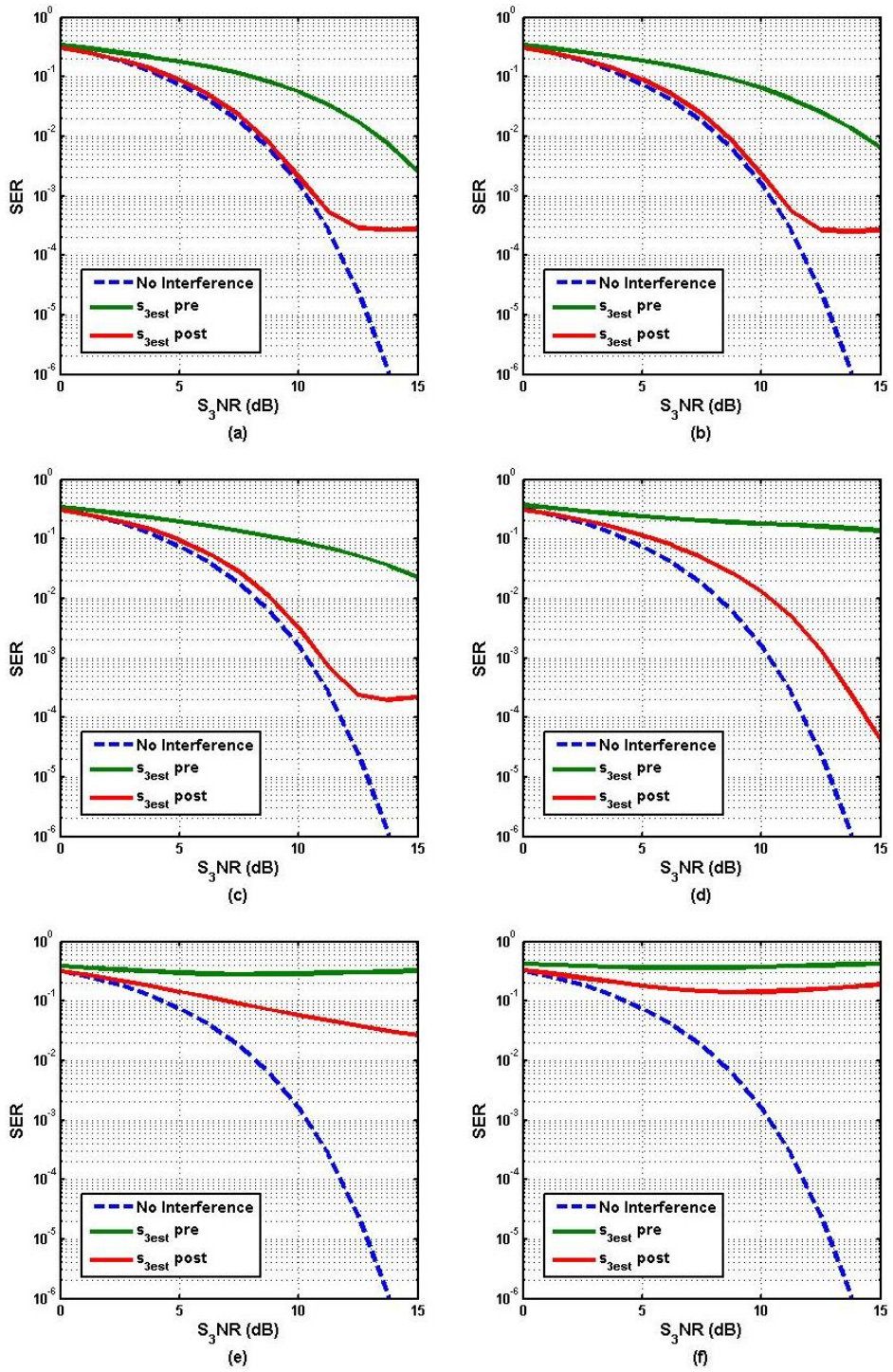

Figure 13. Performance curves of SER vs. S_3NR for *pre*/*post* decisions of $\mathbf{s}_3$ at different interference combinations when $\alpha_{2,3}$ = 0.5: (a) $\alpha_{1,3}$ = 0.01, S_3IR = 6.02 dB; (b) $\alpha_{1,3}$ = 0.1, S_3IR = 5.85 dB; (c) $\alpha_{1,3}$ = 0.2, S_3IR = 5.38 dB; (d) $\alpha_{1,3}$ = 0.4, S_3IR = 3.87 dB; (e) $\alpha_{1,3}$ = 0.6, S_3IR = 2.15 dB; (f) $\alpha_{1,3}$ = 0.8, S_3IR = 0.51 dB.

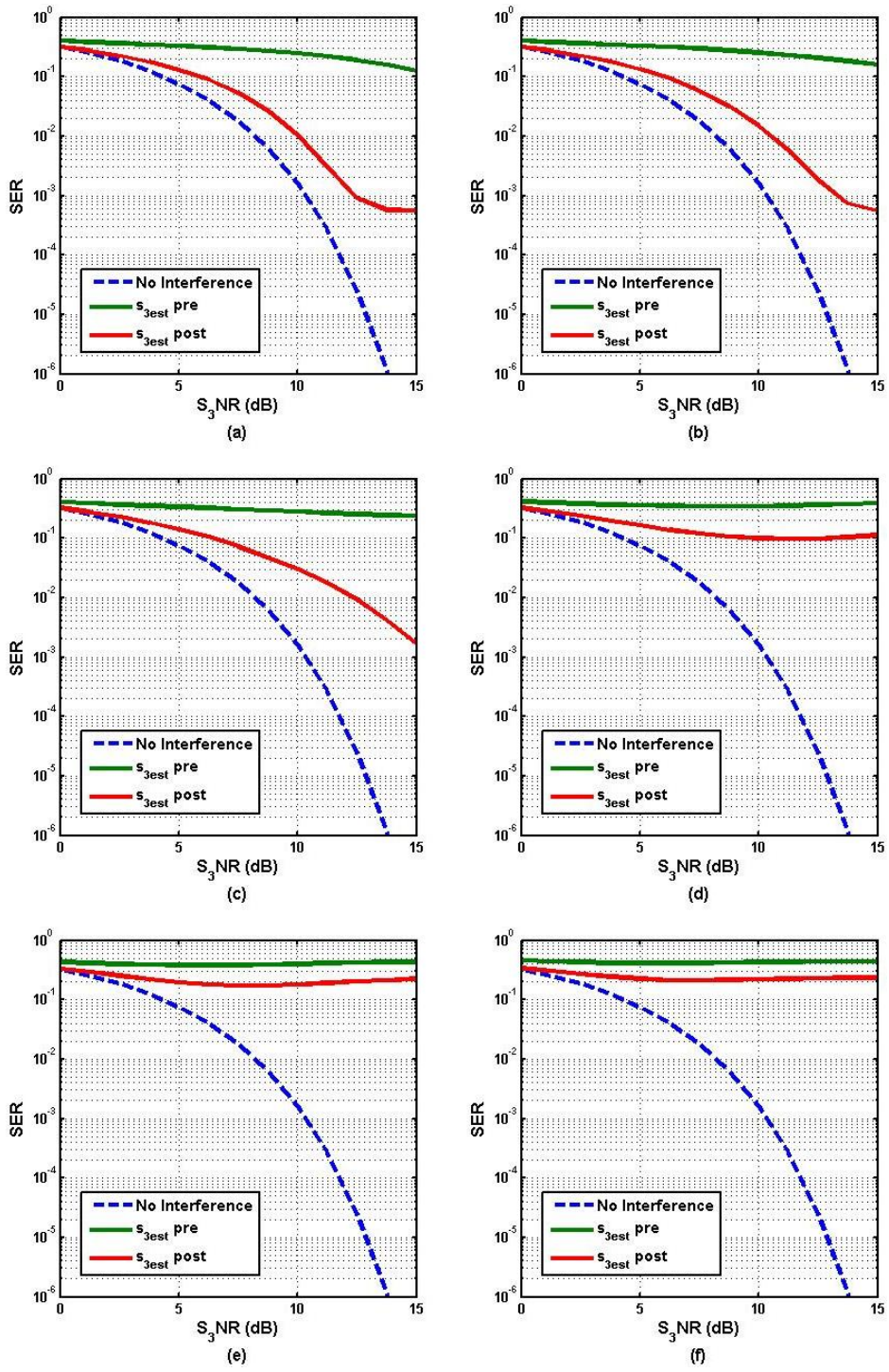

Figure 14. Performance curves of SER vs. S_3NR for *pre*/*post* decisions of $\mathbf{s}_3$ at different interference combinations when $\alpha_{2,3}$ = 0.8: (a) $\alpha_{1,3}$ = 0.01, S_3IR = 1.94 dB; (b) $\alpha_{1,3}$ = 0.1, S_3IR = 1.87 dB; (c) $\alpha_{1,3}$ = 0.2, S_3IR = 1.67 dB; (d) $\alpha_{1,3}$ = 0.4, S_3IR = 0.97 dB; (e) $\alpha_{1,3}$ = 0.6, S_3IR = 0 dB; (f) $\alpha_{1,3}$ = 0.8, S_3IR = -1.07 dB.

Next, the accuracies of the estimates are observed alongside the actual gain parameters in Figures 15–22. Several plots at varying levels of interference are required to show how changing one α parameter affects the estimate β of the other parameter. In every figure, each subplot indicates a different run of the simulation with gain parameters fixed to certain values. For example, from Figures 15 and 16, the initial $\alpha_{2,3}$ parameter is set very low to 0.01 while $\alpha_{1,3}$ moves across a range of a values. The estimates $\beta_{2,3}$ are very accurate throughout these iterations, however, at lower S_3I_1R the estimates $\beta_{1,3}$ require higher S_3NR in order to properly calculate the gain parameter. The next round of simulations are performed with $\alpha_{2,3}$ = 0.2 where an immediate change is observed where the first calculations of $\beta_{2,3}$ lie below the actual value line as seen in Figure 17. These are improved with a higher S_3NR, but again as the $\alpha_{1,3}$ interference approaches 1.0, the estimates $\beta_{2,3}$ and $\beta_{1,3}$ begin to suffer as shown in Figure 18. As both the interference values continue to intensify, the overall accuracy for both estimates decrease, up to the point where even increasing the S_3NR actually begins to have a negative effect on the actual estimation values as shown in Figures 19–22.

The CRLB for a three-receiver shows similar results that are obtained in the two-receiver system. As seen in Figures 23 and 24, each row indicates a specific configuration of gain parameters for the simulation. For example, the top row shown in Figure 24 has $\alpha_{2,3}$ = 0.2 and $\alpha_{1,2}$ = 0.1 whereas the bottom row is setup with $\alpha_{2,3}$ = 0.2 and $\alpha_{1,2}$ = 0.4. The calculated variances from each of the simulations follow the curve of the theoretical variance from (3.14), but deviate a certain degree based on the addition of interference into the system. This is an expected result as additional gain from interfering signals effectively degrades the performance of the estimators, causing the variance to increase in each estimation calculation. As the low interference simulations from Chapter II and III confirm the theoretical variance values of (2.30) as well as of (3.14), the CRLB for a four-receiver system will not be calculated.

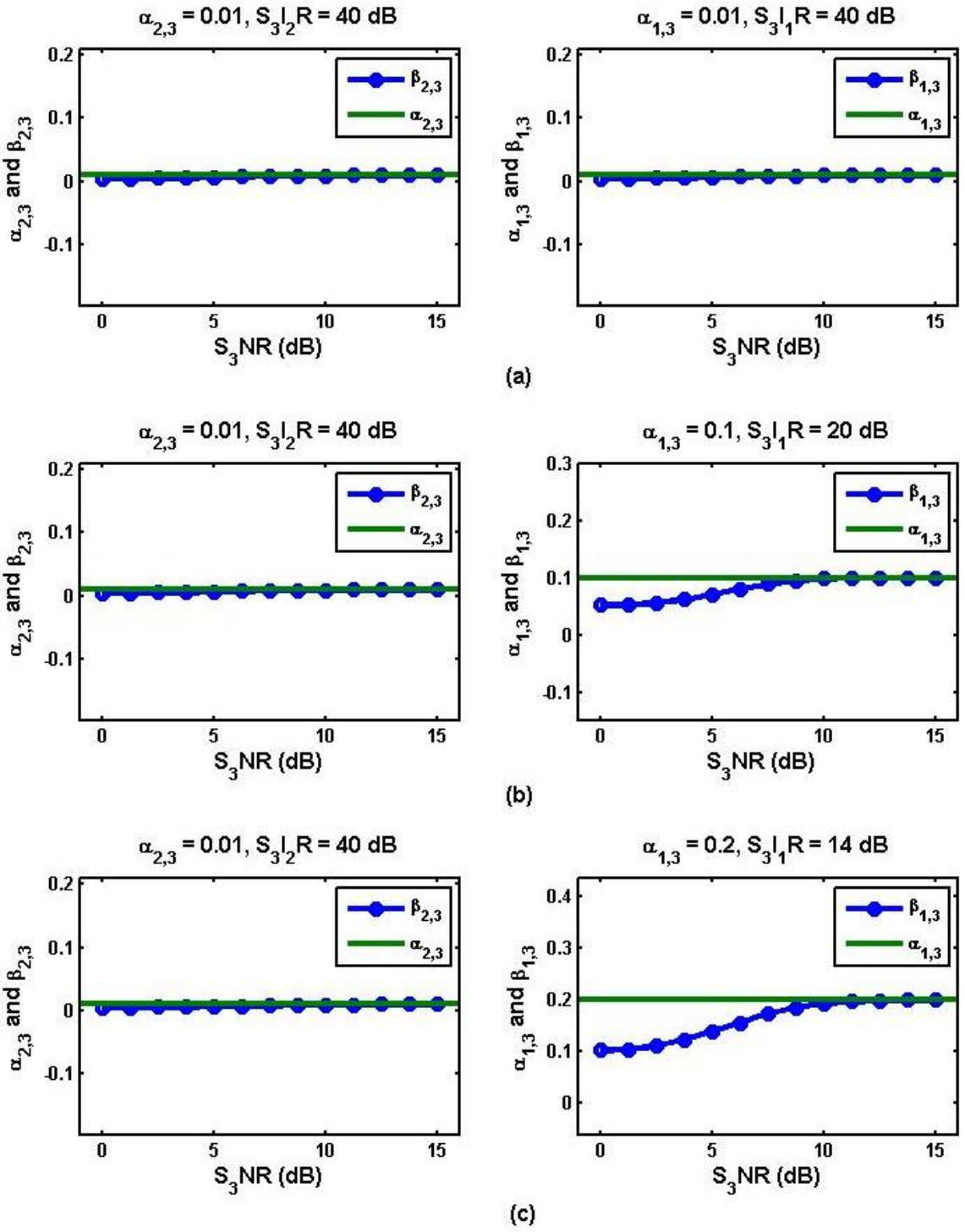

Figure 15. Plots of the actual gain parameters $\alpha_{2,3}$, $\alpha_{1,3}$ and the estimators $\beta_{2,3}$, $\beta_{1,3}$ vs. different S_3NR values for multiple simulations of $\mathbf{y}_3$ while $\alpha_{2,3}$ = 0.01: (a) S_3IR = 37 dB; (b) S_3IR = 20 dB; (c) S_3IR = 14 dB.

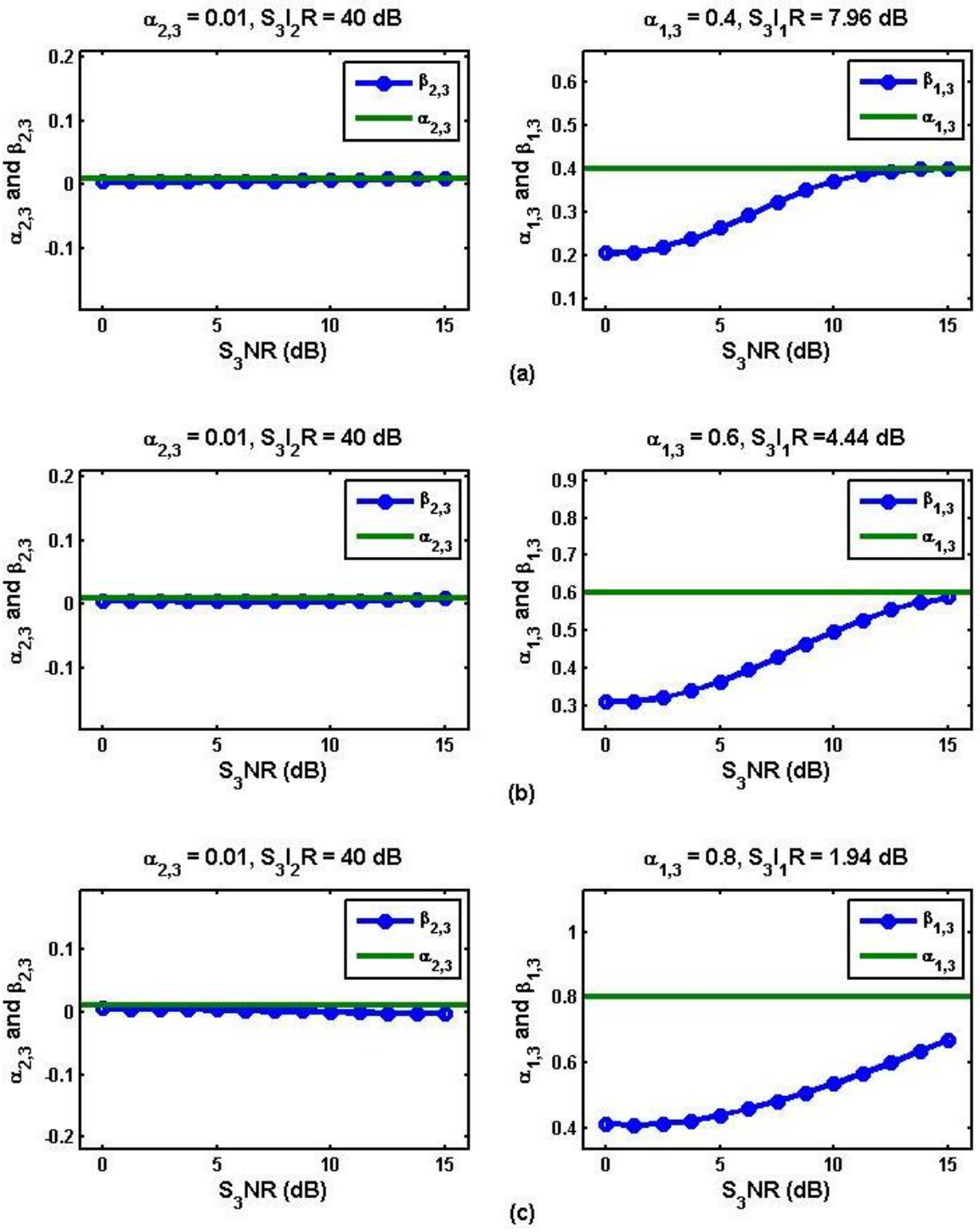

Figure 16. Plots of the actual gain parameters $\alpha_{2,3}$, $\alpha_{1,3}$ and the estimators $\beta_{2,3}$, $\beta_{1,3}$ vs. different S_3NR values for multiple simulations of $\mathbf{y}_3$ while $\alpha_{2,3}$ = 0.01: (a) S_3IR = 7.96 dB; (b) S_3IR = 4.44 dB; (c) S_3IR = 1.94 dB.

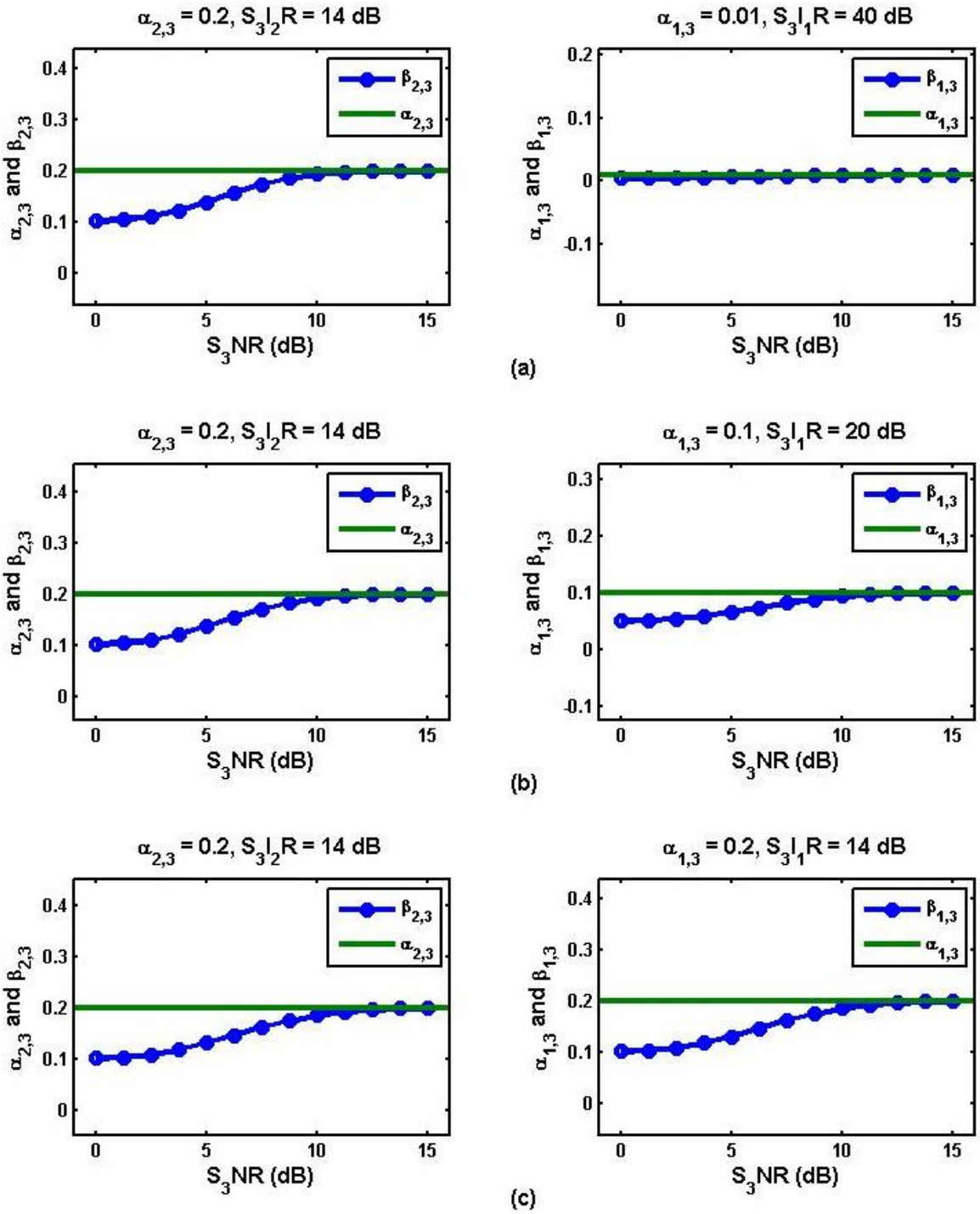

Figure 17. Plots of the actual gain parameters $\alpha_{2,3}$, $\alpha_{1,3}$ and the estimators $\beta_{2,3}$, $\beta_{1,3}$ vs. different S_3NR values for multiple simulations of $\mathbf{y}_3$ while $\alpha_{2,3}$ = 0.2: (a) S_3IR = 14 dB; (b) S_3IR = 13 dB; (c) S_3IR = 11 dB.

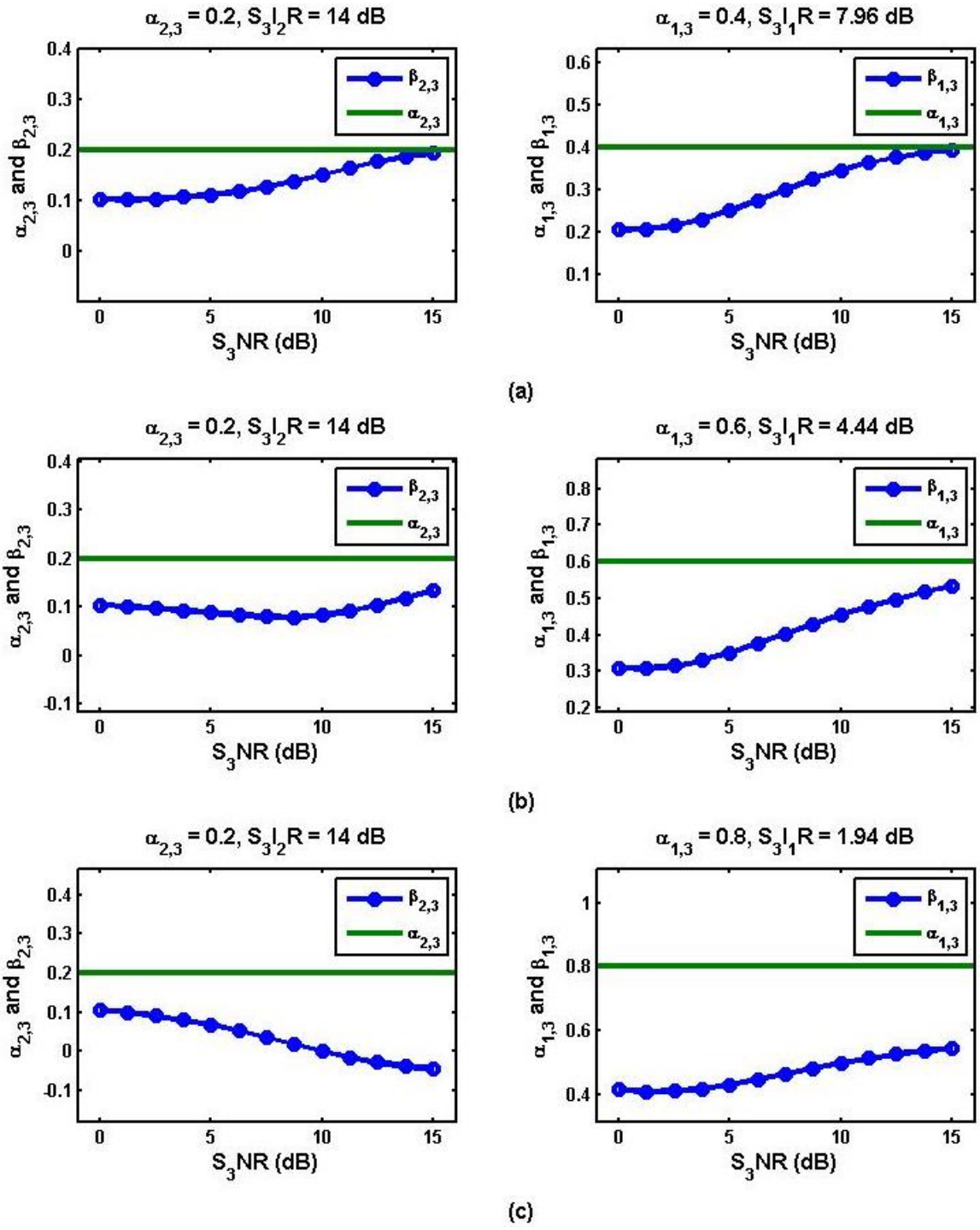

Figure 18. Plots of the actual gain parameters $\alpha_{2,3}$, $\alpha_{1,3}$ and the estimators $\beta_{2,3}$, $\beta_{1,3}$ vs. different S_3NR values for multiple simulations of $\mathbf{y}_3$ while $\alpha_{2,3}$ = 0.2: (a) S_3IR = 6.99 dB; (b) S_3IR = 3.98 dB; (c) S_3IR = 1.67 dB.

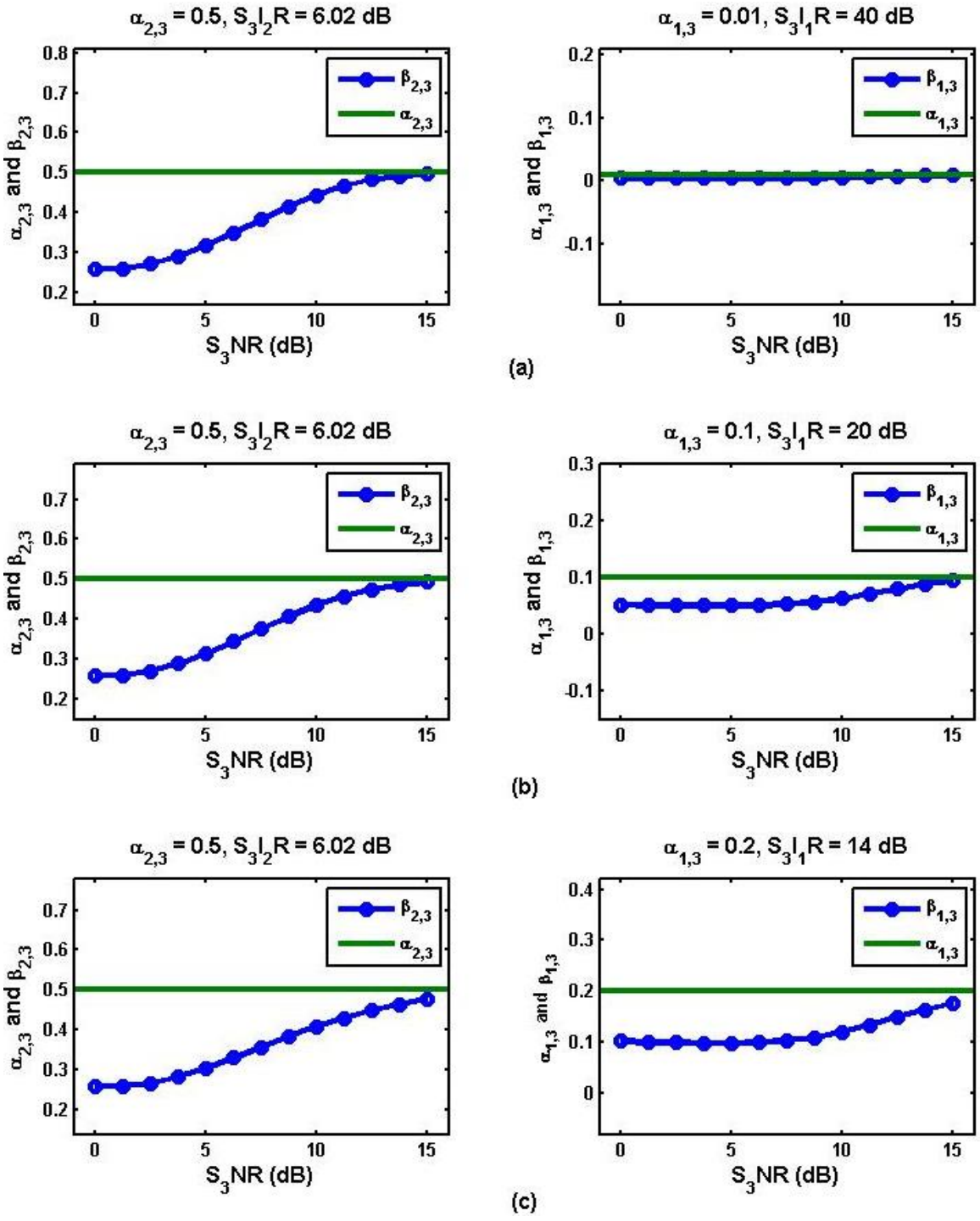

Figure 19. Plots of the actual gain parameters $\alpha_{2,3}$, $\alpha_{1,3}$ and the estimators $\beta_{2,3}$, $\beta_{1,3}$ vs. different S_3NR values for multiple simulations of $\mathbf{y}_3$ while $\alpha_{2,3}$ = 0.5: (a) S_3IR = 6.02 dB; (b) S_3IR = 5.85 dB; (c) S_3IR = 5.38 dB.

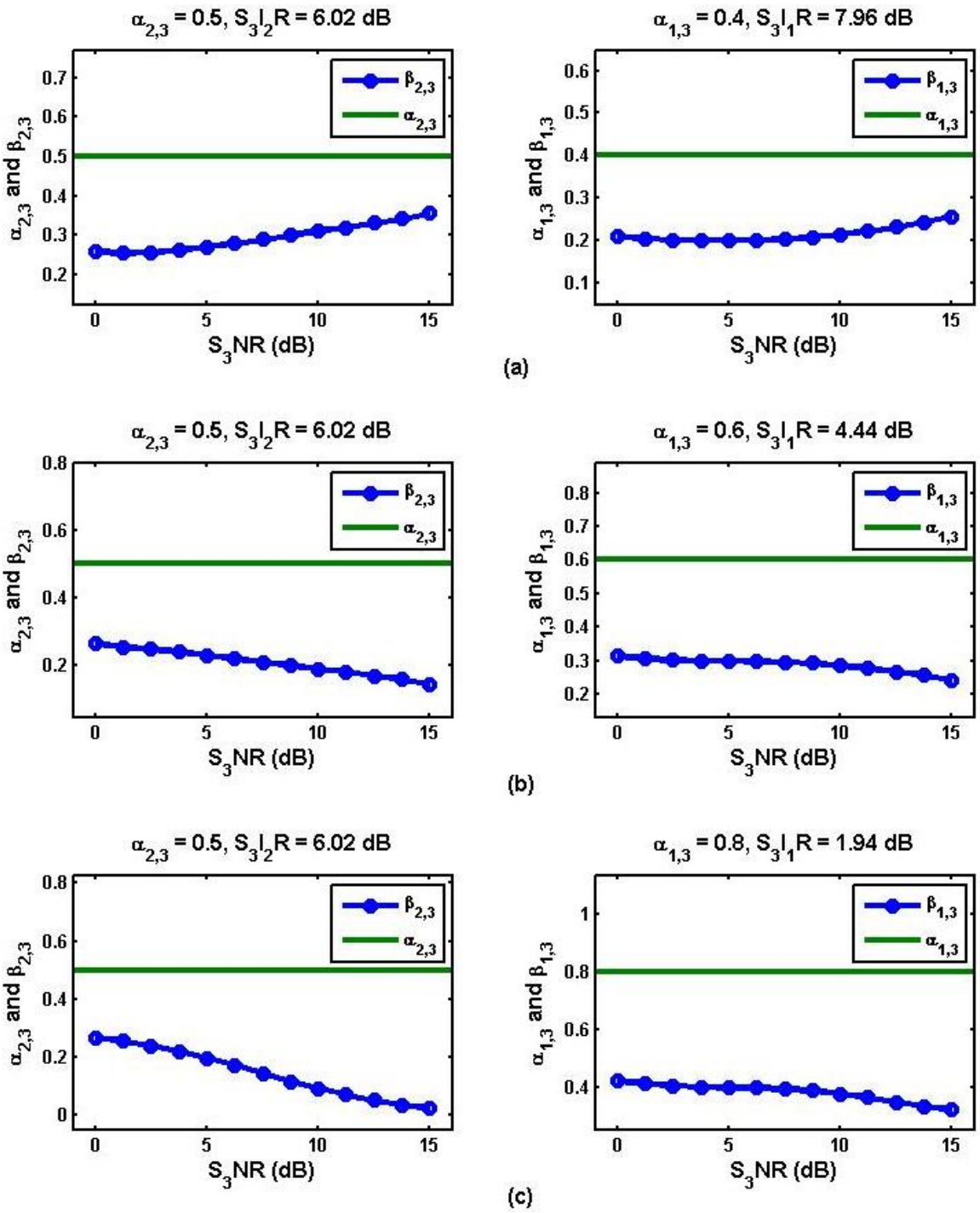

Figure 20. Plots of the actual gain parameters $\alpha_{2,3}$, $\alpha_{1,3}$ and the estimators $\beta_{2,3}$, $\beta_{1,3}$ vs. different S_3NR values for multiple simulations of $\mathbf{y}_3$ while $\alpha_{2,3}$ = 0.5: (a) S_3IR = 3.87 dB; (b) S_3IR = 2.15 dB; (c) S_3IR = 0.51 dB.

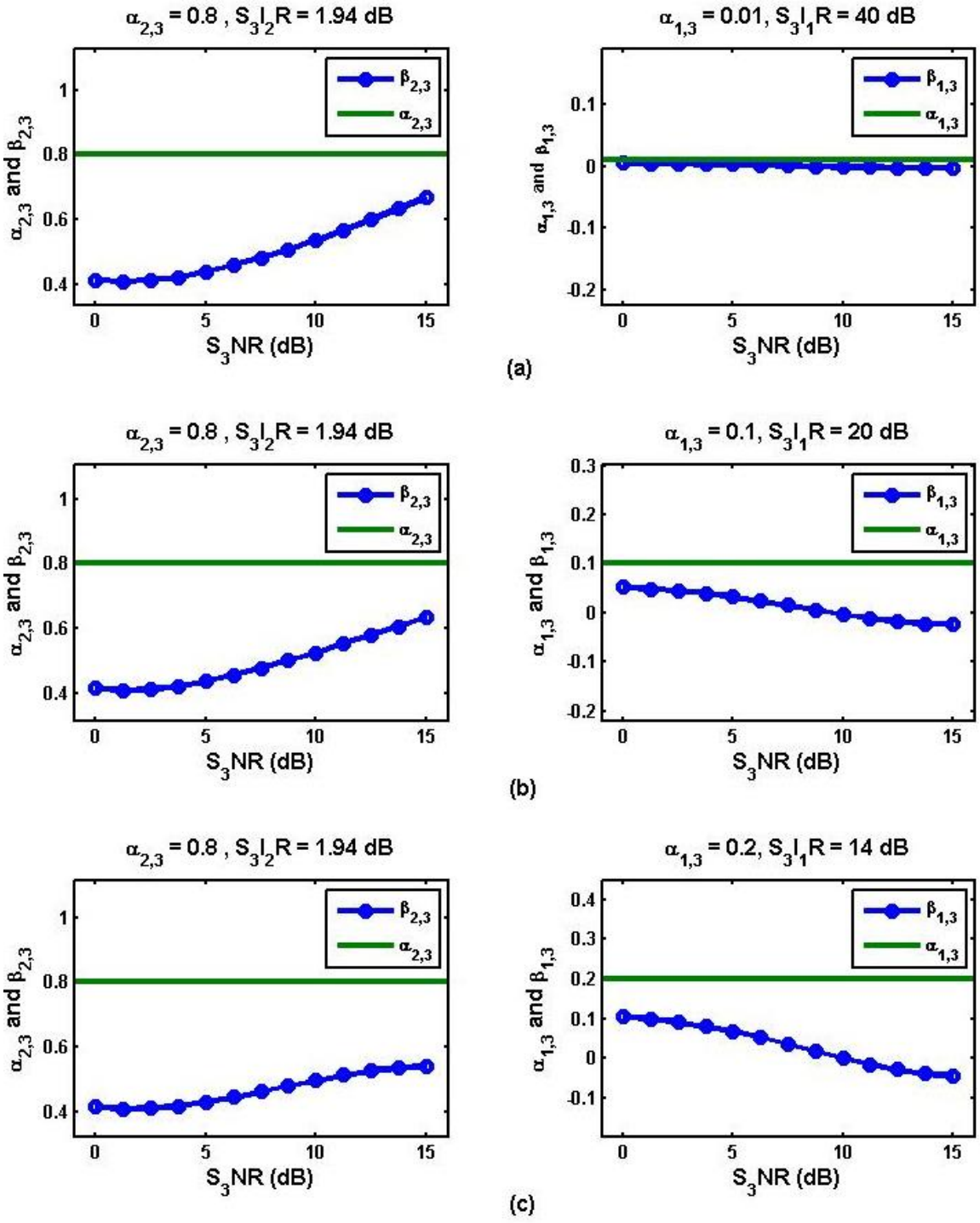

Figure 21. Plots of the actual gain parameters $\alpha_{2,3}$, $\alpha_{1,3}$ and the estimators $\beta_{2,3}$, $\beta_{1,3}$ vs. different S_3NR values for multiple simulations of $\mathbf{y}_3$ while $\alpha_{2,3}$ = 0.8: (a) S_3IR = 1.94 dB; (b) S_3IR = 1.87 dB; (c) S_3IR = 1.67 dB.

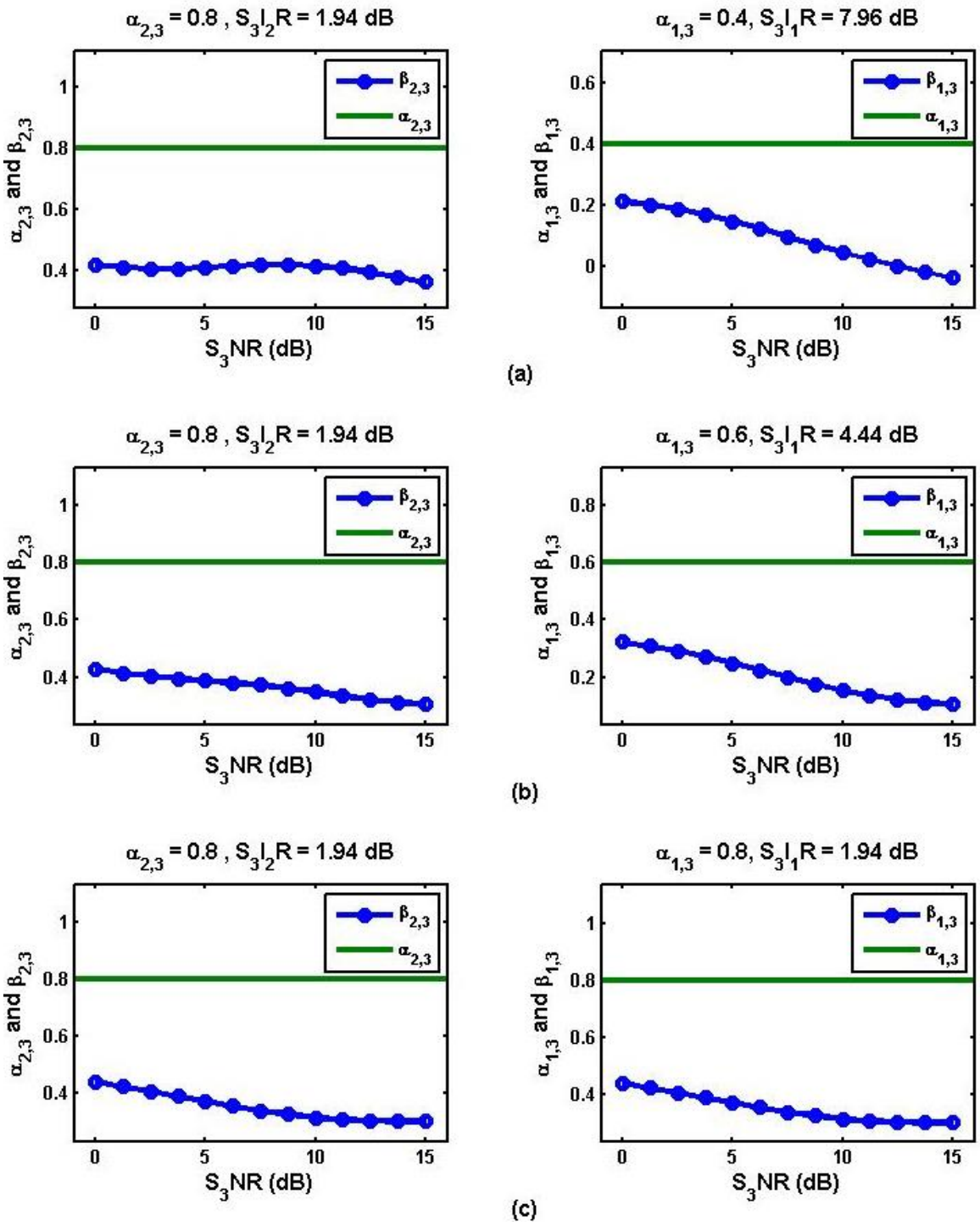

Figure 22. Plots of the actual gain parameters $\alpha_{2,3}$, $\alpha_{1,3}$ and the estimators $\beta_{2,3}$, $\beta_{1,3}$ vs. different S_3NR values for multiple simulations of $\mathbf{y}_3$ while $\alpha_{2,3}$ = 0.8: (a) S_3IR = 0.97 dB; (b) S_3IR = 0 dB; (c) S_3IR = -1.07 dB.

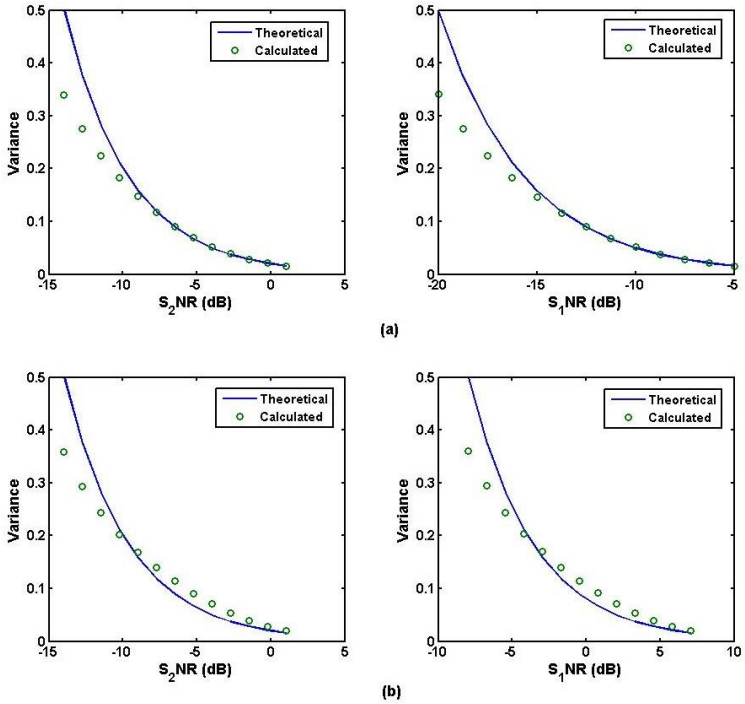

Figure 23. Variance of estimators $\beta_{2,3}, \beta_{1,3}$ vs. their respective SNR with $a_{2,3}$ = 0.2, S_3I_2R = 13.98 dB: (a) $a_{1,3}$ = 0.1, S_3I_1R = 20 dB; (b) $a_{1,3}$ = 0.4, S_3I_1R = 7.96 dB.

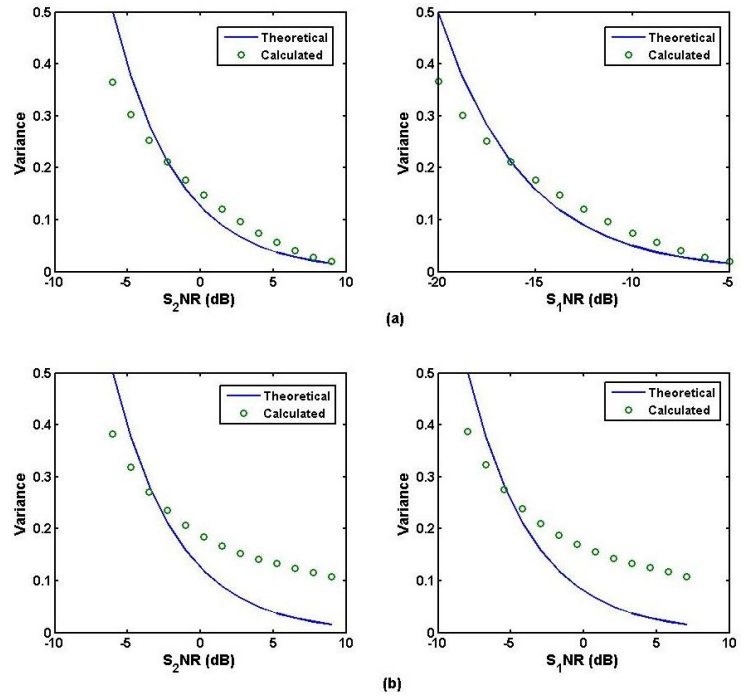

Figure 24. Variance of estimators $\beta_{2,3}, \beta_{1,3}$ vs. their respective SNR with $a_{2,3}$ = 0.5, S_3I_2R = 6.02 dB: (a) $a_{1,3}$ = 0.1, S_3I_1R = 20 dB; (b) $a_{1,3}$ = 0.4, S_3I_1R = 7.96 dB.

A summary of SER performances for multiple configurations, each with different combinations of gain parameter values is shown in Figure 25. The common quantity in the plots is the S_3IR experienced by each of these configurations. The best SER curves correspond to high S_3IR values, which points out the fact that in order to maintain a system with accurate estimations, a reasonable energy difference is needed between the main signal and the interfering ones. Specifically, configurations with S_3IRs values of 6.99 dB or higher have SER curves which follow the theoretical curve quite well.

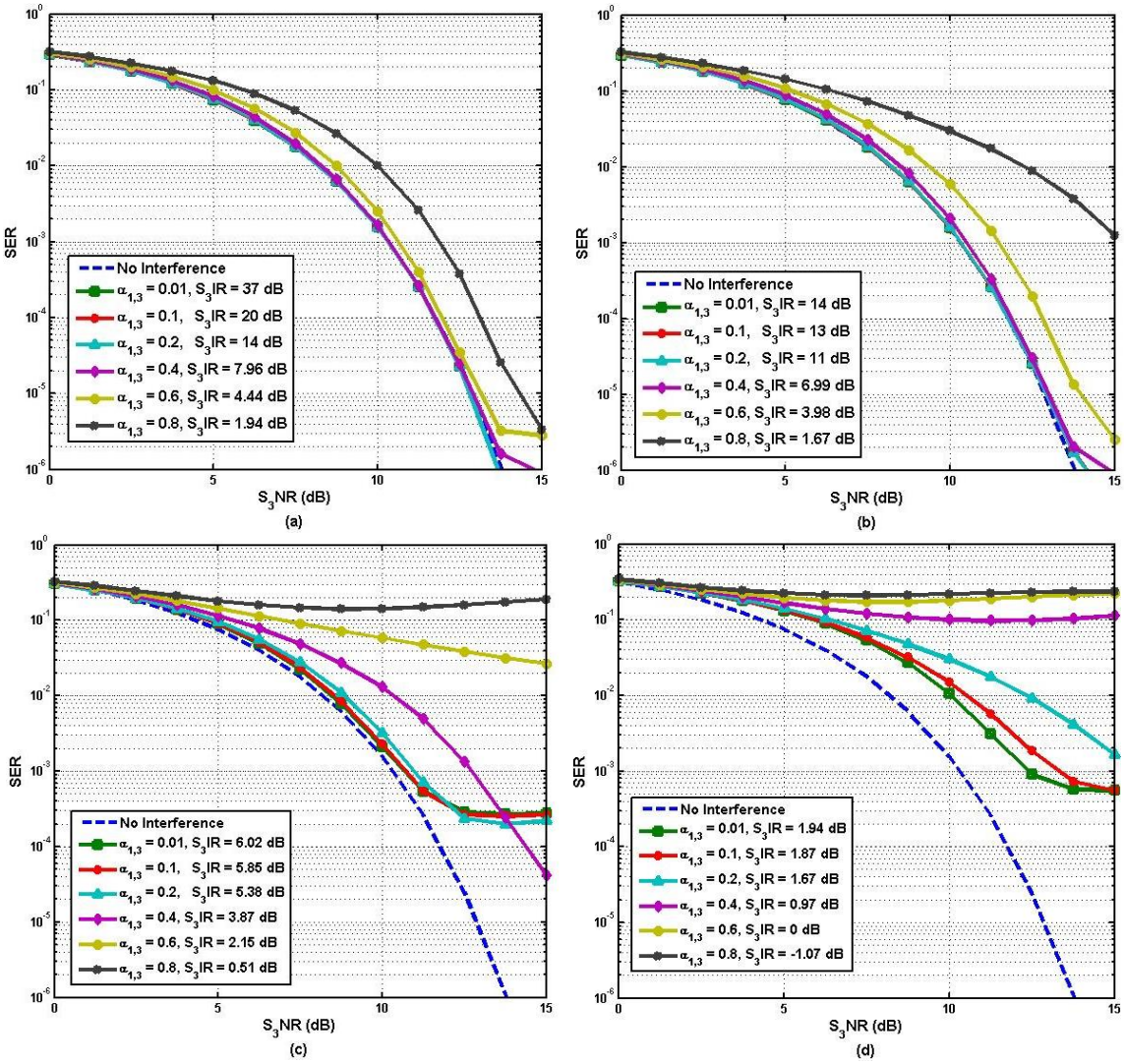

Figure 25. Performance curves of SER vs. S_3NR for *post* $\hat{\mathbf{s}}_3$ decisions at multiple configurations: (a) $\alpha_{2,3} = 0.01$; (b) $\alpha_{2,3} = 0.2$; (c) $\alpha_{2,3} = 0.5$; (d) $\alpha_{2,3} = 0.8$.

IV. ADDITION OF A FOURTH RECEIVER

A. PARAMETER ESTIMATION FOR A FOUR-RECEIVER SYSTEM

Here we consider that a fourth receiver is added to the multi-platform system and takes a position somewhere in Sector D from Figure 26 (shown again for convenience.)

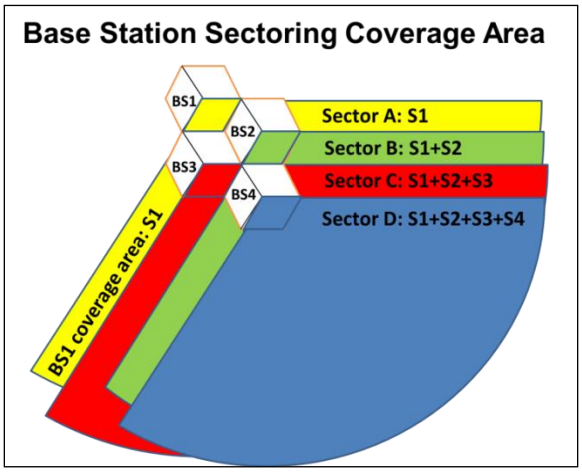

Figure 26. Configuration of multiple BSs with overlapping antenna coverage which has different signal combinations received in each sector. From [3].

If the received signal (2.4) is taken, and the LSE method is applied, we get

$$\begin{aligned} J(\alpha) &= \left\| \mathbf{y}_4 - (\mathbf{s}_4 + \alpha_{3,4}\mathbf{s}_3 + \alpha_{2,4}\mathbf{s}_2 + \alpha_{1,4}\mathbf{s}_1) \right\|^2 \\ &= (\mathbf{y}_4 - \mathbf{s}_4 - \alpha_{3,4}\mathbf{s}_3 - \alpha_{2,4}\mathbf{s}_2 - \alpha_{1,4}\mathbf{s}_1)^H (\mathbf{y}_4 - \mathbf{s}_4 - \alpha_{3,4}\mathbf{s}_3 - \alpha_{2,4}\mathbf{s}_2 - \alpha_{1,4}\mathbf{s}_1). \end{aligned} \tag{4.1}$$

Despite a lengthy derivation, it is shown that the estimators for the gain parameters are

$$\alpha_{3,4} = \frac{\mathrm{Re}\{\mathbf{y}_4{}^H \mathbf{s}_3\} - \mathrm{Re}\{\rho_{4,3}\} - \alpha_{2,4}\,\mathrm{Re}\{\rho_{3,2}\} - \alpha_{1,4}\,\mathrm{Re}\{\rho_{3,1}\}}{2E_{\mathbf{s}_3}},$$

$$\alpha_{2,4} = \frac{\mathrm{Re}\{\mathbf{y}_4{}^H \mathbf{s}_2\} - \mathrm{Re}\{\rho_{4,2}\} - \alpha_{3,4}\,\mathrm{Re}\{\rho_{3,2}\} - \alpha_{1,4}\,\mathrm{Re}\{\rho_{2,1}\}}{2E_{\mathbf{s}_2}}, \tag{4.2}$$

$$\alpha_{1,4} = \frac{\mathrm{Re}\{\mathbf{y}_4{}^H \mathbf{s}_1\} - \mathrm{Re}\{\rho_{4,1}\} - \alpha_{3,4}\,\mathrm{Re}\{\rho_{3,1}\} - \alpha_{2,4}\,\mathrm{Re}\{\rho_{2,1}\}}{2E_{\mathbf{s}_1}}.$$

Unlike in Equation (3.8), which is solved via simple substitution, Equation (4.2) does not lend itself to simple derivation. Conveniently, the three equations and three unknowns allow us to derive the estimates via linear algebraic method. By reordering (4.2) to move the gain parameters to one side, we get

$$\begin{aligned}
\mathrm{Re}\{\mathbf{y}_4{}^H\mathbf{s}_3\} - \mathrm{Re}\{\rho_{4,3}\} &= \alpha_{3,4}(2E_{\mathbf{s}_3}) + \alpha_{2,4}\,\mathrm{Re}\{\rho_{3,2}\} + \alpha_{1,4}\,\mathrm{Re}\{\rho_{3,1}\},\\
\mathrm{Re}\{\mathbf{y}_4{}^H\mathbf{s}_2\} - \mathrm{Re}\{\rho_{4,2}\} &= \alpha_{3,4}\,\mathrm{Re}\{\rho_{3,2}\} + \alpha_{2,4}(2E_{\mathbf{s}_2}) + \alpha_{1,4}\,\mathrm{Re}\{\rho_{2,1}\},\\
\mathrm{Re}\{\mathbf{y}_4{}^H\mathbf{s}_1\} - \mathrm{Re}\{\rho_{4,1}\} &= \alpha_{3,4}\,\mathrm{Re}\{\rho_{3,1}\} + \alpha_{2,4}\,\mathrm{Re}\{\rho_{2,1}\} + \alpha_{1,4}(2E_{\mathbf{s}_1}).
\end{aligned} \tag{4.3}$$

For simplicity, (4.3) is arranged to

$$\begin{bmatrix} A \\ B \\ C \end{bmatrix} = \begin{bmatrix} X_1 & Y_1 & Z_1 \\ X_2 & Y_2 & Z_2 \\ X_3 & Y_3 & Z_3 \end{bmatrix} \begin{bmatrix} \alpha_{3,4} \\ \alpha_{2,4} \\ \alpha_{1,4} \end{bmatrix}, \tag{4.4}$$

where we define $A = \mathrm{Re}\{\mathbf{y}_4{}^H\mathbf{s}_3\} - \mathrm{Re}\{\rho_{4,3}\}$, $B = \mathrm{Re}\{\mathbf{y}_4{}^H\mathbf{s}_2\} - \mathrm{Re}\{\rho_{4,2}\}$, $C = \mathrm{Re}\{\mathbf{y}_4{}^H\mathbf{s}_1\} - \mathrm{Re}\{\rho_{4,1}\}$, $X_1 = 2E_{\mathbf{s}_3}$, $Y_1 = \mathrm{Re}\{\rho_{3,2}\}$, $Z_1 = \mathrm{Re}\{\rho_{3,1}\}$, $X_2 = \mathbf{Re}\{\rho_{3,2}\}$, $Y_2 = 2E_{\mathbf{s}_2}$, $Z_2 = \mathrm{Re}\{\rho_{2,1}\}$, $X_3 = \mathbf{Re}\{\rho_{3,1}\}$, $Y_3 = \mathrm{Re}\{\rho_{2,1}\}$, and $Z_3 = 2E_{\mathbf{s}_1}$. To successfully solve for the three unknowns, the inverse of the X, Y, and Z matrix of constants is multiplied with the A, B, C vector of constants such that

$$\begin{bmatrix} \alpha_{3,4} \\ \alpha_{2,4} \\ \alpha_{1,4} \end{bmatrix} = \begin{bmatrix} X_1 & Y_1 & Z_1 \\ X_2 & Y_2 & Z_2 \\ X_3 & Y_3 & Z_3 \end{bmatrix}^{-1} \begin{bmatrix} A \\ B \\ C \end{bmatrix}. \tag{4.5}$$

Similar to Chapters II and III, there is a need for Rx4 to make a decision on the received signal $\mathbf{y}_4$ and create a *pre* calculation for $\mathbf{s}_4$, or

$$\tilde{\mathbf{s}}_4 = dec(\mathbf{y}_4), \tag{4.6}$$

which when substituted into (4.5) yields the estimates

$$\begin{bmatrix} \beta_{3,4} \\ \beta_{2,4} \\ \beta_{1,4} \end{bmatrix} = \begin{bmatrix} X_1 & Y_1 & Z_1 \\ X_2 & Y_2 & Z_2 \\ X_3 & Y_3 & Z_3 \end{bmatrix}^{-1} \begin{bmatrix} A \\ B \\ C \end{bmatrix}, \tag{4.7}$$

where $A = \mathrm{Re}\{\mathbf{y}_4{}^H \hat{\mathbf{s}}_3\} - \mathrm{Re}\{\tilde{\rho}_{4,3}\}$, $B = \mathrm{Re}\{\mathbf{y}_4{}^H \hat{\mathbf{s}}_2\} - \mathrm{Re}\{\tilde{\rho}_{4,2}\}$, $C = \mathrm{Re}\{\mathbf{y}_4{}^H \hat{\mathbf{s}}_1\} - \mathrm{Re}\{\tilde{\rho}_{4,1}\}$,

$X_1 = 2E_{\mathbf{s}_3}$, $Y_1 = \mathrm{Re}\{\hat{\rho}_{3,2}\}$, $Z_1 = \mathrm{Re}\{\hat{\rho}_{3,1}\}$, $X_2 = \mathrm{Re}\{\hat{\rho}_{3,2}\}$, $Y_2 = 2E_{\mathbf{s}_2}$, $Z_2 = \mathrm{Re}\{\hat{\rho}_{2,1}\}$,

$X_3 = \mathrm{Re}\{\hat{\rho}_{3,1}\}$, $Y_3 = \mathrm{Re}\{\hat{\rho}_{2,1}\}$, and $Z_3 = 2E_{\mathbf{s}_1}$. The solutions from (4.7) are now used in the computation of the *post* decisions, or

$$\hat{\mathbf{s}}_4 = dec(\mathbf{y}_4 - \beta_{3,4}\hat{\mathbf{s}}_3 - \beta_{2,4}\hat{\mathbf{s}}_2 - \beta_{1,4}\hat{\mathbf{s}}_1). \tag{4.8}$$

B. RESULTS FOR A FOUR-RECEIVER SYSTEM

Following the same simulation setup from Chapter III, we assume that Rx4 is provided the reference signals $\hat{\mathbf{s}}_3$, $\hat{\mathbf{s}}_2$, $\hat{\mathbf{s}}_1$ that are mostly interference-free.

1. Fix S_4NR, Vary $\alpha_{3,4}$, $\alpha_{2,4}$ and $\alpha_{1,4}$

The same approach from Chapter III is used to calculate the total SIR, such that

$$S_4IR \triangleq \frac{E_{\mathbf{s}_4}}{E_{\mathbf{s}_3} + E_{\mathbf{s}_2} + E_{\mathbf{s}_1}} = \frac{\|\mathbf{s}_4\|^2}{\|\alpha_{3,4}\mathbf{s}_3\|^2 + \|\alpha_{2,4}\mathbf{s}_2\|^2 + \|\alpha_{1,4}\mathbf{s}_1\|^2}. \tag{4.9}$$

With the energy for each signal set to the same value, (4.9) becomes

$$S_4IR = \frac{1}{\alpha_{3,4}^2 + \alpha_{2,4}^2 + \alpha_{1,4}^2}. \tag{4.10}$$

Again, by first setting specific noise levels in the simulation, we fix S_4NR values and compare the accuracy of the estimates against theoretical values. From Figure 27, we see $\beta_{3,4}$ calculations versus S_4I_3R values, and that at high S_4NR values, the estimations only show good accuracy when the energy of $\mathbf{s}_4$ is much greater than the interference in the rest of the system (i.e., low α values). The performance of the estimators show

increased degradation when more noise is added to the system and the S_4NR values are reduced. This is shown in Figure 28. Taking a look at the direct comparision between the calculations of $\beta_{3,4}$ and the actual values of $\alpha_{3,4}$, we see similar results wherein high S_4NR only provides accurate estimates around gain parameters values of 0.5 as seen in Figure 29. Likewise, increased noise in the system makes accurate gain estimation very difficult as calculations made when there is low S_4NR diverge almost immediately from the theortical line in Figure 30.

If $\alpha_{2,4}$ is increased to 0.4, the overall interference in the system increases and we again see degradation in the accuracies of each estimate. As shown in Figures 31–34, the three interfering signals demonstrate their ability to drastically reduce the performance of the estimators by compounding the effects of the amplitude gain parameters. Even at high S_4NR levels, the estimates barely approach the $\alpha_{3,4}$ line unless the actual gain is set very low to begin with in the simulation.

It is important to emphasize the fact that because of the relationship examined in (4.10), fixed SNR simulations do not require separate runs for each of the individual gain parameters. Due to the overall SIR caused by the additive effects of the interference gains, holding $\alpha_{2,4}$ and $\alpha_{1,4}$ at certain values while cycling through several $\alpha_{3,4}$ values would provide similar (if not exact) results as cycling through a different gain parameter and holding the others constant. These connections are further examined in the Appendix.

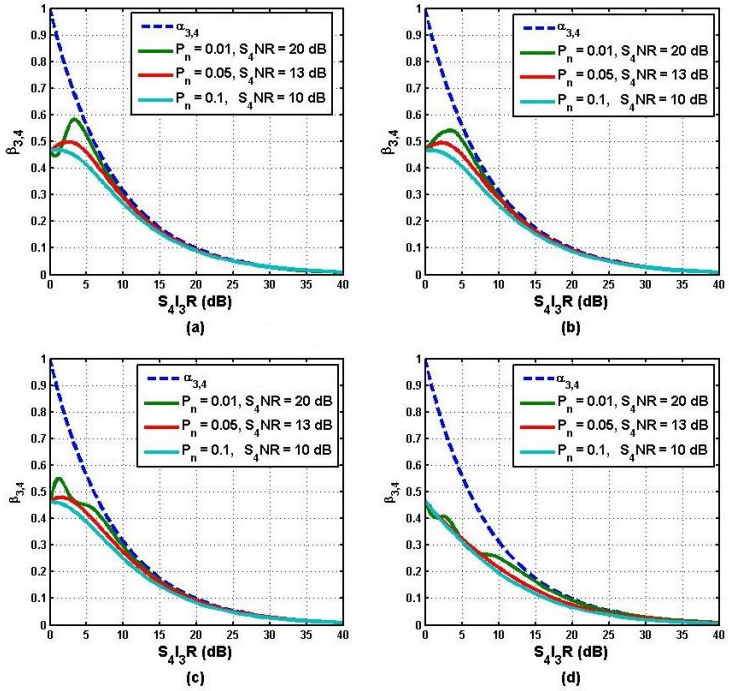

Figure 27. Plots of gain estimates $\beta_{3,4}$ vs. S_4I_3R values with fixed high S_4NR levels while $\alpha_{2,4} = 0.2$: (a) $\alpha_{1,4} = 0.01$; (b) $\alpha_{1,4} = 0.1$; (c) $\alpha_{1,4} = 0.2$; (d) $\alpha_{1,4} = 0.4$.

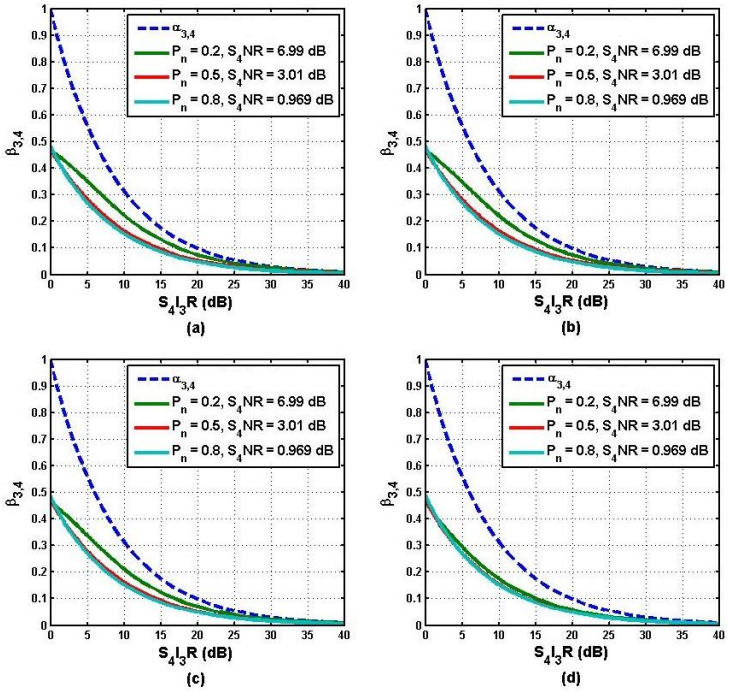

Figure 28. Plots of gain estimates $\beta_{3,4}$ vs. S_4I_3R values with fixed low S_4NR levels while $\alpha_{2,4} = 0.2$: (a) $\alpha_{1,4} = 0.01$; (b) $\alpha_{1,4} = 0.1$; (c) $\alpha_{1,4} = 0.2$; (d) $\alpha_{1,4} = 0.4$.

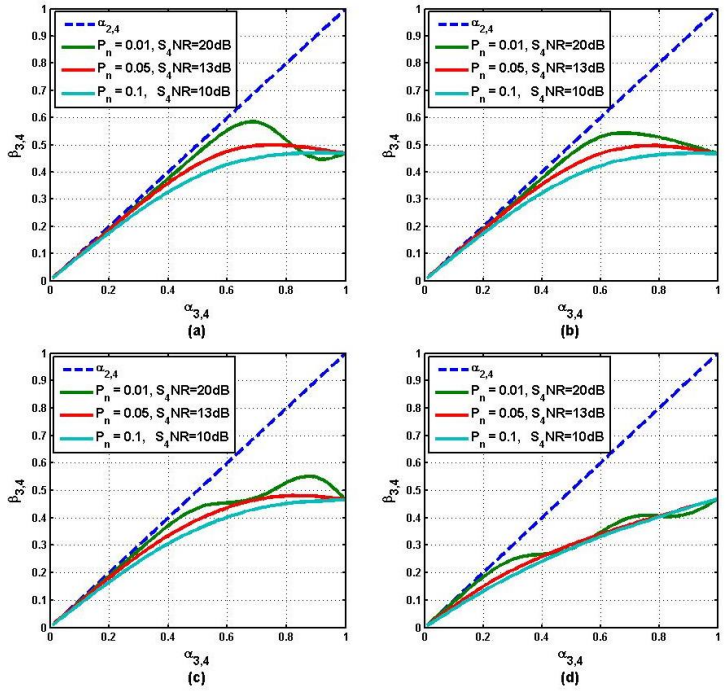

Figure 29. Plots of gain estimates $\beta_{3,4}$ vs. actual $\alpha_{3,4}$ values with fixed high S_4NR levels while $\alpha_{2,4}$ = 0.2: (a) $\alpha_{1,4}$ = 0.01; (b) $\alpha_{1,4}$ = 0.1; (c) $\alpha_{1,4}$ = 0.2; (d) $\alpha_{1,4}$ = 0.4.

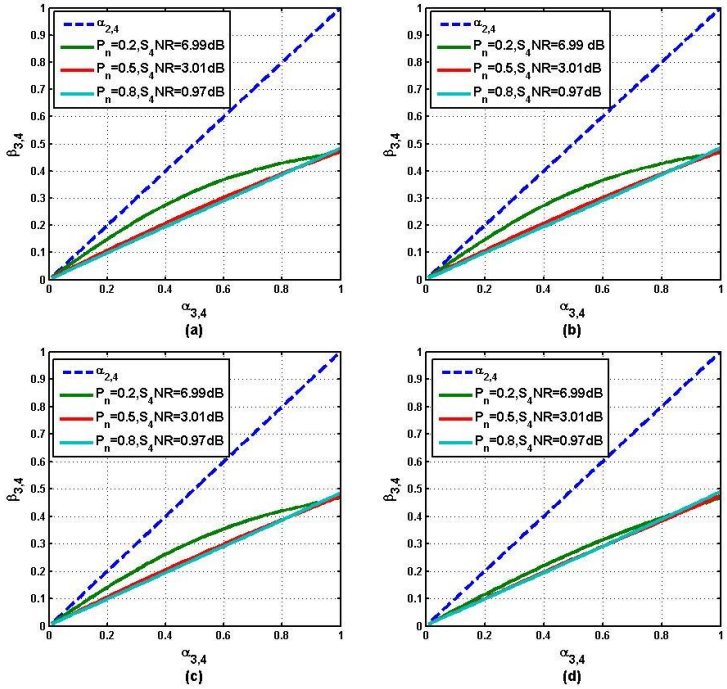

Figure 30. Plots of gain estimates $\beta_{3,4}$ vs. actual $\alpha_{3,4}$ values with fixed low S_4NR levels while $\alpha_{2,4}$ = 0.2: (a) $\alpha_{1,4}$ = 0.01; (b) $\alpha_{1,4}$ = 0.1; (c) $\alpha_{1,4}$ = 0.2; (d) $\alpha_{1,4}$ = 0.4.

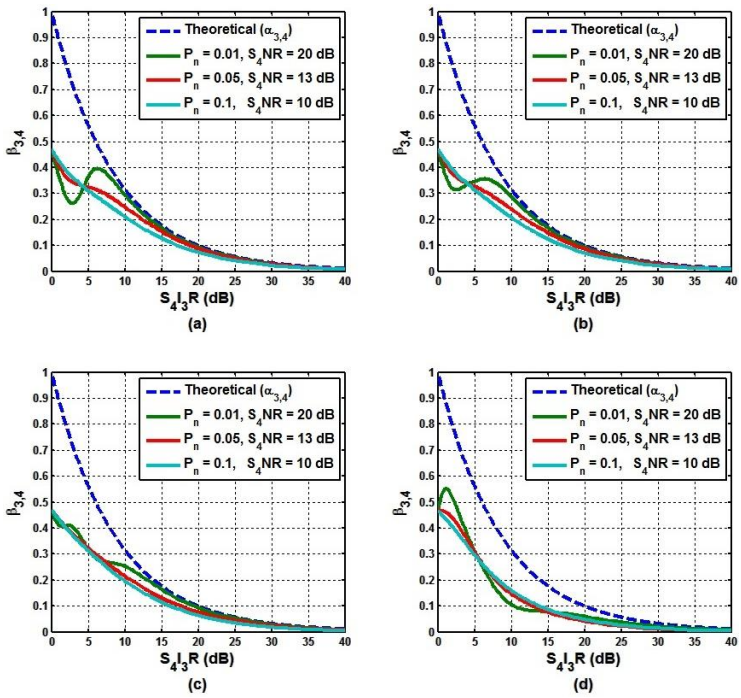

Figure 31. Plots of gain estimates $\beta_{3,4}$ vs. S_4I_3R values with fixed high S_4NR levels while $\alpha_{2,4}$ = 0.4: (a) $\alpha_{1,4}$ = 0.01; (b) $\alpha_{1,4}$ = 0. 1; (c) $\alpha_{1,4}$ = 0.2; (d) $\alpha_{1,4}$ = 0.4.

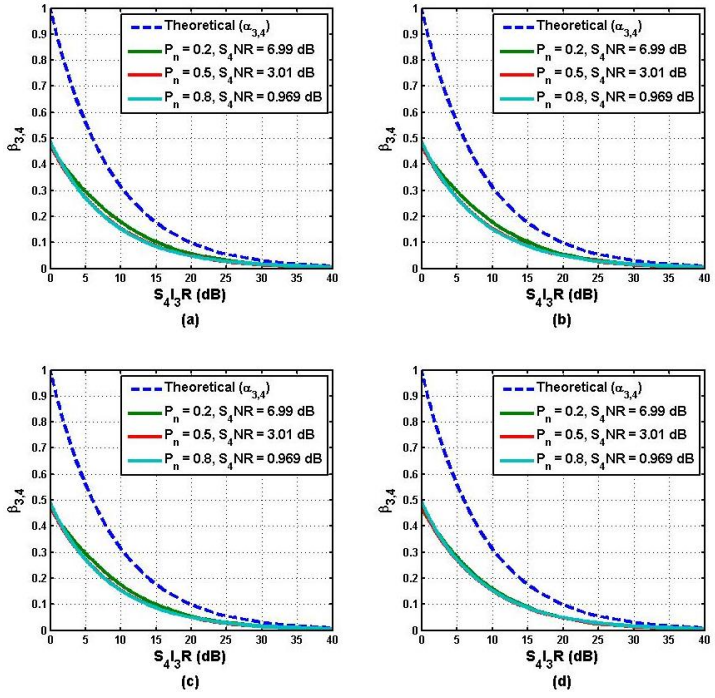

Figure 32. Plots of gain estimates $\beta_{3,4}$ vs. S_4I_3R values with fixed low S_4NR levels while $\alpha_{2,4}$ = 0.4: (a) $\alpha_{1,4}$ = 0.01; (b) $\alpha_{1,4}$ = 0. 1; (c) $\alpha_{1,4}$ = 0.2; (d) $\alpha_{1,4}$ = 0.4.

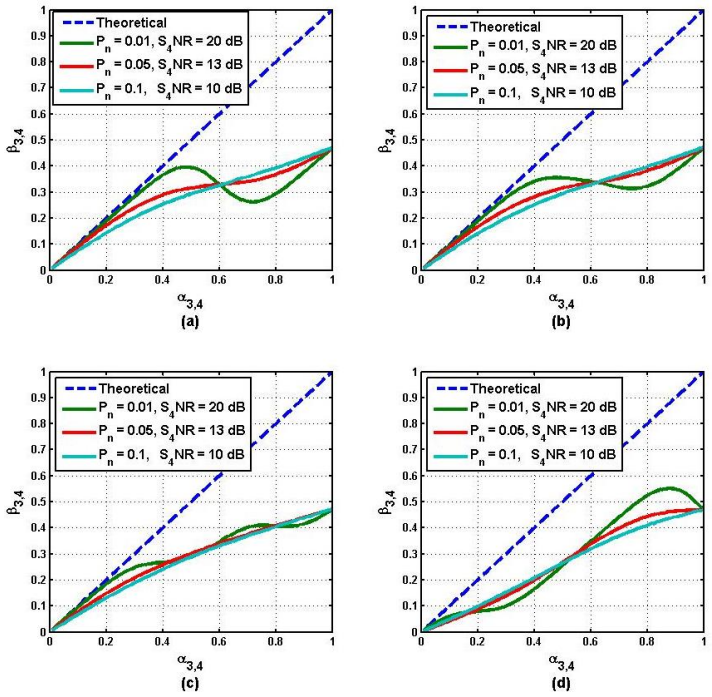

Figure 33. Plots of gain estimates $\beta_{3,4}$ vs. actual $\alpha_{3,4}$ values with fixed high S_4NR levels while $\alpha_{2,4}$ = 0.4: (a) $\alpha_{1,4}$ = 0.01; (b) $\alpha_{1,4}$ = 0.1; (c) $\alpha_{1,4}$ = 0.2; (d) $\alpha_{1,4}$ = 0.4.

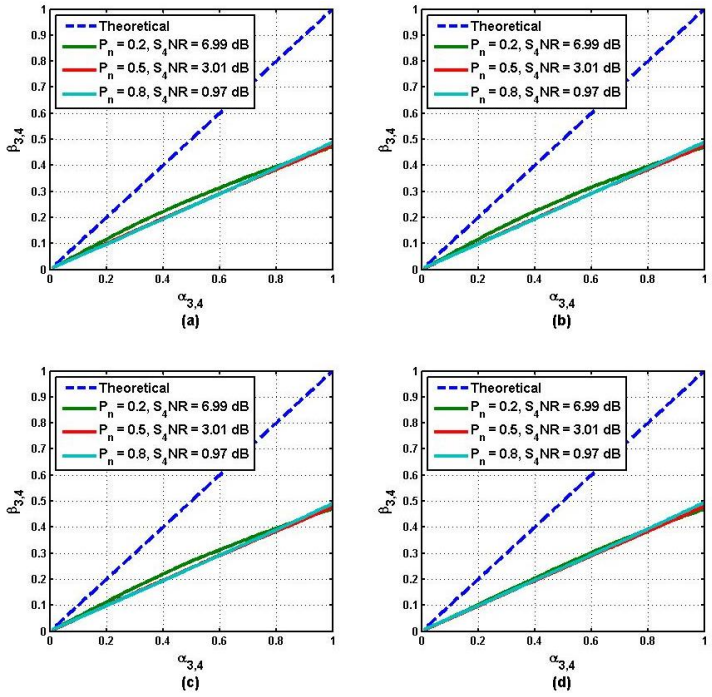

Figure 34. Plots of gain estimates $\beta_{3,4}$ vs. actual $\alpha_{3,4}$ values with fixed low S_4NR levels while $\alpha_{2,4}$ = 0.4: (a) $\alpha_{1,4}$ = 0.01; (b) $\alpha_{1,4}$ = 0.1; (c) $\alpha_{1,4}$ = 0.2; (d) $\alpha_{1,4}$ = 0.4.

2. Fix $\alpha_{3,4}$, $\alpha_{2,4}$ and $\alpha_{1,4}$, Vary S_4NR

Observing the SER of the *post* calculations for each of the combinations of gain parameter values, we better grasp the severity of the compounding effects of interference on the SOI. Only at high S_4IR levels (i.e., greater than 6.0 dB) do the generated $\hat{s}_4$ signals provide results that are considered acceptable for use. For the four-receiver system, it is unnecessary to examine the *pre* calculation results due to expected poor performance in such an interference-filled environment. The simulations that are conducted increase one or two gain parameters at a time, effectively decreasing the accuracy of each of the estimators of Equation (4.7) and therefore the performance of SER is also decreased. From Figure 35, it is seen that at relatively low α values, the SER for the *post* calculations follow the theoretical line for a QPSK system with no interference. Once the S_4IR drops below 6.0 dB, the performance starts to degrade considerably. Increasing the total interference in the system, we see that the SER continues to have a steady decrease and shifts away from an interference-free system, as seen in Figures 36 and 37.

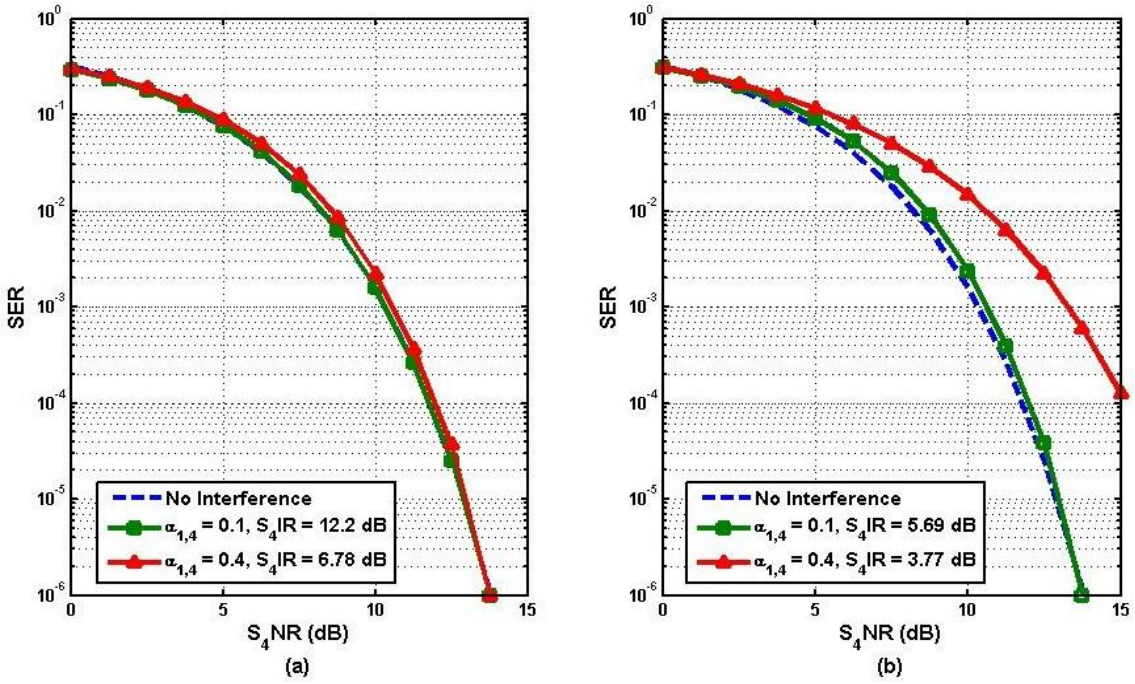

Figure 35. Performance curves of SER vs. S_4NR for *post* decision of $\hat{s}_4$ at different interference combinations when $\alpha_{3,4}$ = 0.1: (a) $\alpha_{2,4}$ = 0.2; (b) $\alpha_{2,4}$ = 0.5.

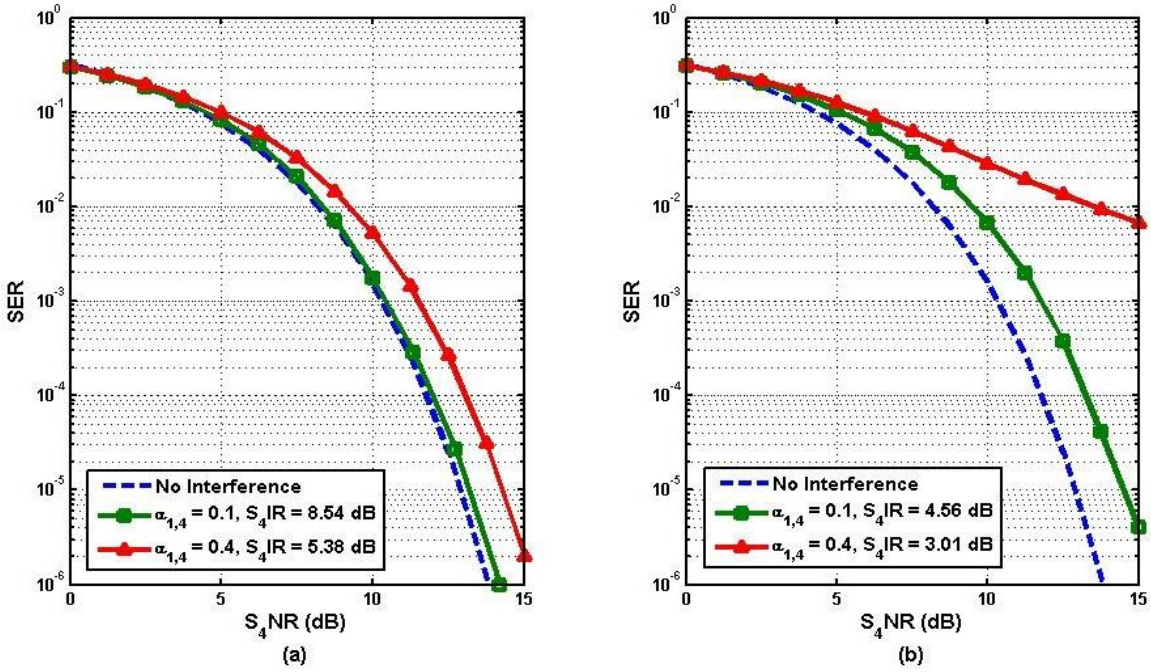

Figure 36. Performance curves of SER vs. S_4NR for *post* decision of $\hat{\mathbf{s}}_4$ at different interference combinations when $\alpha_{3,4}$ = 0.3: (a) $\alpha_{2,4}$ = 0.2; (b) $\alpha_{2,4}$ = 0.5.

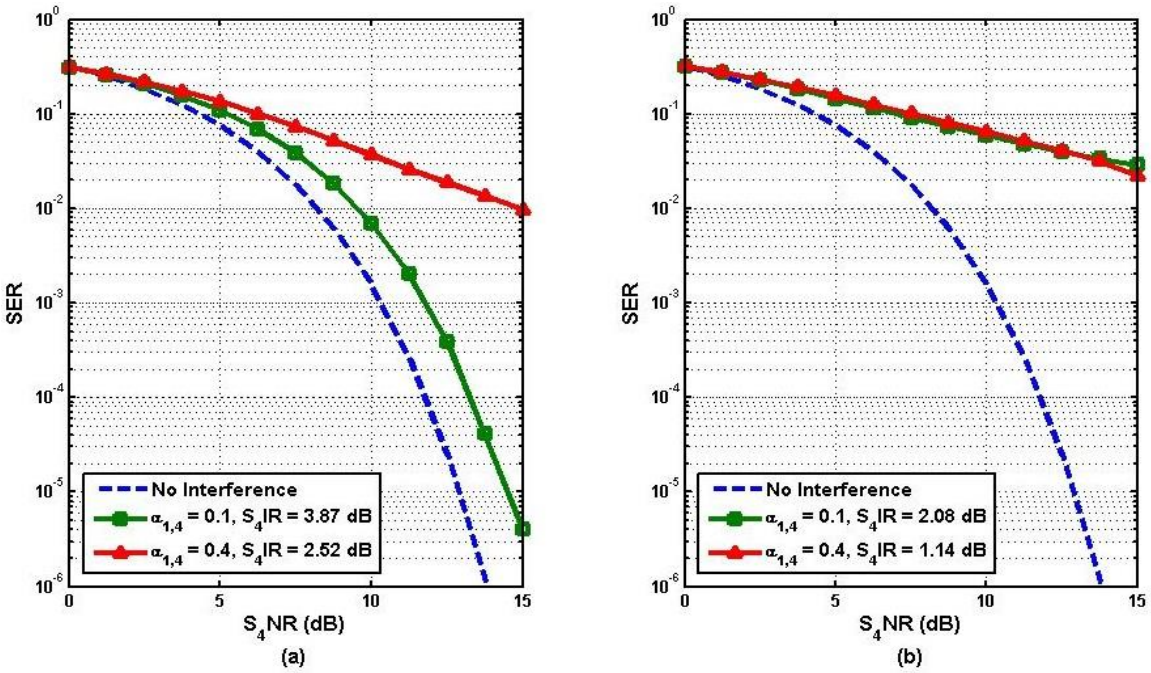

Figure 37. Performance curves of SER vs. S_4NR for *post* decision of $\hat{\mathbf{s}}_4$ at different interference combinations when $\alpha_{3,4}$ = 0.6: (a) $\alpha_{2,4}$ = 0.2; (b) $\alpha_{2,4}$ = 0.5.

Next we observe the accuracy of the estimations against the actual gain parameters that is used in each simulation. The same collection of gain values from the SER performance evaluations are used to show situations with both low and high interference. Each row from Figures 38–43 represents a different configuration of the simulation. For example, from Figure 38 we see two instances of the modeled system with the top row showing gain values and estimates for $\alpha_{3,4}$ = 0.1, $\alpha_{2,4}$ = 0.2 and $\alpha_{1,4}$ = 0.1 while the bottom row shows a different run with $\alpha_{3,4}$ = 0.1, $\alpha_{2,4}$ = 0.2 and $\alpha_{1,4}$ = 0.4.

The performance of the estimations generally show increased accuracy when higher S_4NR or S_4IR is used. As expected, once the S_4IR drops below 6.0 dB, the quality of the estimations begin to deteriorate. Some configurations even experience a reduction of accuracy with the increase of S_4NR as seen in Figure 43. Again, this is likely due to the inability of the estimators to handle scenarios where the energy of the SOI does not strongly overpower the other interference and noise energies. It should be remembered as well that the actual gain parameter estimations β are calculated with use of (4.6), which is heavily interfered by three other signals other than $\mathbf{s}_4$. In the next section, we discuss another technique to take advantage of the cleaner $\hat{\mathbf{s}}_4$ calculation in order to recalculate a better gain estimate.

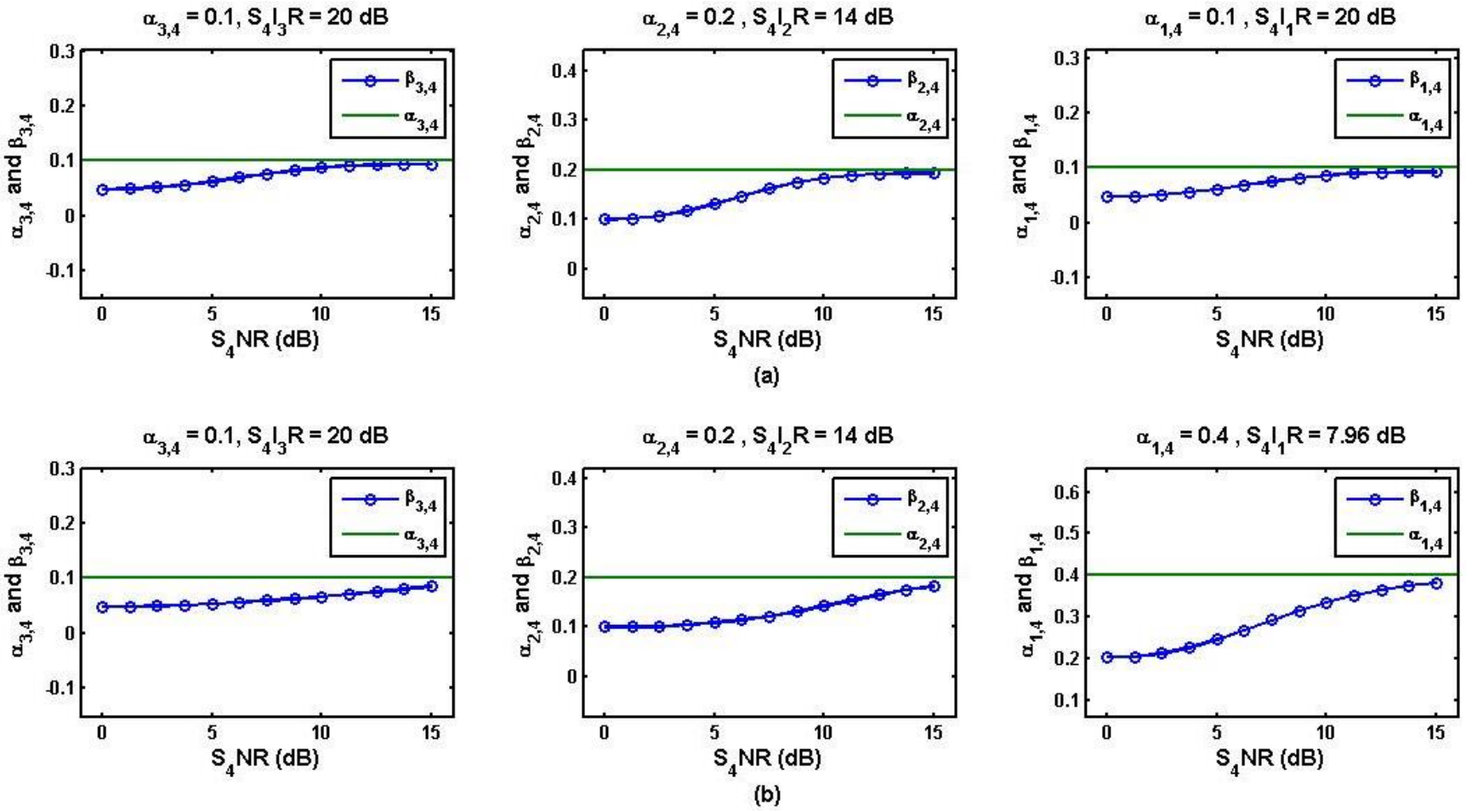

Figure 38. Plots of the actual gain parameters $\alpha_{3,4}$, $\alpha_{2,4}$, $\alpha_{1,4}$ and the estimators $\beta_{3,4}$, $\beta_{2,4}$, $\beta_{1,4}$ vs. different S_4NR values for multiple simulations of $\mathbf{y}_4$: (a) S_4IR = 12.2 dB; (b) S_4IR = 6.78 dB.

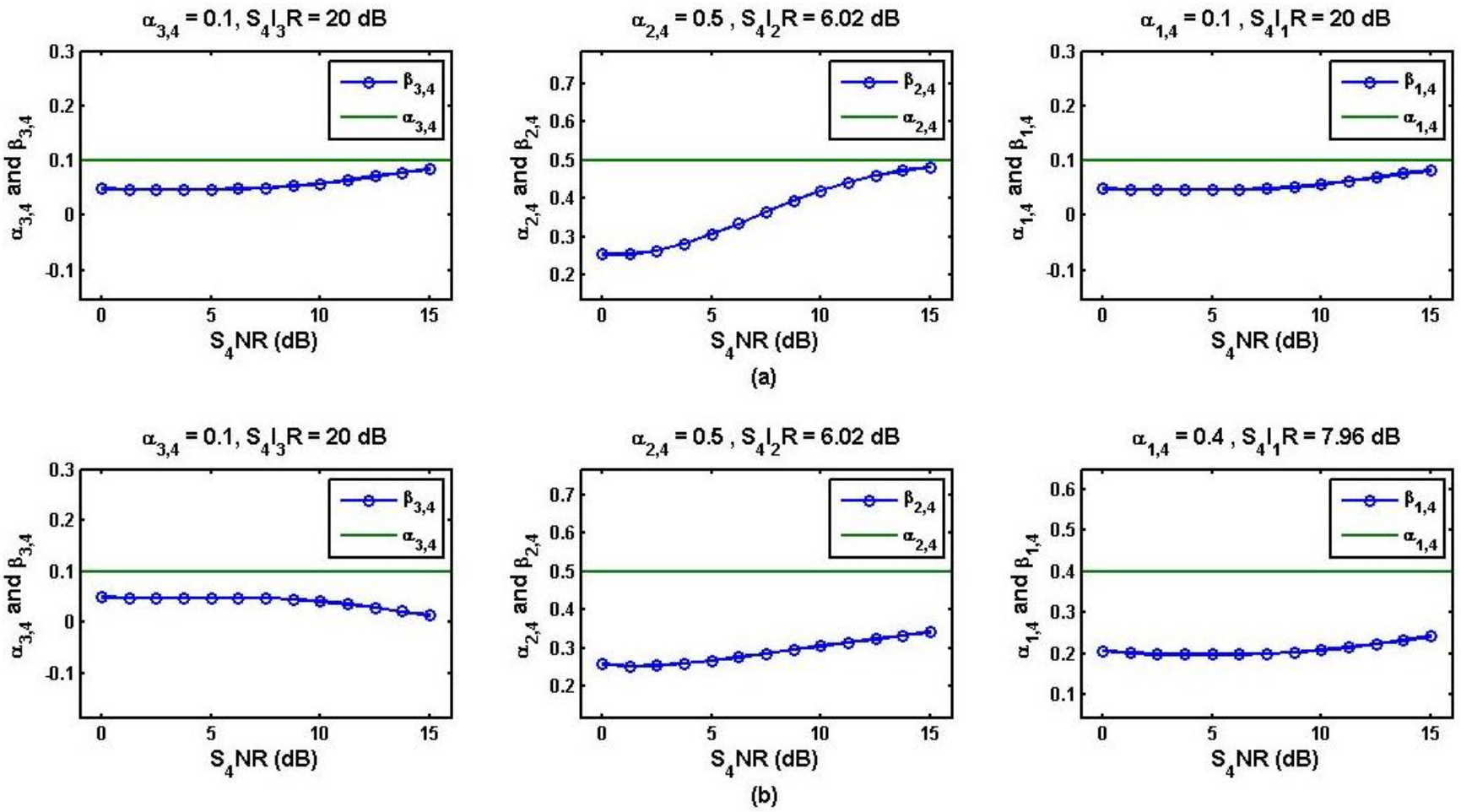

Figure 39. Plots of the actual gain parameters $\alpha_{3,4}$, $\alpha_{2,4}$, $\alpha_{1,4}$ and the estimators $\beta_{3,4}$, $\beta_{2,4}$, $\beta_{1,4}$ vs. different S_4NR values for multiple simulations of $\mathbf{y}_4$: (a) S_4IR = 5.69 dB; (b) S_4IR = 3.77 dB.

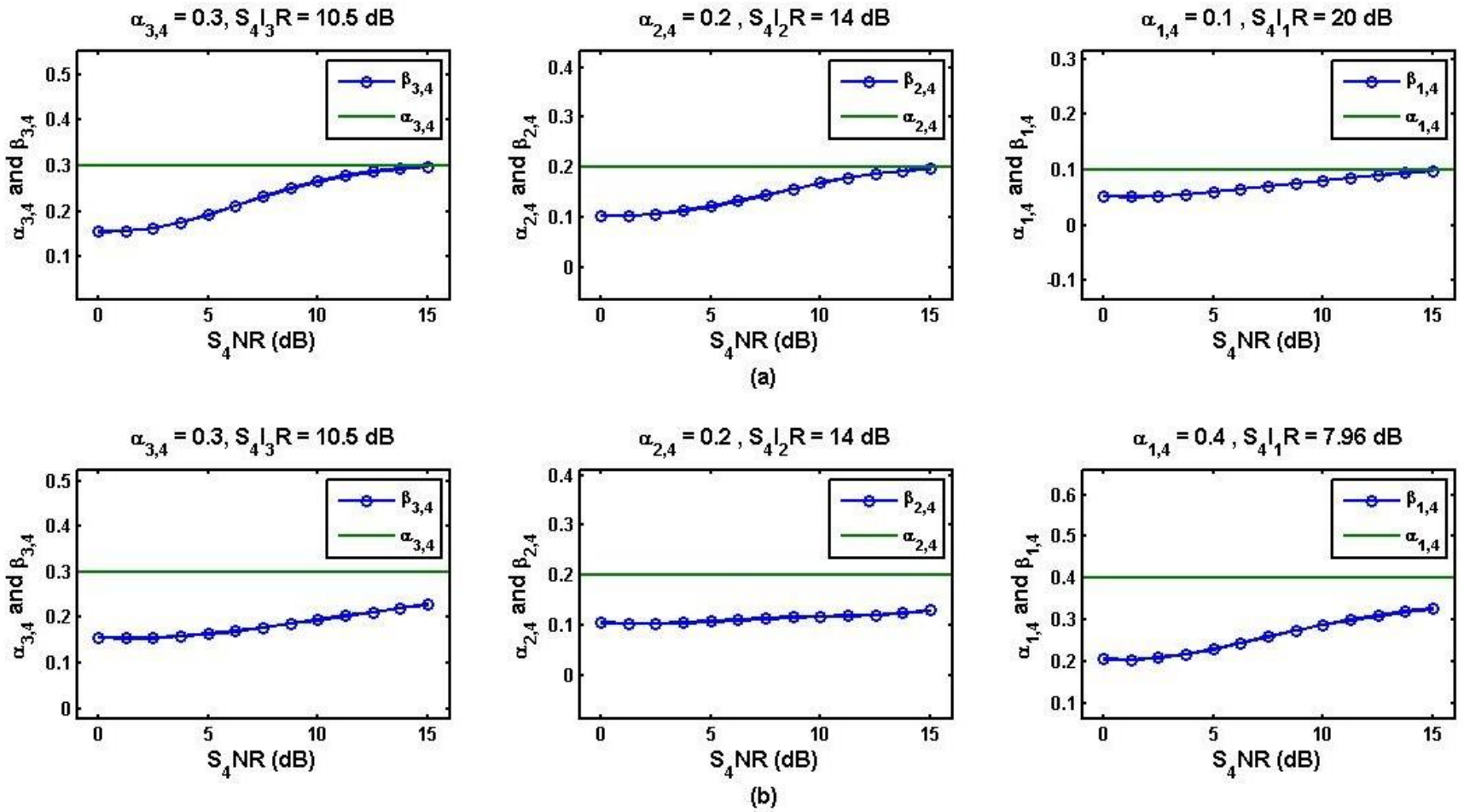

Figure 40. Plots of the actual gain parameters $\alpha_{3,4}$, $\alpha_{2,4}$, $\alpha_{1,4}$ and the estimators $\beta_{3,4}$, $\beta_{2,4}$, $\beta_{1,4}$ vs. different S_4NR values for multiple simulations of $\mathbf{y}_4$: (a) S_4IR = 8.54 dB; (b) S_4IR = 5.38 dB.

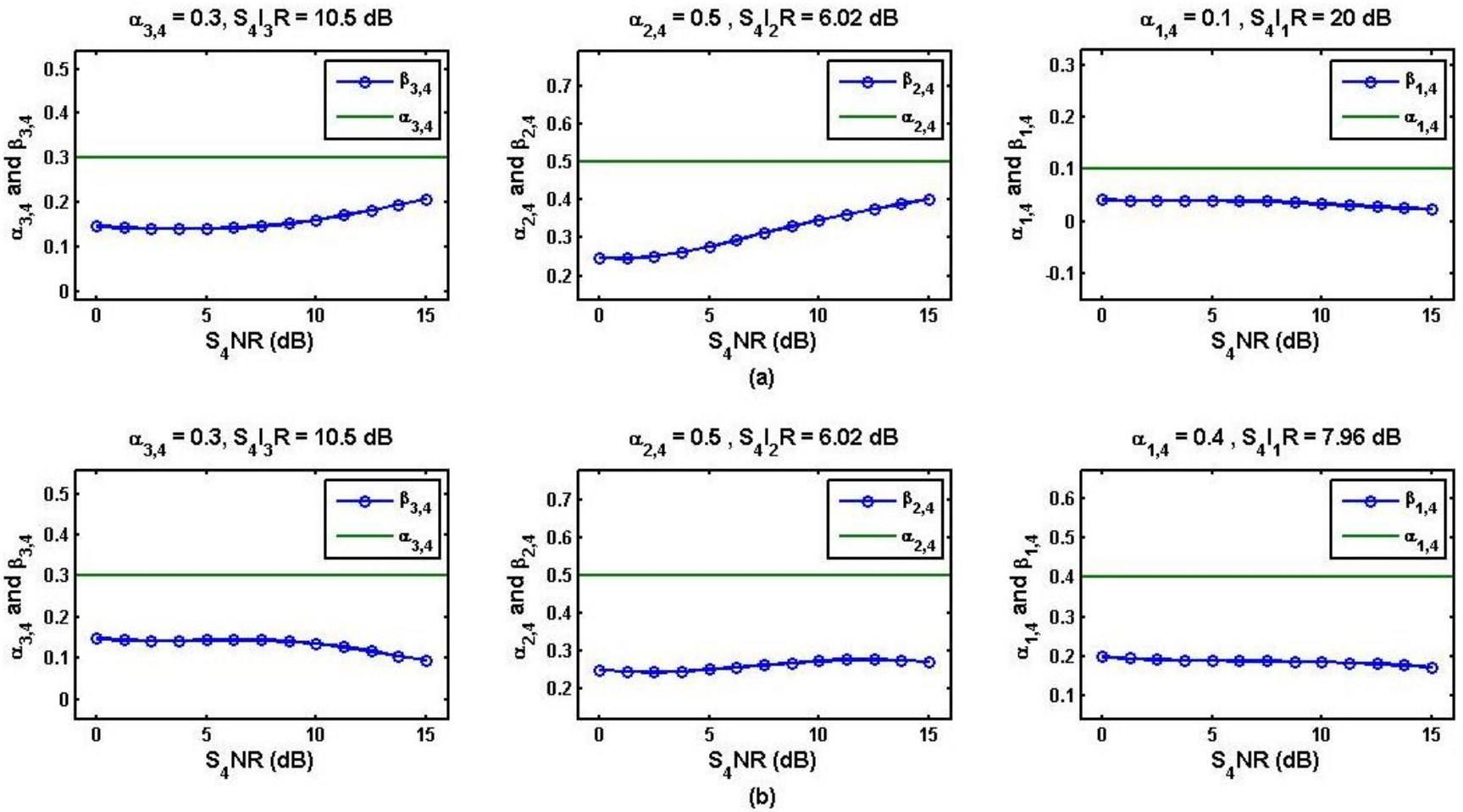

Figure 41. Plots of the actual gain parameters $\alpha_{3,4}$, $\alpha_{2,4}$, $\alpha_{1,4}$ and the estimators $\beta_{3,4}$, $\beta_{2,4}$, $\beta_{1,4}$ vs. different S_4NR values for multiple simulations of $\mathbf{y}_4$: (a) S_4IR = 4.56 dB; (b) S_4IR = 3.01 dB.

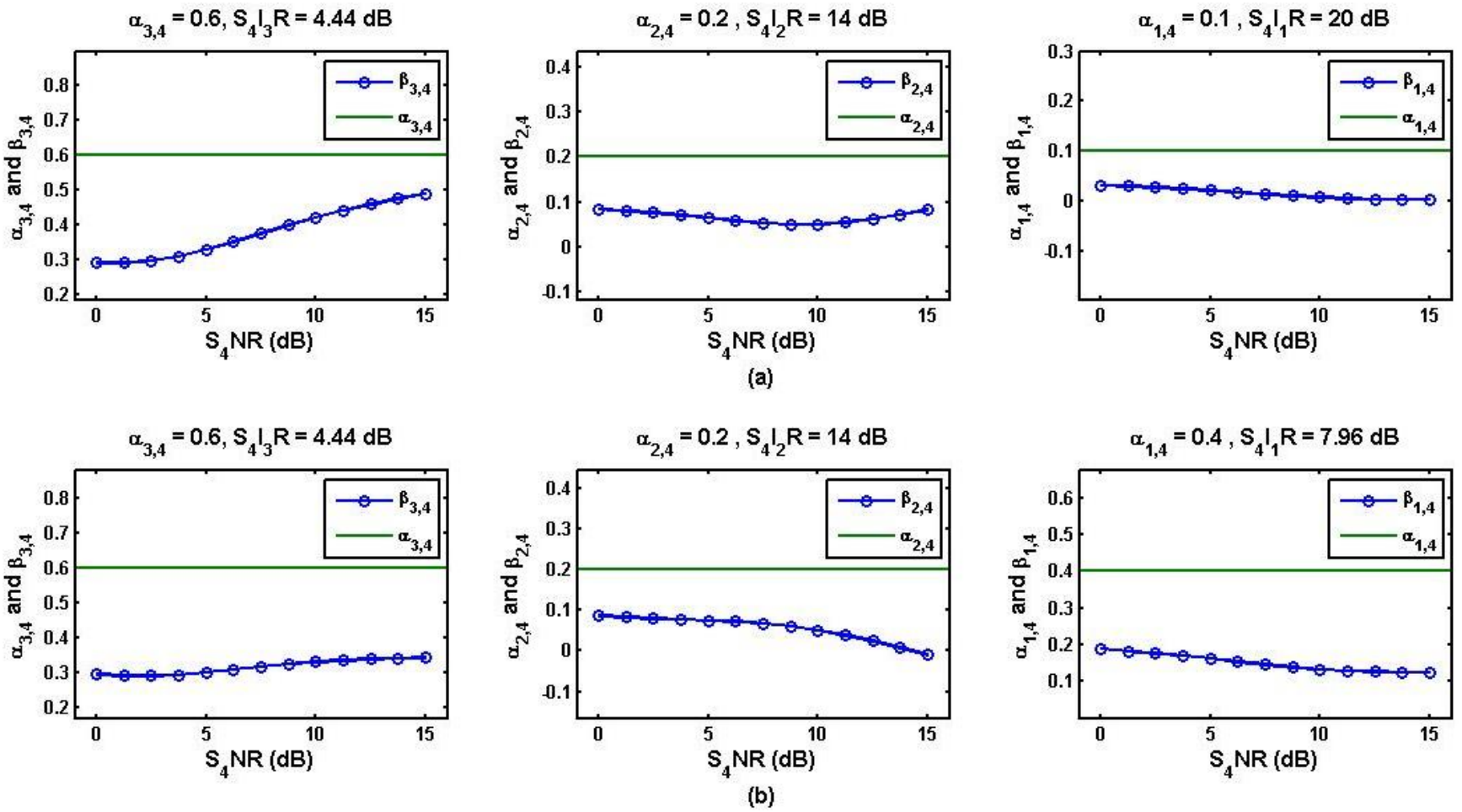

Figure 42. Plots of the actual gain parameters $\alpha_{3,4}$, $\alpha_{2,4}$, $\alpha_{1,4}$ and the estimators $\beta_{3,4}$, $\beta_{2,4}$, $\beta_{1,4}$ vs. different S_4NR values for multiple simulations of $\mathbf{y}_4$: (a) S_4IR = 3.87 dB; (b) S_4IR = 2.52 dB.

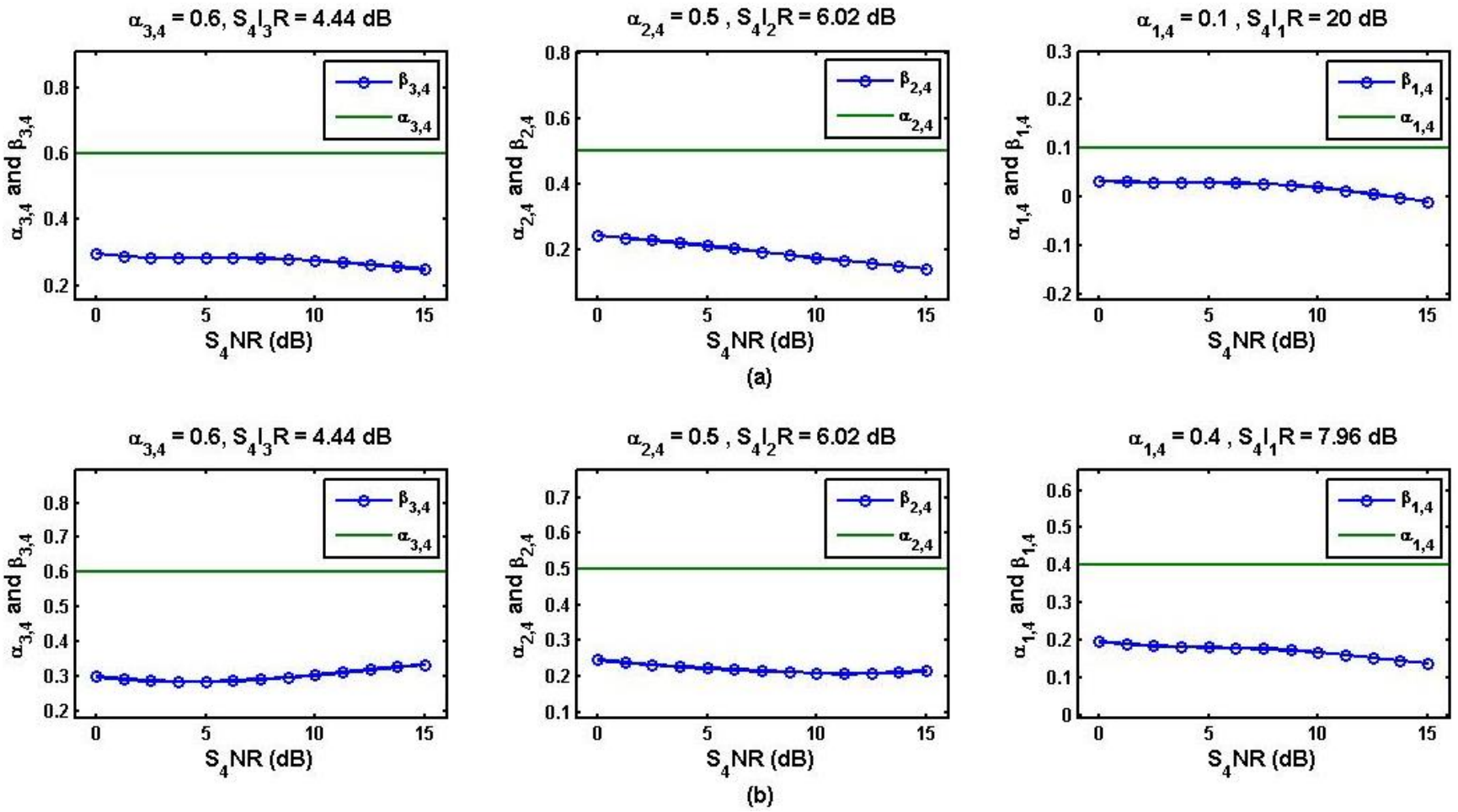

Figure 43. Plots of the actual gain parameters $\alpha_{3,4}$, $\alpha_{2,4}$, $\alpha_{1,4}$ and the estimators $\beta_{3,4}$, $\beta_{2,4}$, $\beta_{1,4}$ vs. different S_4NR values for multiple simulations of $\mathbf{y}_4$: (a) S_4IR = 2.08 dB; (b) S_4IR = 1.14 dB.

C. RESULTS OF ITERATIVE ESTIMATION CALCULATION

With the combination of the multiple interferences negatively affecting the performance of the estimators, another technique is employed to improve the accuracy of the β calculations. From Equation (4.7), we see that the estimators make use of the *pre* calculation $\tilde{\mathbf{s}}_4$ in order to make a calculation. By inspection, it is clear this is not optimal as Rx4 is required to make a decision based simply on the value of $\mathbf{y}_4$ which is heavily interfered by the other signals in the environment. Therefore, by reusing the cleaner *post* decision $\hat{\mathbf{s}}_4$ with the estimate equations, we are able to produce a more accurate estimator through a second round of calculation. Substituting $\tilde{\mathbf{s}}_4$ with Equation (4.8) and incorporating it back into (4.7), we get

$$\begin{bmatrix} \beta_{3,4} \\ \beta_{2,4} \\ \beta_{1,4} \end{bmatrix} = \begin{bmatrix} X_1 & Y_1 & Z_1 \\ X_2 & Y_2 & Z_2 \\ X_3 & Y_3 & Z_3 \end{bmatrix}^{-1} \begin{bmatrix} A \\ B \\ C \end{bmatrix}, \tag{4.11}$$

where the updated A, B and C terms are now $A = \mathrm{Re}\{\mathbf{y}_4{}^H \hat{\mathbf{s}}_3\} - \mathrm{Re}\{\hat{\rho}_{4,3}\}$, $B = \mathrm{Re}\{\mathbf{y}_4{}^H \hat{\mathbf{s}}_2\} - \mathrm{Re}\{\hat{\rho}_{4,2}\}$ and $C = \mathrm{Re}\{\mathbf{y}_4{}^H \hat{\mathbf{s}}_1\} - \mathrm{Re}\{\hat{\rho}_{4,1}\}$. Increasing the number of recalculations, or rounds, also continues to improve performance of the estimators, in turn creating even cleaner estimates of $\hat{\mathbf{s}}_4$. The Monte Carlo simulations are performed again, this time iterating the decision process, providing updated estimate and re-demodulated *post* signals. As can be seen in Figures 44 and 45, two P_n levels are set to illustrate one system with high SNR and another with low SNR. The first and third iterated rounds are illustrated and it is clear that the use of $\hat{\mathbf{s}}_4$ in (4.11) vastly improves the quality of the estimates in Round 3 (Rd3).

Even with $\alpha_{2,4}$ = 0.7, the performance of the estimators at the end of Rd3 shows the considerable improvement in estimation accuracy as seen in Figures 46 and 47. Without this iterative recalculation, there is little chance of successfully extracting SOIs from the received signals.

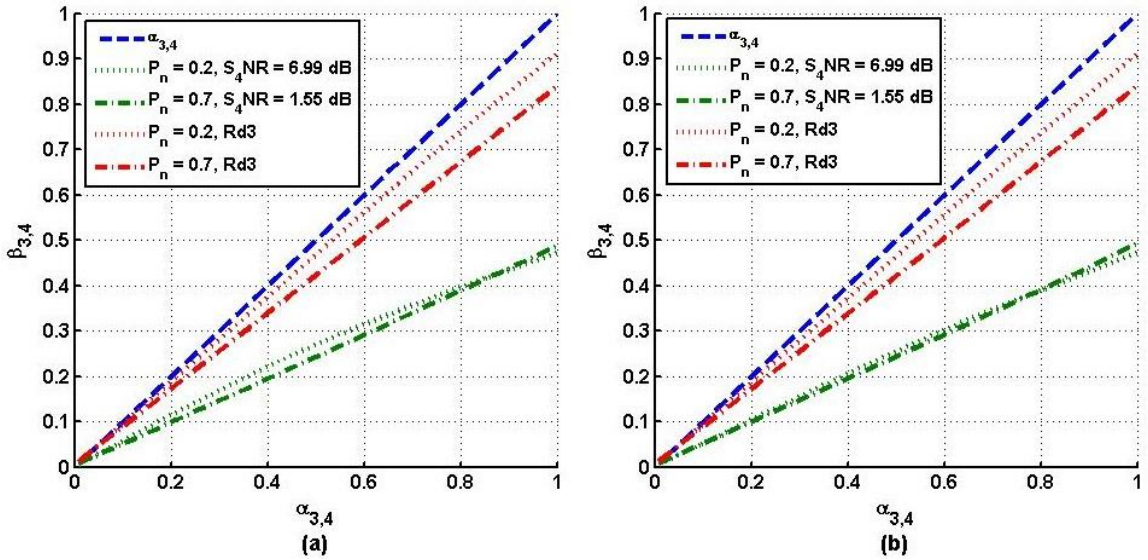

Figure 44. Iterative gain estimates of $\beta_{3,4}$ vs. $\alpha_{3,4}$ with fixed S_4NR levels while $\alpha_{2,4}$ = 0.4: (a) $\alpha_{1,4}$ = 0.2; (b) $\alpha_{1,4}$ = 0.4.

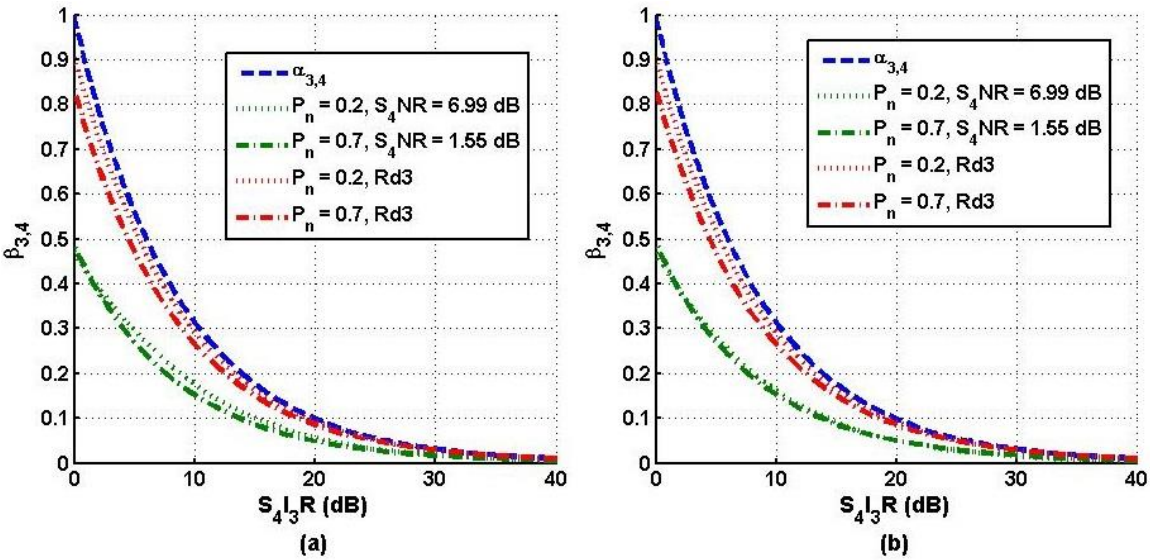

Figure 45. Iterative gain estimates of $\beta_{3,4}$ vs. S_4I_3R with fixed S_4NR while $\alpha_{2,4}$ = 0.4: (a) $\alpha_{1,4}$ = 0.2; (b) $\alpha_{1,4}$ = 0.4.

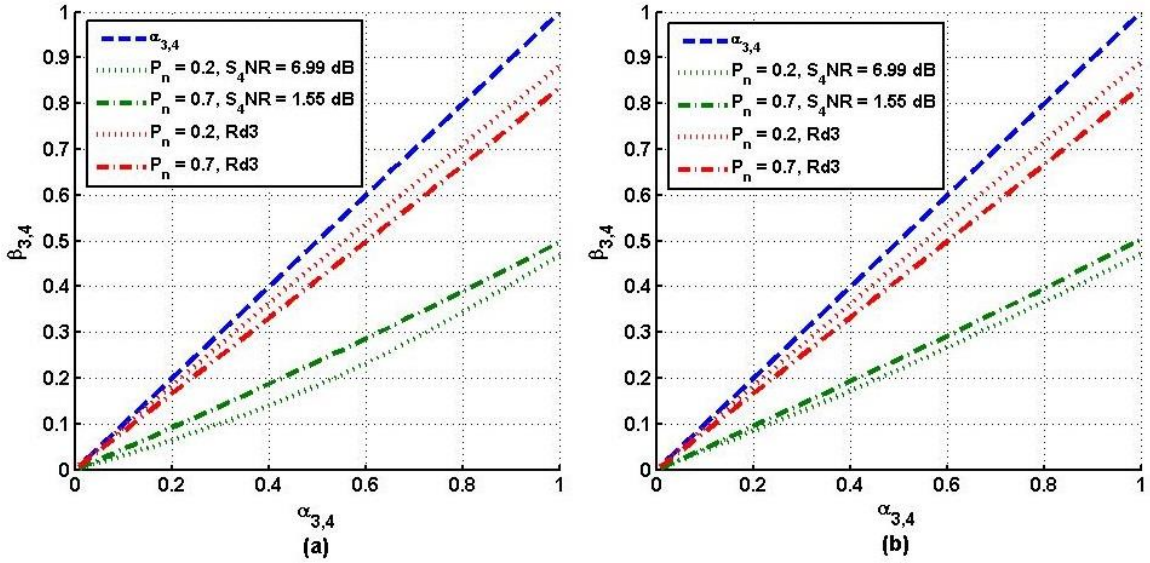

Figure 46. Iterative gain estimates of $\beta_{3,4}$ vs. $\alpha_{3,4}$ with fixed S_4NR levels while $\alpha_{2,4}$ = 0.7: (a) $\alpha_{1,4}$ = 0.2; (b) $\alpha_{1,4}$ = 0.4.

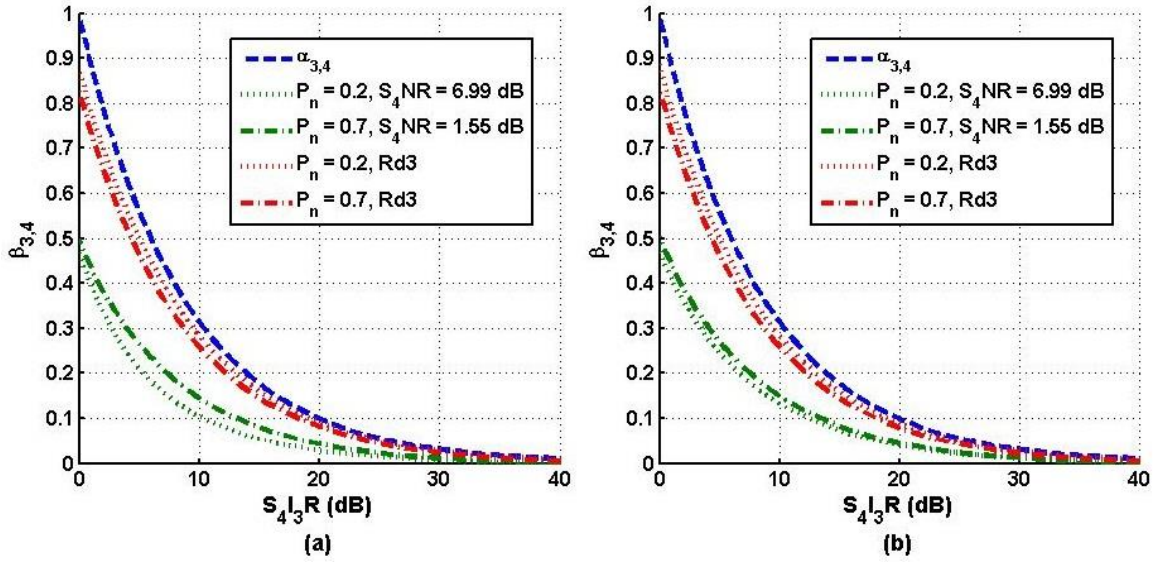

Figure 47. Iterative gain estimates of $\beta_{3,4}$ vs. S_4I_3R with fixed S_4NR while $\alpha_{2,4}$ = 0.7: (a) $\alpha_{1,4}$ = 0.2; (b) $\alpha_{1,4}$ = 0.4.

To really see the positive effect of this iterative gain estimation, we again view the estimates as they are recalculated alongside the actual gain parameter used in the specific configuration. As seen in Figures 48–51, each row demonstrates the three amplitude gain parameters associated with the interfering signals of $\mathbf{y}_4$ for one run of the simulation. Each plot also shows the results of the original gain estimate calculation as well as two additional rounds (i.e., Rd2 and Rd3) of re-estimation. For the configurations which previously suffered immense performance degradation due to high amount of interference in the received signal, this new technique greatly enhances estimation accuracy. Even when the S_4IR is very low (e.g., Figure 51b with 0.46 dB), the third round of iterative estimate calculation provides nearly perfect estimates at high S_4NR.

In addition to the improved accuracy of the gain estimates, another result from this iterative technique is that each new round also yields a more accurate $\hat{\mathbf{s}}_4$ calculation. The performance curves for this IC approach show significantly improved SER for low to medium values of S_4NR levels, as seen in Figures 52 and 53. The resulting SERs from the second and third rounds now follow the theoretical curve from low to medium S_4NR. However, it is important to notice that at high S_4NR levels, there appears to be a performance "floor", where no amount of reduction of noise reduces SER below about 10^{-3}. We believe that is likely due to the fact that $\hat{\mathbf{s}}_1$, $\hat{\mathbf{s}}_2$, $\hat{\mathbf{s}}_3$ are themselves estimates which are slightly corrupted with specific noise power in the simulation. Perhaps if these reference signals were set up with higher SNR, then the performance floor could be lowered.

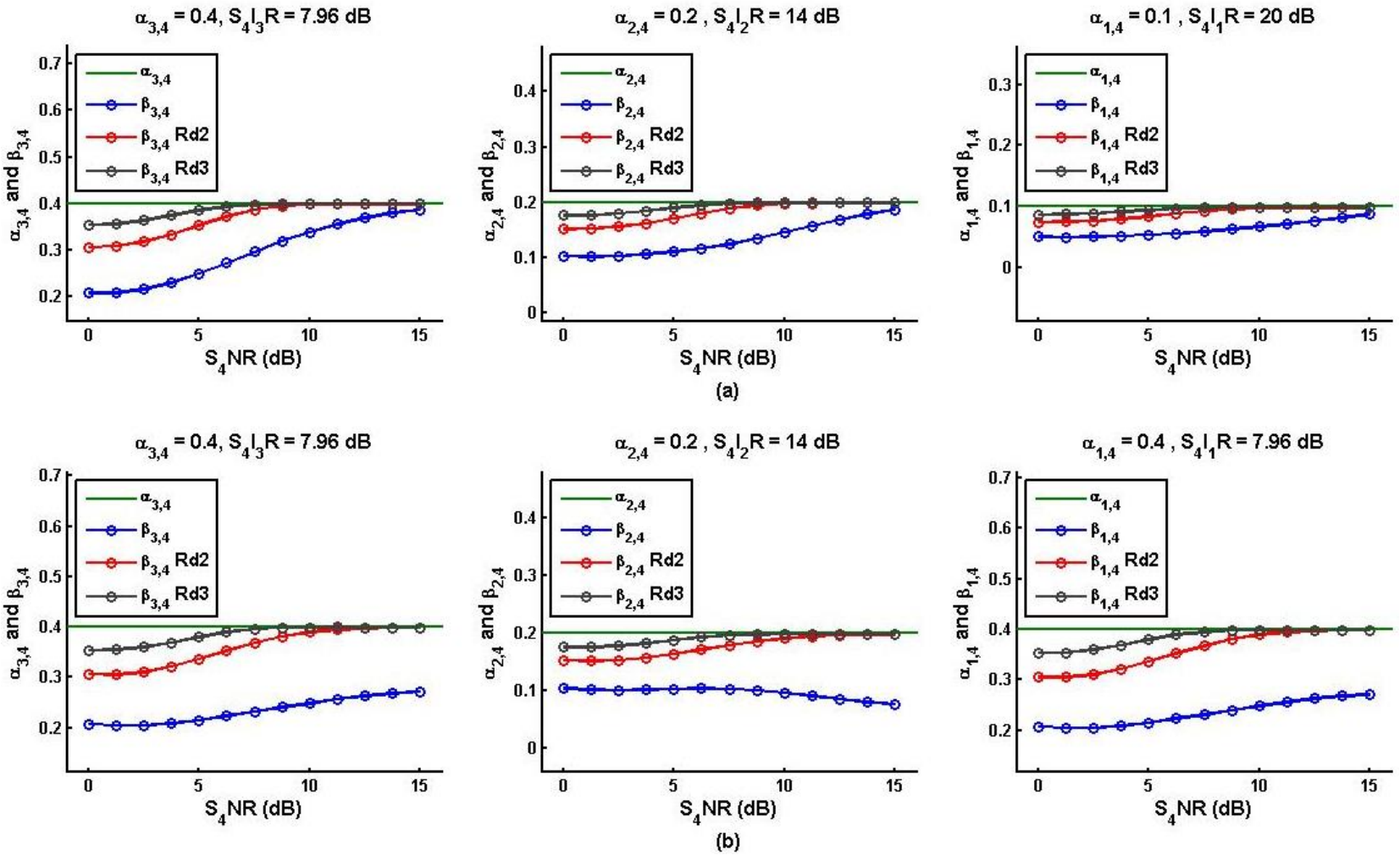

Figure 48. Plots of the actual gain parameters $\alpha_{3,4}$, $\alpha_{2,4}$, $\alpha_{1,4}$ and the iterated estimations of $\beta_{3,4}$, $\beta_{2,4}$, $\beta_{1,4}$ vs. different S_4NR values for multiple simulations of $\mathbf{y}_4$: (a) S_4IR = 6.78 dB; (b) S_4IR = 4.44 dB.

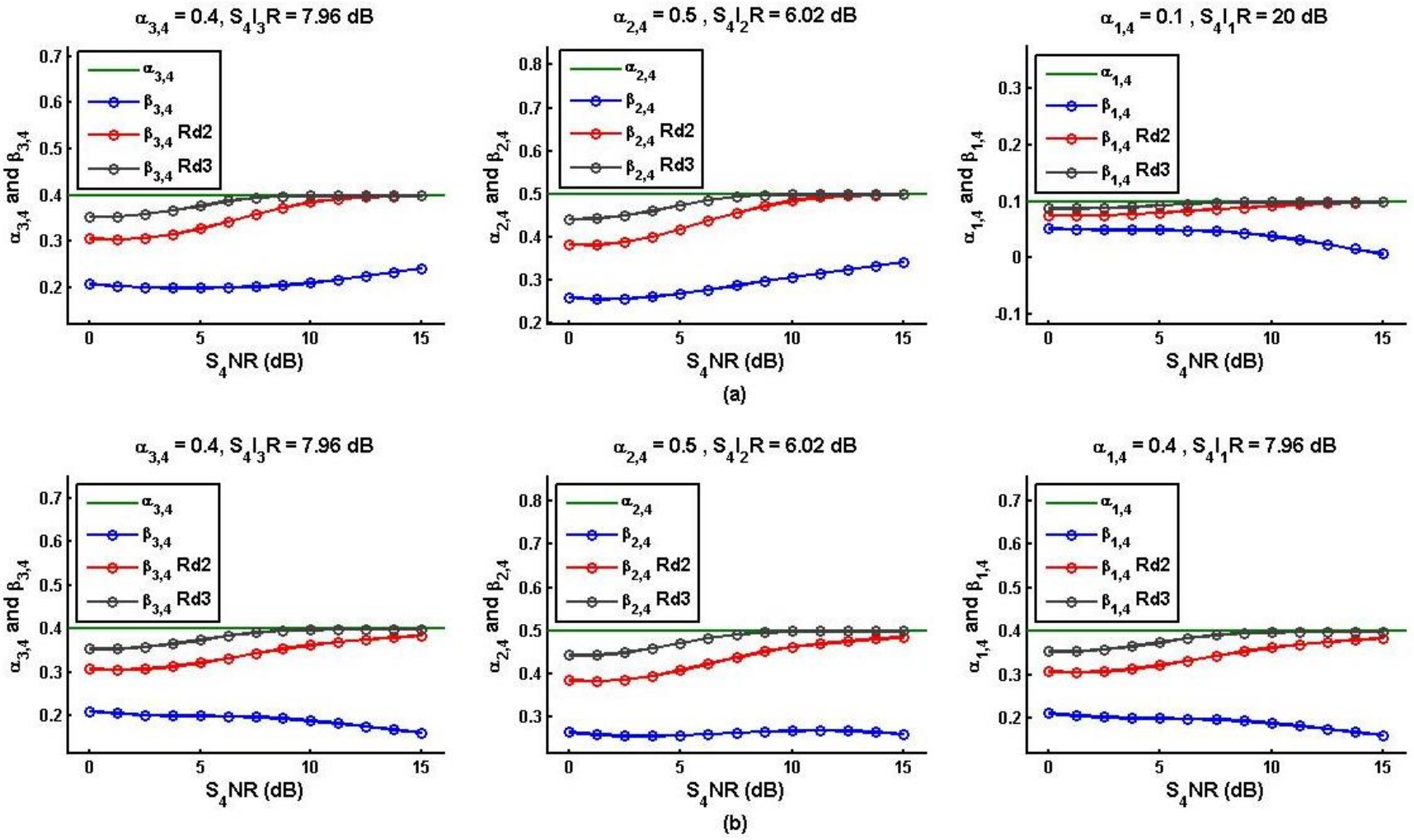

Figure 49. Plots of the actual gain parameters $\alpha_{3,4}$, $\alpha_{2,4}$, $\alpha_{1,4}$ and the iterated estimations of $\beta_{3,4}$, $\beta_{2,4}$, $\beta_{1,4}$ vs. different S_4NR values for multiple simulations of $\mathbf{y}_4$: (a) S_4IR = 3.77 dB; (b) S_4IR = 2.44 dB.

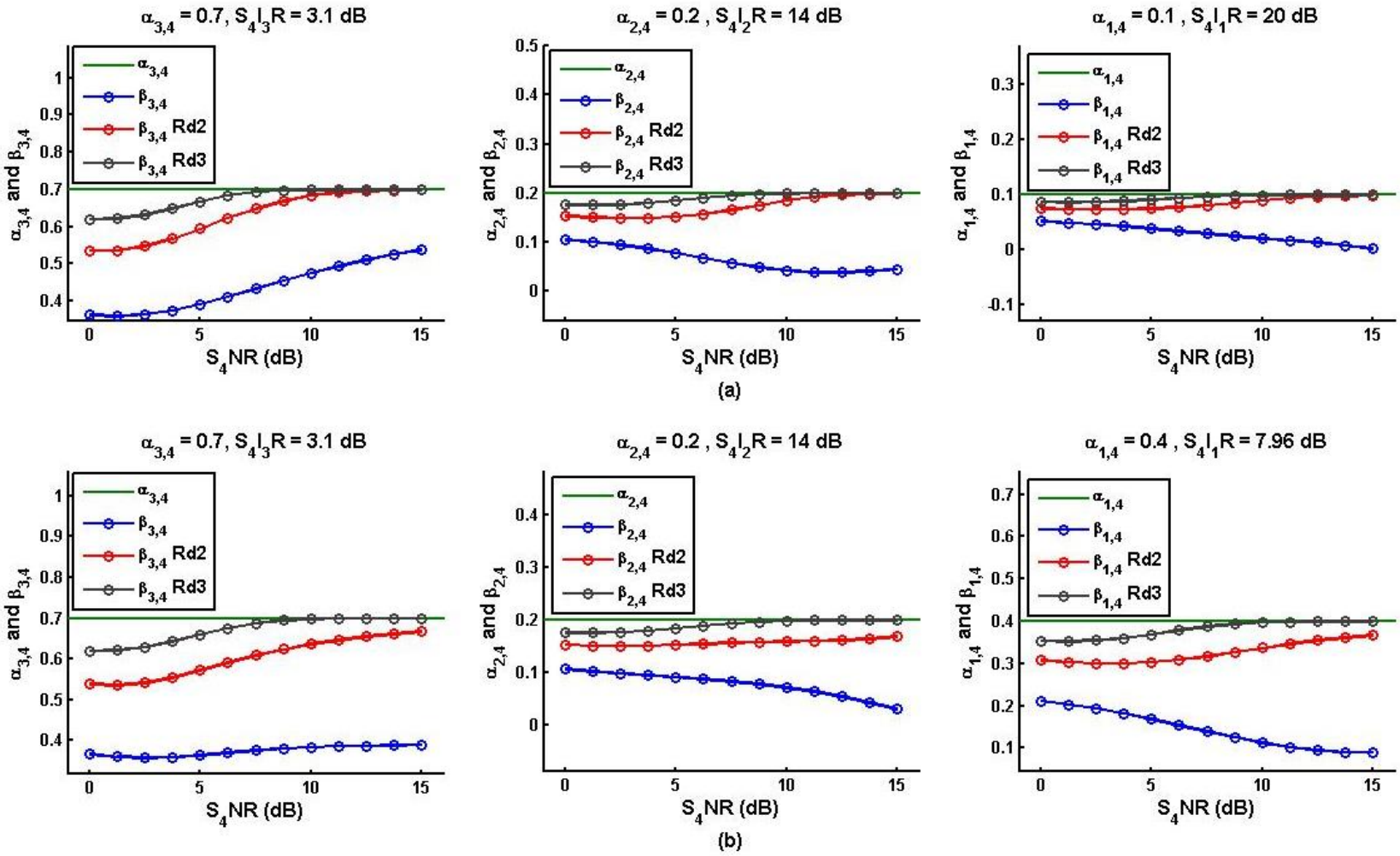

Figure 50. Plots of the actual gain parameters $\alpha_{3,4}$, $\alpha_{2,4}$, $\alpha_{1,4}$ and the iterated estimations of $\beta_{3,4}$, $\beta_{2,4}$, $\beta_{1,4}$ vs. different S_4NR values for multiple simulations of $\mathbf{y}_4$: (a) S_4IR = 2.68 dB; (b) S_4IR = 1.61 dB.

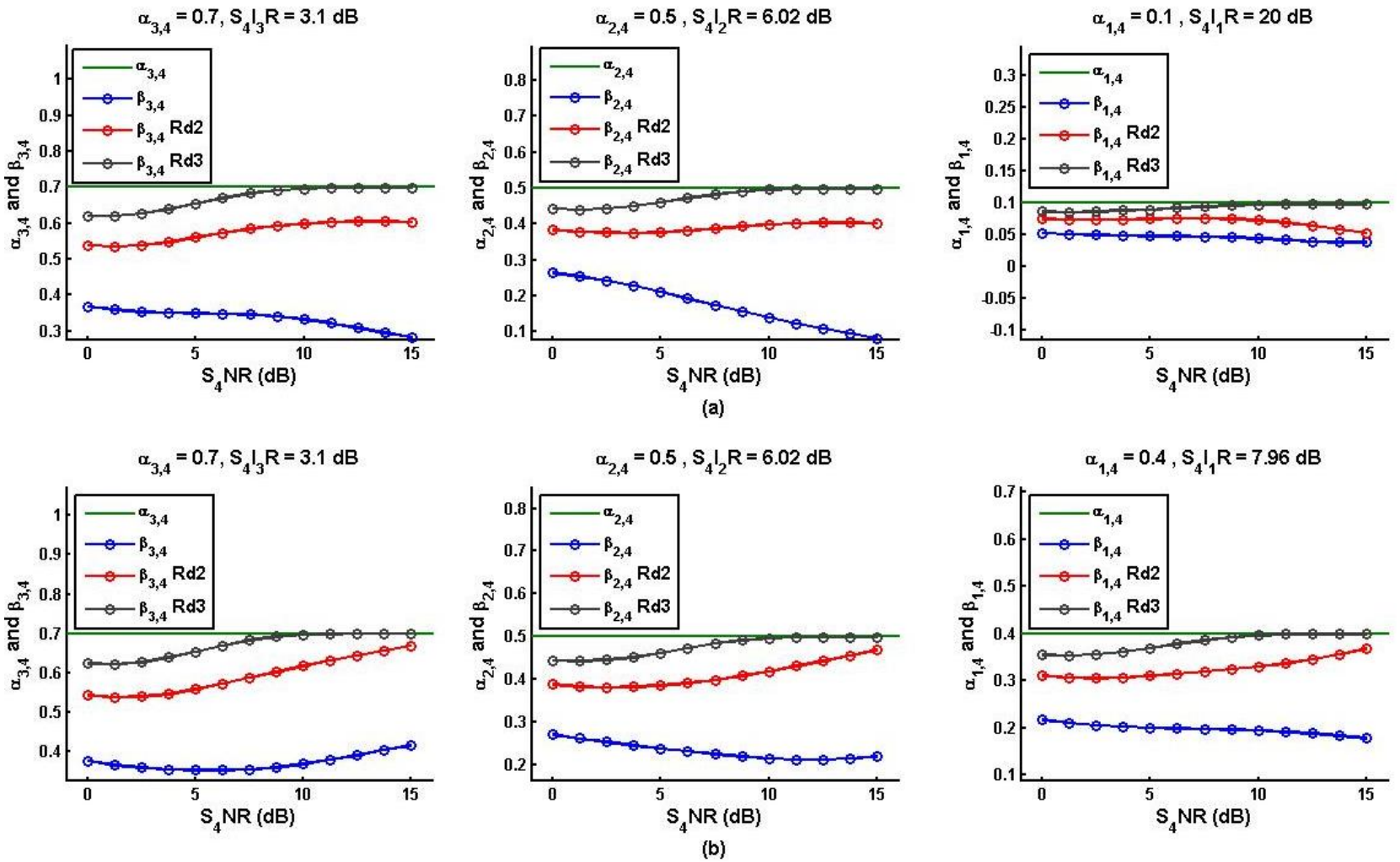

Figure 51. Plots of the actual gain parameters $\alpha_{3,4}$, $\alpha_{2,4}$, $\alpha_{1,4}$ and the iterated estimations of $\beta_{3,4}$, $\beta_{2,4}$, $\beta_{1,4}$ vs. different S_4NR values for multiple simulations of $\mathbf{y}_4$: (a) S_4IR = 1.25 dB; (b) S_4IR = 0.458 dB.

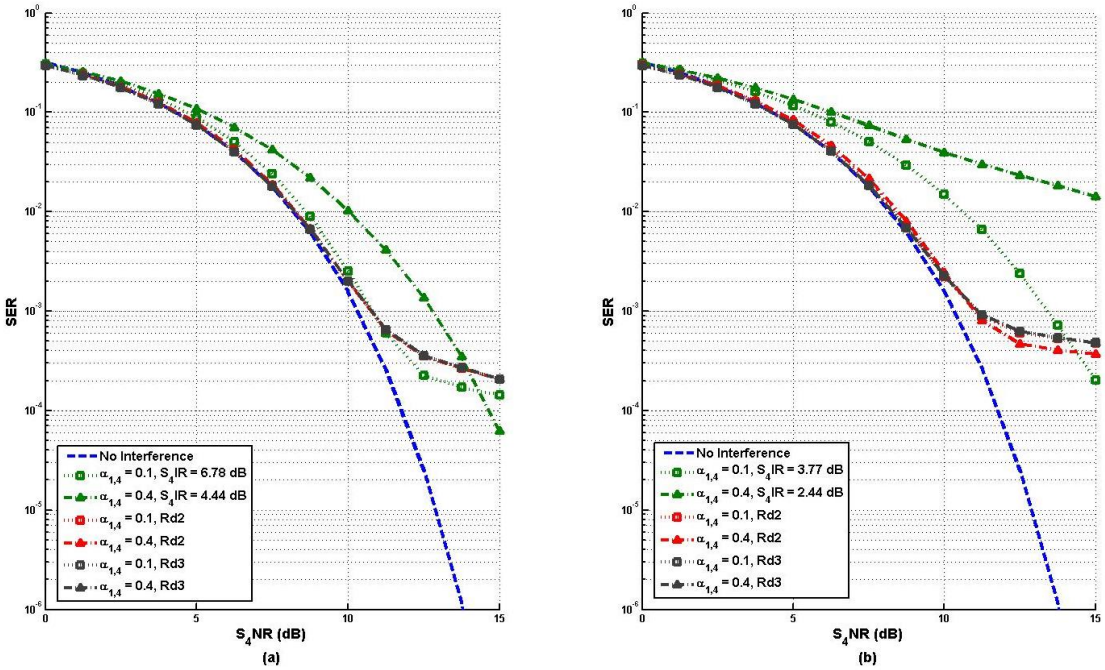

Figure 52. Performance curves of SER vs. S_4NR for iterated $\hat{\mathbf{s}}_4$ calculation at different interference combinations when $\alpha_{3,4}$ = 0.4: (a) $\alpha_{2,4}$ = 0.2; (b) $\alpha_{2,4}$ = 0.5.

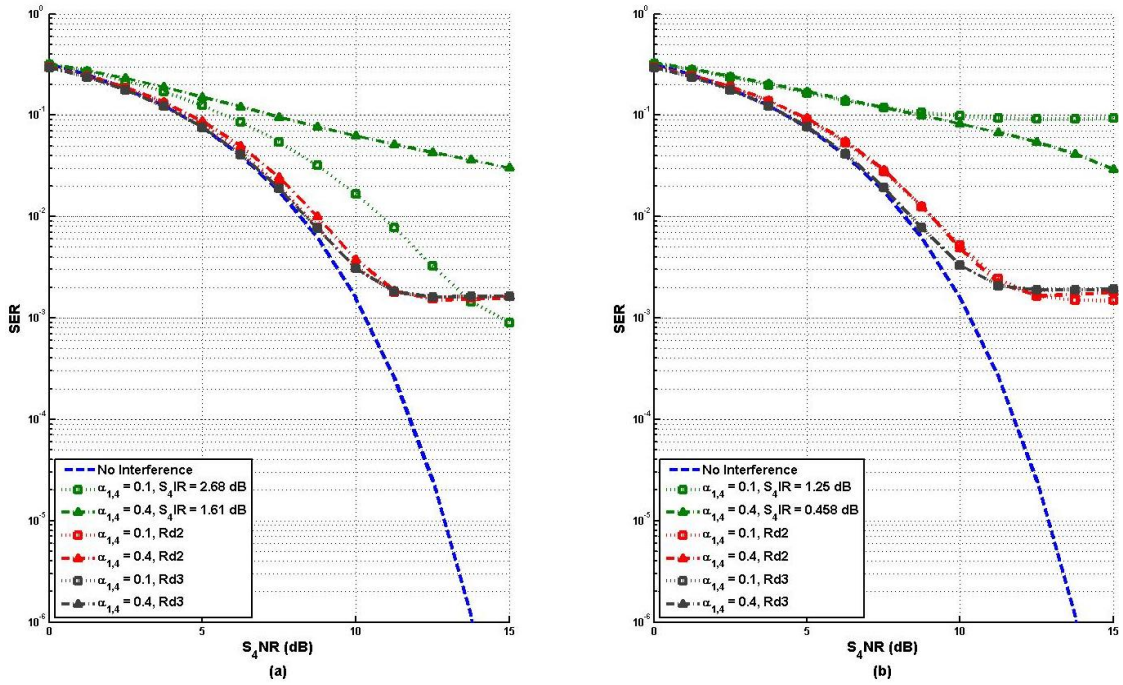

Figure 53. Performance curves of SER vs. S_4NR for iterated $\hat{\mathbf{s}}_4$ calculations at different interference combinations when $\alpha_{3,4}$ = 0.7: (a) $\alpha_{2,4}$ = 0.2; (b) $\alpha_{2,4}$ = 0.5.

V. CONCLUSIONS AND RECOMMENDATIONS

The success of RSIC relies on the initial reception of an interference-free reference signal and the accuracy of the amplitude gain estimation of the interfering signal. This estimation is crucial in correctly subtracting the interference a system experiences from multiple transmitters. It was observed that factors such as noise and compounding interference greatly impact the accuracy of the estimators used in the Monte Carlo simulations.

A. CONCLUSIONS

For this thesis, it was assumed that clean reference signals were available for subtracting interference from subsequent receivers. Obviously, the placement of said receivers in favorable locations is vital to ensuring cancellation of wanted interference. For the best results, it is advised to have the receiver placed so that the energy of the desired signal is much greater than the energy of interfering signals in the area.

The LSE estimation method was utilized in this thesis and while capable of finding accurate estimates for systems with low interference, its limitation was observed when attempting to estimate values of α that approached 1.0. At these levels, the amount of interference in the received signals affected the symbols such that calculations for the estimators could not produce a satisfactory β value. Introduction of an iterative gain estimation technique vastly improved the performance of estimates in a four-receiver system. The technique may also work for whatever number of receivers.

Cleary, the noise and interference present in the systems play a major part in determining the amplitude gain parameters, and the higher the SNR values are for a signal, the more accurate an estimation is expected to become. In turn, this provides for a more accurate *post* demodulation the desired signal.

B. RECOMMENDATIONS

While QPSK is still a relevant modulation, more powerful and complex communication methods exist that would most likely perform differently with the IC

technique described in this thesis. Follow on work that focuses on SIC for multi-carrier and MIMO systems would be most beneficial.

Other estimation methods exist that could possibly provide better estimator performance for this multi-platform system. Future work could observe the implementation of different methods to better estimate α, perhaps at levels higher than 1.0, or when the gain is complex.

APPENDIX

Due to the relationship of the terms in Equation (3.16) for a three-receiver system, certain combinations of gain parameters yield similar if not exact performance SER outcomes as seen in Figure 54.

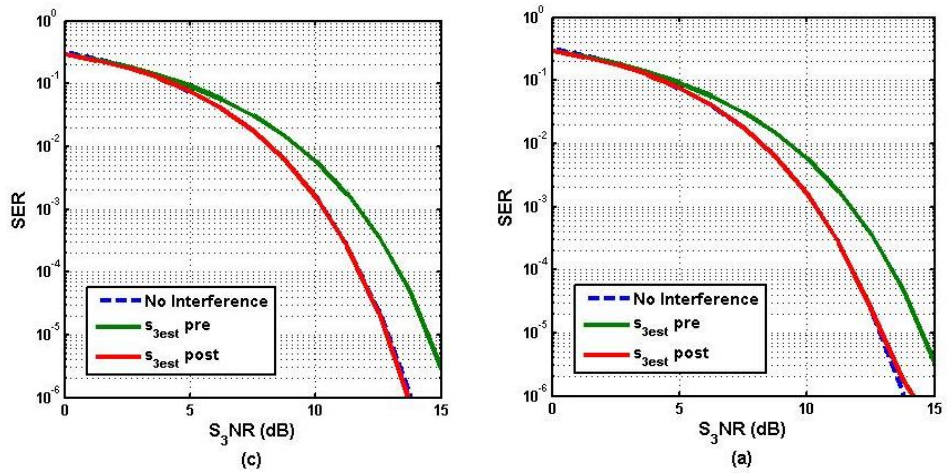

Figure 54. Performance results observed from Figure 11c with $\alpha_{2,3}$ = 0.01 and $\alpha_{1,3}$ = 0.2 compared against Figure 12a where $\alpha_{2,3}$ = 0.2 and $\alpha_{1,3}$ = 0.1. The S_3IR for both simulations is 14 dB.

The same outcome is illustrated in terms of the performance of the estimators, where switching the values between $\alpha_{2,3}$ and $\alpha_{1,3}$ would result in related accuracies of the gain estimations, as is seen in Figure 55. This association mitigates the requirement of multiple simulations with each gain parameter individually being held constant.

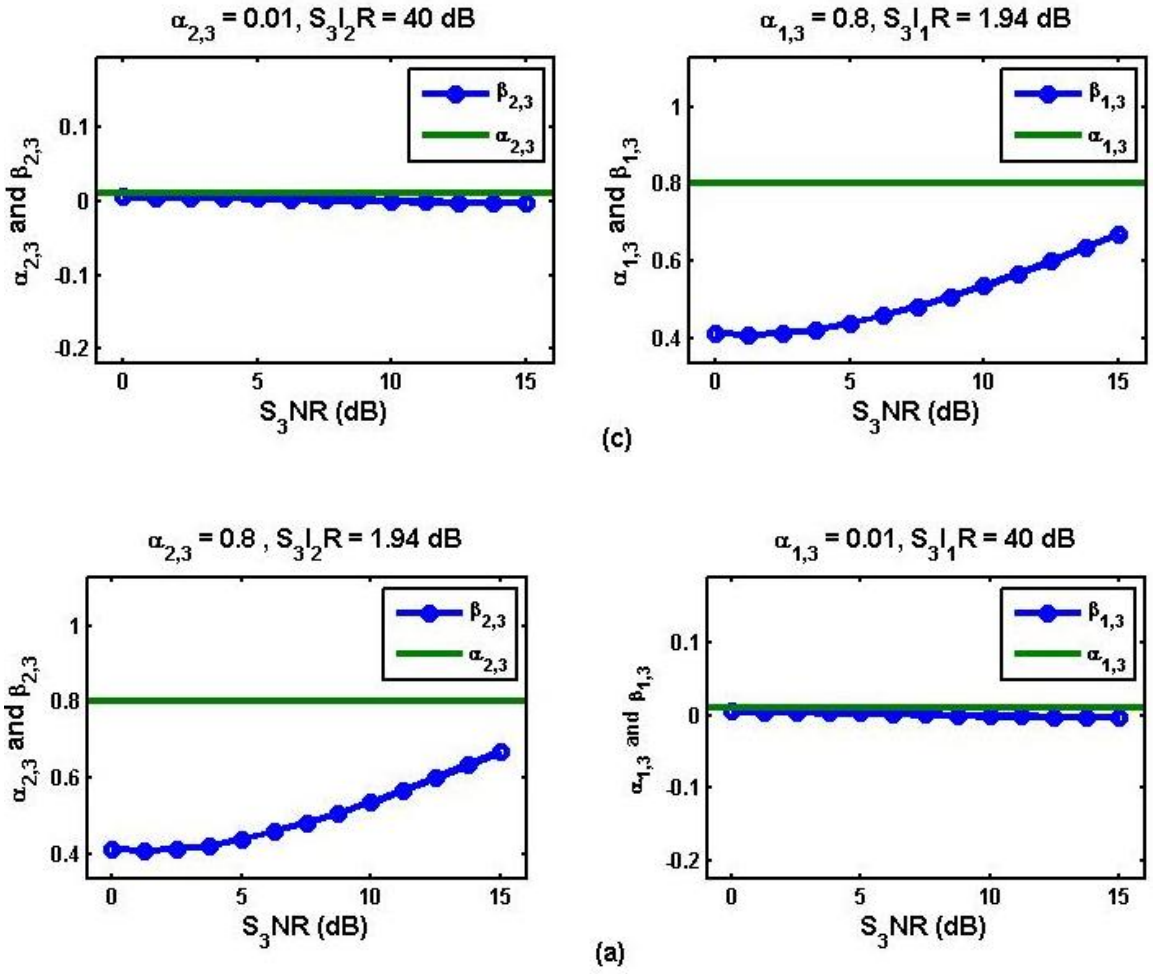

Figure 55. Performance results observed from Figure 16c with $\alpha_{2,3}$ = 0.01 and $\alpha_{1,3}$ = 0.8 compared against Figure 21a where $\alpha_{2,3}$ = 0.8 and $\alpha_{1,3}$ = 0.01. The S_3IR for both simulations is 1.94 dB.

In a four-receiver system, this same relationship is observed in Equation (4.10), and the performances of the SER and estimators are seen in Figures 56 and 57.

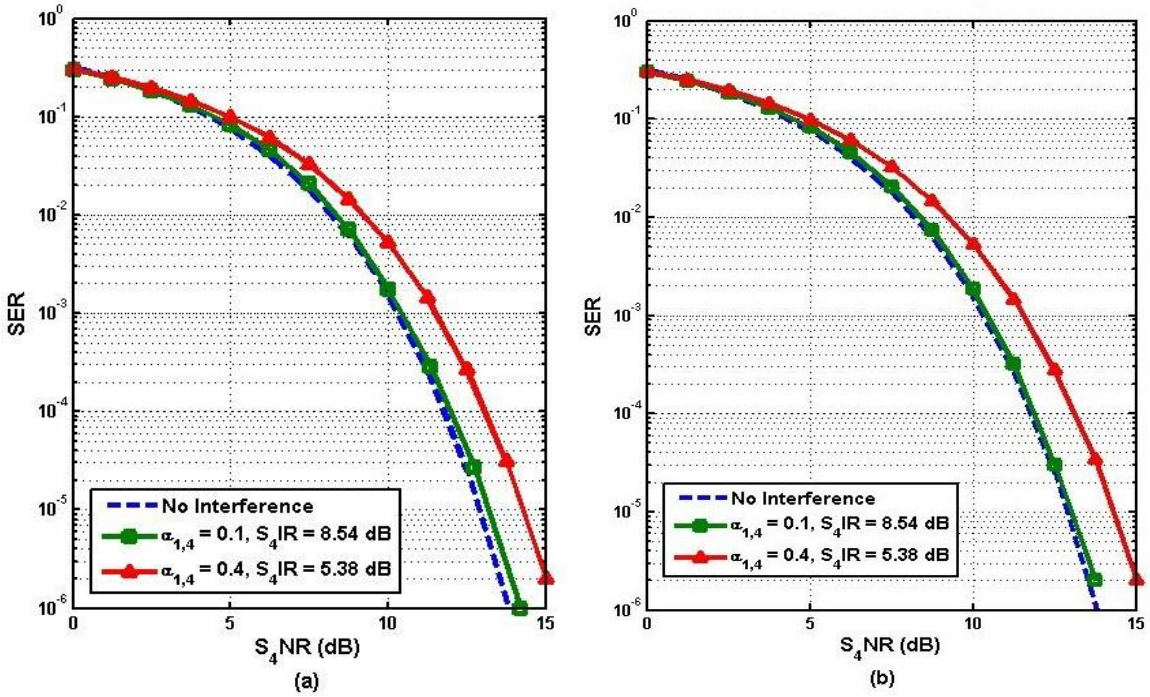

Figure 56. Performance results observed from Figure 36a with $\alpha_{3,4}$ = 0.3, $\alpha_{2,4}$ = 0.2 and compared against Figure 56b (a separate configuration simulation) where $\alpha_{3,4}$ = 0.2 and $\alpha_{2,4}$ = 0.3. The S_4IRs for both simulations are 8.54 and 5.38 dB for $\alpha_{1,4}$ = 0.1 and 0.4, respectively.

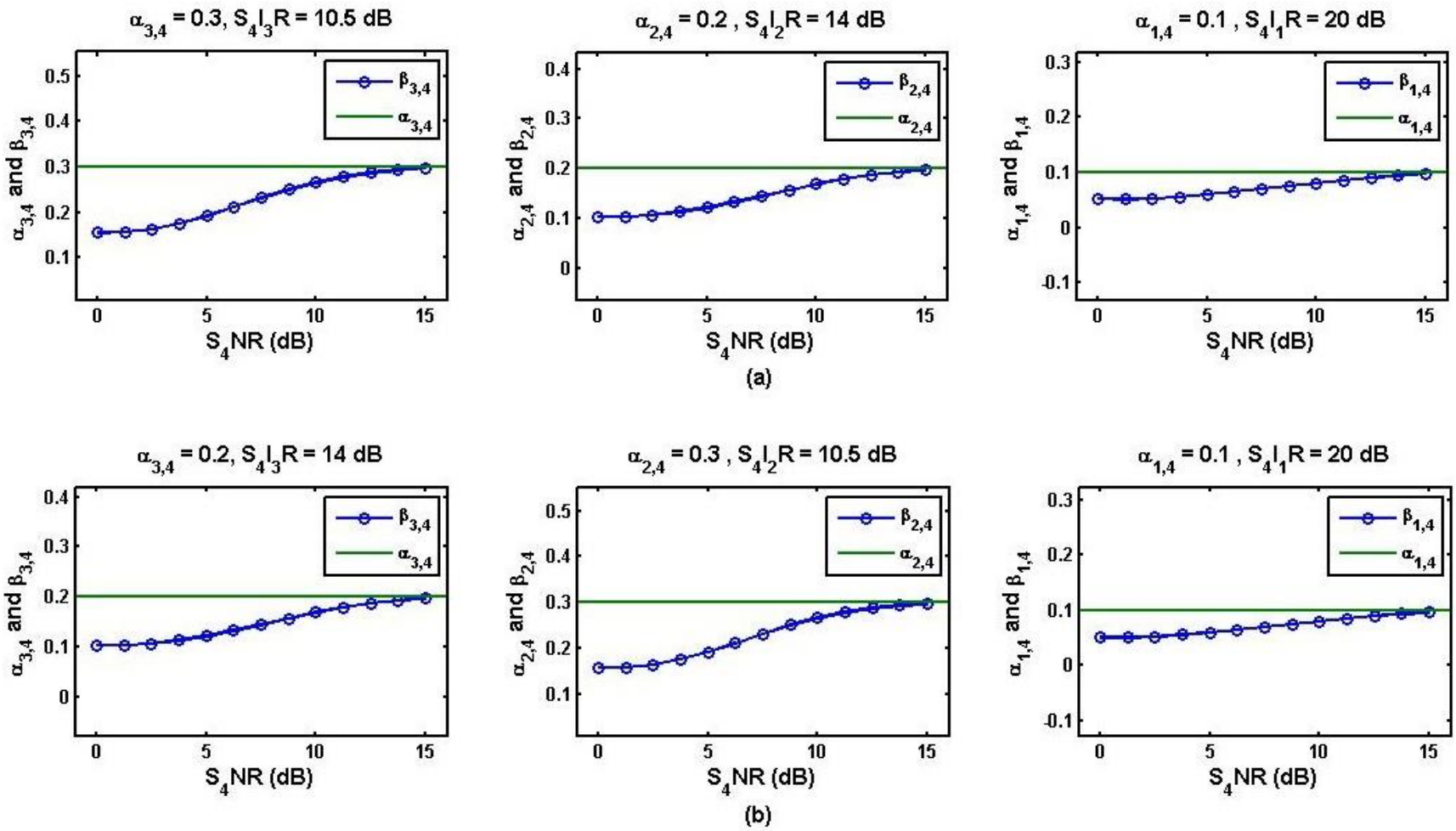

Figure 57. Performance results observed from Figure 40a with $\alpha_{3,4}$ = 0.3, $\alpha_{2,4}$ = 0.2 and $\alpha_{1,4}$ = 0.1 compared against Figure 57b (a separate configuration simulation) where $\alpha_{3,4}$ = 0.2, $\alpha_{2,4}$ = 0.3 and $\alpha_{1,4}$ = 0.1. The S_4IR for both simulations is 8.54 dB.

LIST OF REFERENCES

[1] N. I. Miridakis and D. D. Vergados, "A survey on the successive interference cancellation performance for single-antenna and multiple-antenna OFDM systems," *IEEE Comms. Surveys & Tutorials*, vol.15, no. 1, pp. 312–335, 2013.

[2] J. G. Andrews, "Interference cancellation for cellular systems: a contemporary overview," *IEEE Wireless Comms.*, pp. 19–29, 2005.

[3] C. Ni, "Signal Reception Via Multi-Platform Receivers," M.S. thesis, Naval Postgraduate School, Monterey, CA, 2012.

[4] S. M. Kay, *Fundamentals of Statistical Signal Processing, Volume I: Estimation Theory*, Upper Saddle River, NJ: Prentice Hall PTR, 1993.

[5] S. M. Kay, *Fundamentals of Statistical Signal Processing, Volume II: Detection Theory*, Upper Saddle River, NJ: Prentice Hall PTR, 1998.

THIS PAGE INTENTIONALLY LEFT BLANK

INITIAL DISTRIBUTION LIST

1. Defense Technical Information Center
   Ft. Belvoir, Virginia

2. Dudley Knox Library
   Naval Postgraduate School
   Monterey, California